Bartosz Bednarz

The functions of CpkO and CpkN regulators in coelimycin synthesis and other antibiotic production pathways in *Streptomyces coelicolor* A3(2)

(doctoral thesis)

Supervisor

Dr hab. Jacek Rybka

Auxiliary supervisor

Dr Krzysztof Pawlik

Institute of Immunology and Experimental Therapy

Polish Academy of Sciences

Wrocław 2021

Bartosz Bednarz

Rola białek regulatorowych CpkO i CpkN w procesie syntezy coelimycyny oraz w szlakach produkcji innych antybiotyków u *Streptomyces coelicolor* A3(2)

(rozprawa doktorska)

Promotor

Dr hab. Jacek Rybka

Kopromotor

Dr Krzysztof Pawlik

Instytut Immunologii i Terapii Doświadczalnej

Polska Akademia Nauk

Wrocław 2021

The research for the doctoral thesis was carried out in Laboratory of Molecular Biology of Microorganisms at the Institute of Immunology and Experimental Therapy, Polish Academy of Sciences.

I would like to thank Dr hab. Jacek Rybka and Dr Krzysztof Pawlik for creating a space where I could focus on science and creativity.

I would like to thank Dr Magdalena Kotowska for the enthralling discussions on molecular biology and other topics.

TABLE OF CONTENTS

ABSTRACT 1
STRESZCZENIE 3
LIST OF FIGURES 5
LIST OF TABLES 7
LIST OF ABBREVIATIONS 8

1. INTRODUCTION 11
1.1. The genus *Streptomyces* 11
1.2. The model organism *S. coelicolor* A3(2) 13
1.2.1. Complexity of differentiation and morphogenesis 13
1.2.2. Genome architecture 15
1.2.3. Antibiotics produced by *S.coelicolor* A3(2) M145 16
1.2.3.1. Actinorhodin (ACT) 16
1.2.3.2. Undecylprodigiosin (RED) 17
1.2.3.3. Calcium-dependent antibiotic (CDA) 18
1.3. Regulation of secondary metabolism in *Streptomyces* 19
1.3.1. Sigma factors 20
1.3.2. Two-component systems (TCSs) 21
1.3.3. TetR-like regulators 22
1.3.4. *Streptomyces* antibiotic regulatory proteins (SARPs) 23
1.4. Coelimycin 25
1.4.1. The *cpk* gene cluster 26
1.4.2. Coelimycin synthesis pathway 27
1.4.3. Coelimycin synthesis regulation 31

2. AIM OF THIS WORK 33

3. MATERIALS AND METHODS 34
3.1. Reagents and commercial kits 34

3.2. Microorganisms 35
3.3. Plasmids/constructs 37
3.4. Oligonucleotides 40
3.5. Buffers and solutions 41
3.6. Culturing media 42
3.7. DNA manipulation techniques 43
3.7.1. Agarose gel electrophoresis 43
3.7.2. Spectrophotometric DNA concentration measurement 43
3.7.3. Cosmid DNA minipreparation by phenol:chloroform extraction 43
3.7.4. DNA extraction and purification from agarose gel 44
3.7.5. DNA purification after enzymatic reactions 44
3.7.6. Plasmid DNA minipreparation 44
3.7.7. *S. coelicolor* A3(2) genomic DNA preparation 44
3.7.8. Blunting of 5' or 3' DNA ends 45
3.7.9. Dephosphorylation of 5' DNA ends 45
3.7.10. Phosphorylation of 5' DNA ends 46
3.7.11. Restriction digest 46
3.7.12. Ligation 47
3.7.13. PCR (polymerase chain reaction) 47
3.8. Microorganism manipulation techniques 48
3.8.1. *Escherichia coli* culturing 48
3.8.2. Preparation of *S. coelicolor* A3(2) spore glycerol stocks 49
3.8.3. Intergenic conjugation between *E. coli* and *S. coelicolor* A3(2) 49
3.8.4. Construction of *S. coelicolor* A3(2) deletion mutants and their derivatives 50
3.8.5. Construction of CpkO and CpkN protein-overproducing strains 51
3.8.6. Preparation of competent *E. coli* for heat-shock transformation 52
3.8.7. Competent *E. coli* cell transformation by heat-shock 52
3.8.8. *E. coli* cell transformation by electroporation 52
3.8.9. Phenotypic characterization of *S. coelicolor* A3(2) strains 54
3.8.10. Transcriptional profiling of *cpk* cluster genes 54
3.9. Protein manipulation techniques 54
3.9.1. Protein overproduction 54
3.9.2. Protein purification by affinity chromatography 55

3.9.3. Bradford assay 56
3.9.4. SDS-PAGE 56
3.10. Proteomics 57
3.10.1. Sample preparation 57
3.10.2. LC-MS/MS analysis 57
3.10.3. Protein identification and quantification 58

4. RESULTS 60
4.1. Analysis of CpkO and CpkN amino acid sequences 60
4.2. CpkO and CpkN protein overproduction and DNA binding site determination 61
4.3. Generation of *cpkO* and *cpkN* deletion mutants and their derivatives 64
4.4. Phenotypic characterization of Δ*cpkO*, Δ*cpkN* and derivative mutants 67
4.5. Proteomic analysis of Δ*cpkO* and Δ*cpkN* mutants 70
4.5.1. Coelimycin biosynthetic gene cluster (*cpk*) 72
4.5.2. Undecylprodigiosin biosynthetic gene cluster (*red*) and expression corelated with *red* cluster (*ecr*) 73
4.5.3. Calcium-dependent antibiotic biosynthetic gene cluster (*cda*) 73
4.5.4. Antibiotic precursor flux 73
4.6. In *vivo* expression profiling of *cpk* cluster genes in Δ*cpkO* and Δ*cpkN* mutants 75

5. DISCUSSION 79
5.1. CpkO and CpkN activate coelimycin biosynthetic gene cluster in a cascade manner 79
5.2. CpkO and CpkN act as pleiotropic regulators of secondary metabolism 81
5.3. Deletion of the major coelimycin synthesis activator CpkO directs the precursor flux to the production of other antibiotics 84

6. REFERENCES 86

7. APPENDIX 96

ABSTRACT

Bacteria of the genus *Streptomyces* produce a multitude of secondary metabolites, many of which are pharmaceutically-relevant antibiotics, immunosuppressants and anti-cancer drugs. Secondary metabolite synthesis genes are grouped together on the chromosome into biosynthetic gene clusters (BGCs) that also encode cluster-specific regulatory proteins. Among these regulators are *Streptomyces* antibiotic regulatory proteins (SARPs), which are direct transcription activators of biosynthetic genes.

Coelimycin (CPK) is a transition growth phase secondary metabolite, produced in specific conditions by the model organism *Streptomyces coelicolor* A3(2). After its synthesis as a hydroxyaldehyde and additional enzymatic modifications, the colorless polyketide antibiotic abCPK is formed and subsequently undergoes reactions with specific compounds in the medium, loses its antibacterial properties and gives rise to the yellow coelimycins P1 and P2. Because of synthesis dependence on complex regulatory mechanisms, including quorum-sensing, carbon catabolite repression and pleiotropic regulators, coelimycin remained to be undiscovered for over 50 years of *Streptomyces* research despite being visible to the human eye.

The final putative effectors of *cpk* cluster regulation cascade are CpkO and CpkN – the two cluster-situated SARPs, which are predicted to activate the expression of Cpk type I polyketide synthase genes. Previous studies have found that CpkO is required for CPK synthesis and have linked deletion of its gene to decreased/silenced transcription of chosen *cpk* genes. However, no studies were published on CpkN – a protein belonging to the same family. Previous studies of other SARP proteins (i.e. ActII-orf4, RedD, RedZ, CdaR) have shown that these formerly „cluster-specific" regulators could also exert pleiotropic acitivities and influence other secondary metabolite synthesis pathways.

The aim of this work was to further characterize the functions of CpkO and CpkN in the regulation of coelimycin synthesis and to identify other antibiotic production pathways that are controlled, indirectly or directly, by these regulators in *Streptomyces coelicolor* A3(2). To achieve these goals, *cpkO* deletion- and *cpkN* disruption (insertion) mutants were generated and assayed for antibiotic production. Next, their proteomes were analysed using label-free, shotgun proteomics and compared to that of the wild-type strain M145. Finally, an *in vivo* reporter assay was performed to obtain detailed expression profiles of chosen *cpk* cluster genes in the wild-type and the mutant strains.

The results presented in this work confirm that CpkO is the main activator of *cpk* cluster, inducing the transcription of most of the *cpk* genes (including that of *cpkN*). CpkN, on the other hand, is responsible for activating the transcription of *scoT,* encoding a type II thioesterase necessary for CPK production. These findings, together with literature analysis, resulted in the proposal of a more-detailed mechanism of coelimycin synthesis regulation. Phenotypic and proteomic analysis revealed that CpkO and CpkN influence other antibiotic biosynthetic pathways in *Streptomyces coelicolor* A3(2), including that of actinorhodin, undecylprodigiosin and calcium-dependent antibiotic synthesis. Possible molecular background for these effects is presented and discussed.

STRESZCZENIE

Bakterie z rodzaju *Streptomyces* są producentami rozległego szeregu metabolitów wtórnych, z których wiele znalazło zastosowanie w przemyśle farmaceutycznym jako antybiotyki, immunosupresanty i leki przeciwnowotworowe. Geny syntezy metabolitów wtórnych są na chromosomie zgrupowane w tzw. klastry genów biosyntetycznych (ang. biosynthetic gene clusters – BGCs), które zawierają w sobie również geny białek regulatorowych, specyficznych dla danego klastra. Wśród nich wyróżniamy rodzinę białek regulatorowych syntezy antybiotyków u *Streptomyces* – SARPs (ang. *Streptomyces* antibiotic regulatory proteins), których przedstawiciele są bezpośrednimi aktywatorami transkrypcji genów biosyntetycznych.

Coelimycyna (CPK) jest metabolitem wtórnym produkowanym przez organizm modelowy *Streptomyces coelicolor* A3(2) w ściśle określonych warunkach, podczas przejścia hodowli bakteryjnej z fazy wzrostu eksponencjalnego w fazę stacjonarną. Syntaza poliketydowa Cpk tworzy hydroksyaldehyd, który po dodatkowych modyfikacjach enzymatycznych przekształca się w bezbarwny związek o właściwościach antybiotycznych (abCPK). Następnie abCPK ulega spontanicznym reakcjom z wybranymi związkami zawartymi w medium hodowlanym, traci swoje właściwości antybiotyczne i tworzy żółty barwnik, którego zidentyfikowanymi do tej pory składnikami są coelimycyna P1 i P2. Przez ponad 50 lat badań nad *S. coelicolor* A3(2) brak było artykułów naukowych opisujących obserwację tego metabolitu wtórnego, pomimo jego wyraźnego zabarwienia. Wynika to ze ścisłej kontroli produkcji coelimycyny przez skomplikowane mechanizmy regulacyjne, w tym zjawisko quorum sensing i represję kataboliczną oraz działanie regulatorów plejotropowych.

W kaskadzie sygnałów regulujących ekspresję genów klastra *cpk* biorą udział dwa białka z rodziny SARP – CpkO i CpkN. Przewidywaną funkcją tych regulatorów jest bezpośrednia aktywacja ekspresji genów syntazy Cpk – syntazy poliketydowej typu I. W dotychczasowych badaniach udowodniono, iż białko CpkO jest wymagane w procesie syntezy CPK oraz wykazano, że delecja kodującego je genu skutkuje obniżoną/wyciszoną transkrypcją wybranych genów *cpk*. Brak natomiast informacji na temat białka CpkN, należącego to tej samej rodziny regulatorów. Badania nad innymi białkami z rodziny SARP (ActII-orf4, RedD, RedZ, CdaR) dowiodły, iż te regulatory, uważane dotychczas za specyficzne względem własnych klastrów genów, mogą również działać jako regulatory plejotropowe i kontrolować szlaki produkcji innych metabolitów wtórnych.

Celem niniejszej pracy było dokładniejsze scharakteryzowanie funkcji białka CpkO i zbadanie funkcji białka CpkN w procesie syntezy coelimycyny oraz zidentyfikowanie ścieżek produkcji innych antybiotyków, będących pod bezpośrednią lub pośrednią kontrolą tych regulatorów w *Streptomyces coelicolor* A3(2). By osiągnąć te cele stworzono mutanta *S. coelicolor* A3(2) z delecją genu *cpkO* oraz mutanta z przerwaną ciągłością genu *cpkN,* po czym zbadano ich profile produkcji antybiotyków. Następnie przeanalizowano proteomy mutantów przy użyciu proteomicznej metody „bottom-up, label-free shotgun" i porównano z profilem białkowym szczepu dzikiego M145. W ostatnim etapie pracy ustalono dokładne profile transkrypcji wybranych genów klastra *cpk* w mutantach oraz szczepie dzikim *in vivo,* przy użyciu systemu reporterowego opartego na lucyferazie.

Osiągnięciem niniejszej pracy jest potwierdzenie, iż białko CpkO jest głównym aktywatorem klastra *cpk*, aktywującym transkrypcję większości genów *cpk*, włącznie z *cpkN*, natomiast białko CpkN jest odpowiedzialne za aktywację genu *scoT*, kodującego tioesterazę typu II, niezbędną do produkcji coelimycyny. Te obserwacje oraz analiza danych literaturowych umożliwiły zaproponowanie dokładniejszego mechanizmu regulacji syntezy CPK. Co więcej, dzięki analizie fenotypowej i proteomicznej wykazano, iż białka regulatorowe CpkO i CpkN wywierają również wpływ na inne szlaki biosyntezy – aktynorodyny, undecylprodigiozyny i antybiotyku zależnego od wapnia. W pracy przedyskutowano możliwe wyjaśnienie tych zjawisk na poziomie molekularnym.

LIST OF FIGURES

Figure 1. Scanning electron microscopy images of streptomycetes' life-cycle stages 11

Figure 2. Schematic representation of *Streptomyces* life-cycle 12

Figure 3. The classical and the new model of *S. coelicolor* A3(2) life-cycle 14

Figure 4. Actinorhodin 17

Figure 5. Undecylprodigiosin..... 18

Figure 6. Calcium-dependent antibiotic 19

Figure 7. Coelimycin synthesis *cpk* cluster organization 26

Figure 8. Coelimycin P1 synthesis pathway. 30

Figure 9. Coelimycin synthesis regulation mechanism..... 31

Figure 10. Common domains identified in CpkN and CpkO proteins using CDD/SPARCLE algorithm integrated into BLAST.. 60

Figure 11. Schematic representation of *cpkO* and *cpkN* gene deletion/disruption in *S. coelicolor* A3(2). 65

Figure 12. Confirmation of *cpkO* and *cpkN* gene deletion/disruption in *S. coelicolor* A3(2).. 65

Figure 13. Phenotypes of *S. coelicolor* A3(2) wild-type (M145), *ΔcpkO* and *ΔcpkN* strains cultivated on solid medium 79NG 69

Figure 14. Analysis of the proteomes of *S. coelicolor* A3(2) wild-type (M145), *ΔcpkO* and *ΔcpkN* 70

Figure 15. Comparison of relative levels of proteins involved in antibiotic biosynthesis and antibiotic precursor flux in *S. coelicolor* A3(2) M145, *ΔcpkO* and *ΔcpkN* strains. 71

Figure 16. Transcriptional profiles of *cpk* cluster genes.. 77

Figure 17. Updated mechanism of coelimycin biosynthetic gene cluster regulation by cluster-situated regulators 80

Appendix Figure 1. Map of the expression vector pIJ10257 96

Appendix Figure 2. Map of the expression vector pET28a 97

Appendix Figure 3. Map of the expression vector pGEX-6P-1 98

Appendix Figure 4. Map of the expression vector pMAL-c2TEV 98

Appendix Figure 5. Map of the expression vector pCJW93 99

Appendix Figure 6. Map of the recombineering vector pIJ790 99

Appendix Figure 7. Calcium-dependent antibiotic (CDA) bioassay in *S. coelicolor* A3(2) M145, Δ*cpkO* and Δ*cpkN* 100

Appendix Figure 8. Primary component analysis as an indicator of proteomics sample preparation quality/reproducibility 100

LIST OF TABLES

Table 1. List of chemical reagents and commercial kits used in this work..... 34

Table 2. List of microorganisms used in this work 35

Table 3. List of genetic constructs used in this work. 37

Table 4. List of oligonucleotides used in this work. Restriction sites are in bold..... 40

Table 5. Summary of the attempts at obtaining functional CpkO and CpkN proteins..... 63

Appendix Table 1. List of all proteins quantified in *S. coelicolor* A3(2) M145, Δ*cpkO* and Δ*cpkN* strains by XIC, SC or PC quantification methods after proteomics data post-processing..... 101

Appendix Table 2. Proteomic comparison of *S. coelicolor* A3(2) M145, Δ*cpkO* and Δ*cpkN* strains - proteins with statistically significant abundance changes (ANOVA-adjusted p value < 0.01). 116

LIST OF ABBREVIATIONS

ACP	acyl carrier protein
ACT	actinorhodin
AGC	automatic gain control
APS	ammonium persulfate
AT	acyltransferase domain
BLAST	basic local alignment search tool
BTAD	bacterial trancription activation domain
BGC	biosynthetic gene cluster
bp	base-pairs
BSA	bovine serum albumin
CDA	calcium-dependent antibiotic
cfu	colony forming unit
ChIP-seq	chromatin immunoprecipitation-sequencing
CPK	coelimycin
CSR	cluster-situated regulator
ddH_2O	double-distilled water
DBD	DNA-binding domain
DH	dehydratase domain
DMSO	dimethyl sulfoxide
DNA	deoxyribonucleic acid
ECR	expression correlated with *red*
EDTA	ethylenediaminetetraacetic acid
EMSA	electrophoretic mobility shift assay

ER	enoyl reductase domain
FDR	false discovery rate
Fig	figure
GBL	γ-butyrolactone
gDNA	genomic deoxyribonucleic acid
GST	glutathione S-transferase
HK	histidine kinase
HTH	helix-turn-helix
IPTG	isopropyl β-D-1-thiogalactopyranoside
KR	ketoreductase domain
KS	ketosynthase domain
LB	lysogeny broth
LD	loading dye
MBP	maltose binding protein
NRPs	non-ribosomal peptides
ori	origin of replication
PC	peak counting
PCA	primary component analysis
PCR	polymerase chain reaction
PEG	polyethylene glycol
RED	undecylprodigiosin
rpm	rounds per minute
RR	response regulator
SAP	shrimp alkaline phosphatase

SARP	*Streptomyces* antibiotic regulatory protein
SC	spectral counting
SDS-PAGE	sodium dodecyl sulphate - polyacrylamide gel electrophoresis
SMM	supplemented minimal medium
SOB	super optimal broth
SOC	super optimal broth with catabolites repression
spp	species
T4 PNK	T4 phage polynucleotide kinase
TBE	tris-borate-EDTA
TCS	two-component system
TEV	tobacco etch virus
TPR	tetratricopeptide repeat
TR	thioester reductase
U	enzyme unit
X-gal	5-bromo-4-chloro-3-indolyl-β-D-galactopyranoside
XIC	extracted ion chromatograms

1. INTRODUCTION

1.1. The genus *Streptomyces*

Streptomyces are Gram-positive, filamentous, saprophytic, soil-dwelling bacteria belonging to the phylum *Actinobacteria*, order *Streptomycetales,* family *Streptomycetaceae* (NCBI: Taxonomy, abbreviated lineage). As inhabitants of terrestrial and marine sediments, and being capable of hydrolyzing a wide range of natural macromolecules (i.e. polysaccharides, proteins, nucleic acids and lipids), they contribute to the turnover of biogenic elements in nature (Chater et al. 2010). However, members of *Streptomyces* genus are mostly renowned for producing more than two-thirds of clinically relevant antibiotics among other bioactive molecules such as immunosupressants, anti-helmintics and anti-cancer drugs (Hopwood 2007).

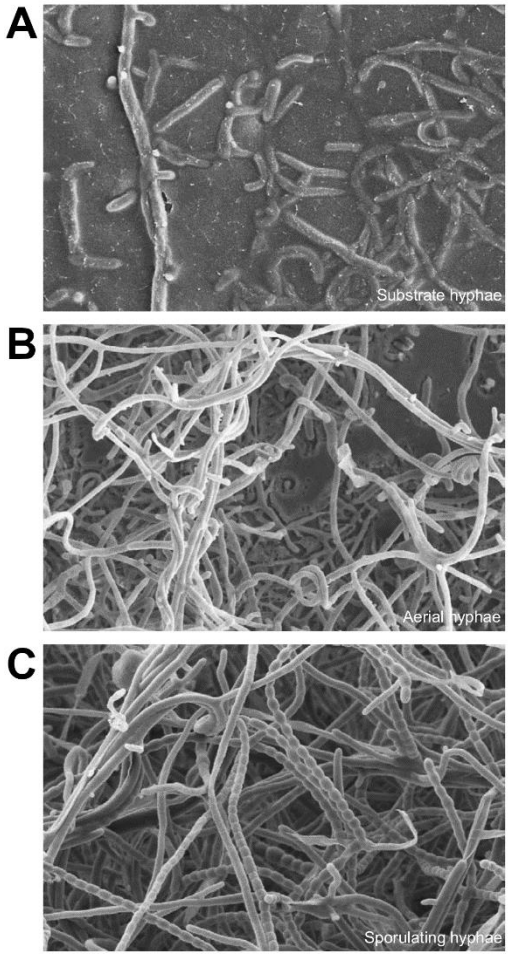

Figure 1. Scanning electron microscopy images of streptomycetes' life-cycle stages. A) vegetative mycelium, B) aerial mycelium, C) spore chains (Claessen et al. 2006).

Optimal growth conditions for *Streptomyces* span around the temperature of 30ºC and pH 6.5 - 8. On solid substrate the bacteria undergo a complex multicellular life-cycle of vegetative growth, aerial mycelium formation and sporulation, resembling the processes of filamentous fungi (Hopwood 2007) (Fig. 1 and 2). For around 2 – 3 days after spore germination, *Streptomyces* grow into the substrate in the form of a vegetative (substrate) mycelium. Its morphological differentiation corresponds to the production of secondary metabolites. Transcription of their respective biosynthetic genes is induced by environmental, physiological or nutrient-limitation signals and is coupled to vegetative mycelium autolysis and recycling of its constituents for aerial mycelium formation. Upon septation, the tips of aerial mycelium form spore chains. The deposition of spore pigment is indicative of spore maturation (Bibb 2005) (Fig. 1 and 2). Spores are means of survival in potential unfavorable conditions of nutrient scarcity, oxygen limitation or dessication. In liquid cultures *Streptomyces* do not usually undergo sporulation, however exceptions to this rule exist (Hopwood 2007).

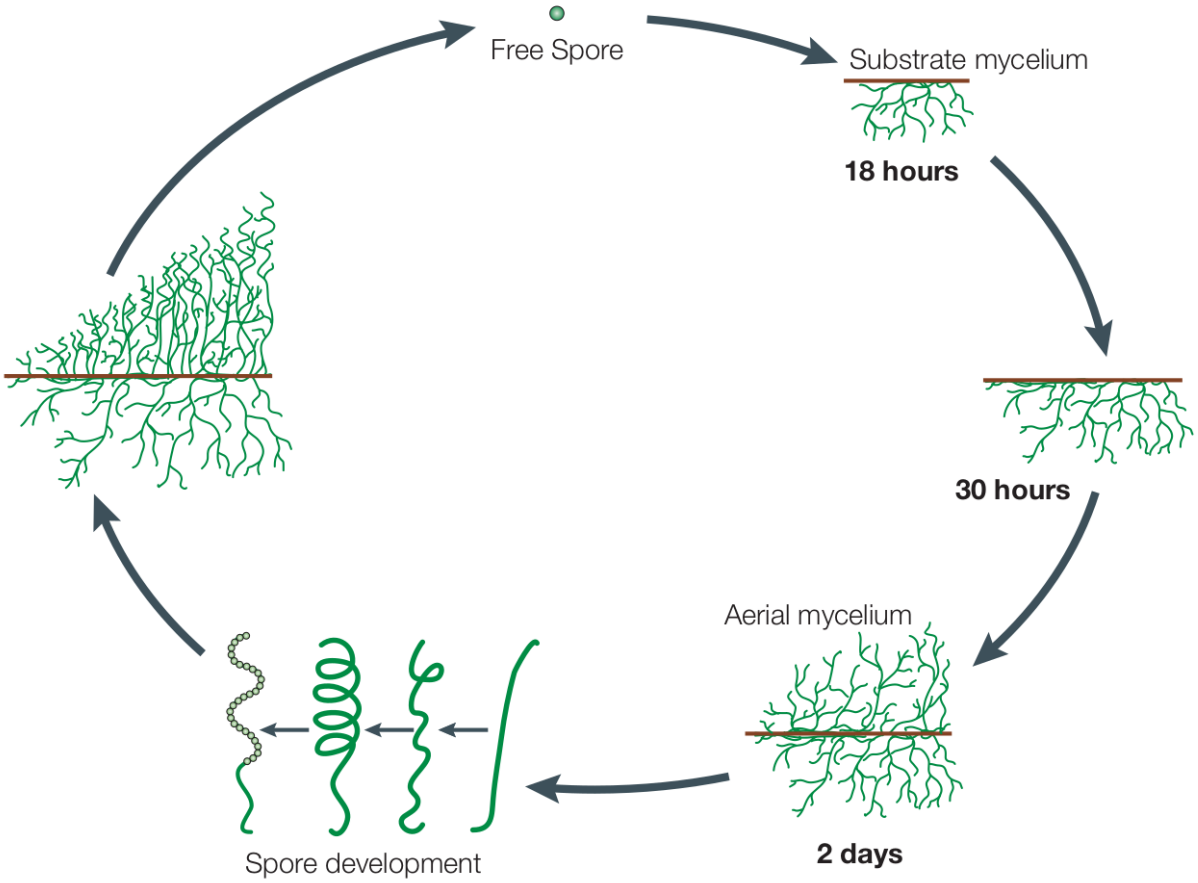

Figure 2. Schematic representation of *Streptomyces* life-cycle (Angert 2005).

1.2. The model organism *S. coelicolor* A3(2)

Streptomyces coelicolor A3(2) is the best studied representative of *Streptomyces*. It undergoes all of the growth phases typical for the genus. The research on *S. coelicolor* A3(2) genetics was initiated by David A. Hopwood in the late 1950s (Hopwood 1957). The early availability of its genome sequence, genetic manipulation tools such as genomic- and mutagenesis- ordered cosmid libraries, and the strain's capability to produce three colored metabolites: actinorhodin, undecylprodigiosin and coelimycin, made it a perfect model for morphogenesis, development and antibiotic production studies.

1.2.1. Complexity of differentiation and morphogenesis

Two models are used to describe the development of *Streptomyces coelicolor* A3(2). The general, „classical" model (Fig. 1 and 2), distinguishes three phases of growth on agar surface: 1) the branched, multinucleoid vegetative (substrate) mycelium, 2) hydrophobic aerial mycelium that extends to the air from the former hyphae, and 3) uninucleoid spores, which are formed from aerial mycelium by its septation and compartmentalization. It is generally agreed that the onset of antibiotic production coincides with aerial mycelium formation (Hopwood 2007). The newer, detailed model (Manteca and Sanchez 2009) divides life-cycle of a solid *S. coelicolor* A3(2) culture into: 1) early, compartmentalized mycelium MI that undergoes partial programmed cell death, and 2) multinucleated mycelium MII that stems from the remaining viable cells of MI. MII is further classified into: 2a) early MII without hydrophobic layers and 2b) late MII with hydrophobic layers. The classical „vegetative hyphae" corresponds to early MII while „aerial hyphae" corresponds to MII coated with hydrophobic layers (Fig. 3). MI is the predominant phase in natural environment. According to the updated model, MII is the antibiotic-producing mycelium.

The vegetative and aerial mycelia are multinucleated syncytia, with occasional peptidoglycan cross-walls, that grow by extension at apical sites (Flärdh et al. 2012). Interestingly, in *Streptomyces*, cell division is non-essential for viability. *ftsZ* gene, encoding a bacterial tubulin-homologue protein that is necessary for cross-wall formation and reproductive cell division, can be deleted and the resulting mutant can be propagated from mycelium fragments. Moreover, such non-compartmentalized mycelium is still highly resistant to mechanical damage (McCormick 2009). This phenomenon remained unexplained until recently when two groups demonstrated the existence of another compartmentalization

mechanism in *Streptomyces* – the cross-membranes that are impermeable to large molecules and delimit nucleoid-restricted zones. It was also suggested that they may protect nucleoid from cell-wall rearrangement events (Celler et al. 2016; Yagu et al. 2016).

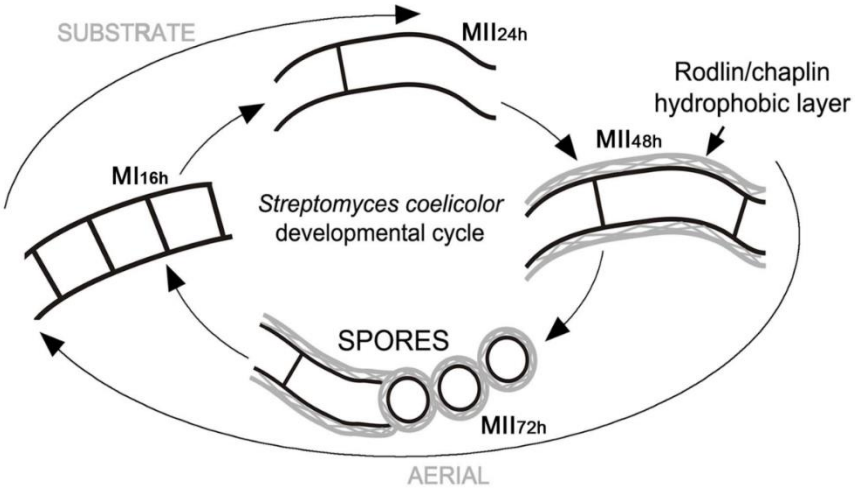

Figure. 3. The classical and the new model of *S. coelicolor* A3(2) life-cycle (Yagüe et al. 2013).

The most well-studied genetic mechanisms regulating *S. coelicolor* A3(2) development are the so called „*bld*", and „*whi*" pathways, named after the respective gene groups involved. *bld* gene mutants grow only as a substrate mycelium and fail to produce aerial hyphae – thus present the „bald" phenotype. It is accepted that *bld* cascade integrates signals of intracellular and environmental conditions which results in activation of *ramS* gene, encoding an enzyme responsible for producing surfactant lantipeptide SapB that enables bacterial colony to break the water surface tension and elevate aerial hyphae into the air (Claessen et al. 2006). *whi* mutants display the characteristic „white" phenotype because they produce aerial mycelium, which is however incapable of sporulation – a process that ends in the deposition of grey spore pigment in the mature spores (Champness 1988; Chater 2001). Subsequently, a novel developmental cascade named the „*sky*" pathway was discovered, that regulates the expression of chaplin and rodlin genes (Claessen et al. 2006). Chaplins and rodlins are proteins that form the hydrophobic rodlet layer on the surface of late MII mycelium and spores (Claessen et al. 2004). Chaplins also constitute fimbriae that enable *S. coelicolor* A3(2) attachment to surfaces (Jong et al. 2009). *sky* pathway is presumably activated by *bld* cascade and it is accepted that its activity is timed in between the *bld* and *whi* pathways (Claessen et al. 2006).

1.2.2. **Genome architecture**

Genome of *S. coelicolor* A3(2) consists of a linear, 8.7 Mbp chromosome with a 72% G+C content, encoding 7825 predicted genes (one of the largest numbers present in a bacterium), and two plasmids – linear SCP1 (365 kbp) and circular SCP2 (31 kbp). The capacity to produce such an enormous repertoire of proteins is associated with a complex life-cycle and the diversity of possible ecological niches, nutrient sources and possible competitors of this bacterium. Centrally located on the chromosome is the *oriC* (origin of replication), while the terminal inverted repeats carry covalently attached proteins at the free 5' ends (Bentley et al. 2002). Functional analysis of genes led to the discovery that *S. coelicolor* A3(2) chromosome has a biphasic structure – it is comprised of the conserved core region (from ~ 1.5 Mbp to 6.4 Mbp) and a pair of arms. The core region generally encodes primary metabolism proteins, essential for viability of the cell, while the distal arms encode secondary metabolite synthesis proteins along with hydrolytic enzymes and gas vesicle proteins. Genes located on the chromosomal arms most probably originated from incorporation of foreign genes by a horizontal gene transfer (Bentley et al. 2002). An interesting feature is the genetic instability of these chromosomal regions – they frequently undergo deletions and multiplications, resulting in diversified secondary metabolite production capacity as means of adaptive division of labor within a culture (Zhang et al. 2020). In laboratories around the world, a prototrophic derivative of strain A3(2), designated M145, is routinely used for *Streptomyces coelicolor* A3(2) studies. The strain lacks two plasmids: SCP1 and SCP2.

A remarkable feature of *S. coelicolor* A3(2) chromosome is the overwhelming number of regulatory genes it encodes. Out of 7825 predicted genes, 965 encode putative regulatory proteins (Bentley et al. 2002). These include: two-component systems (100 sensor histidine kinases and 87 response regulators), sigma-factors (65), serine/threonine kinases (44), TetR-family proteins (153) and others (Bentley et al. 2002; Cuthbertson and Nodwell 2013; Rodríguez et al. 2013). Their transcription often induces a coordinated, global response, linking multiple metabolic pathways for growth modulation, stress-response or secondary metabolite synthesis, all of which are interconnected.

1.2.3. **Antibiotics produced by *Streptomyces coelicolor* A3(2) M145**

Actinomycete species often produce more than 25 secondary metabolites each (Nett et al. 2009). The genes responsible for the synthesis of the respective specialized metabolites are colocalized on the chromosome, forming biosynthetic gene clusters (BGCs). Plethora of biosynthetic gene clusters found in actinomycetes' genomes reflect the complexities of their ecological niches. The bacteria must face everchanging environmental conditions such as dehydration, hypoxia and osmotic stress, compete with other microbes and live in symbiosis with other organisms such as plants, fungi and insects (Meij et al. 2017). Novel predictive strategies and bioinformatic tools such as antiSMASH (Blin et al. 2017) identified more than 30 potential BGCs in *S. coelicolor* A3(2). Many of the products have already been studied. They belong to several chemical classes such as polyketides, fatty acids, peptides, terpenoids, hydroxamate-type siderophores and others (van Keulen and Dyson 2014). Functionally, they are classified as signaling molecules (i.e. gamma-butyrolactones), protectants (i.e. melanin), surfactants (SapB), chemoatractants (2-methylisoborneol), antibiotics and many more classes. *S. coelicolor* A3(2) chromosome encodes proteins for the production of four antibiotics: two polyketides - coelimycin (CPK, *cpk* cluster) and the blue-colored actinorhodin (ACT, *act* cluster), the pyrrole-based red pigment undecylprodigiosin (RED, *red* cluster) and the lipopeptide calcium-dependent antibiotic (CDA, *cda* cluster) (Bentley et al. 2002). Methylenomycin, the cyclopentanone antibiotic encoded on the SCP1 plasmid of *S. coelicolor* A3(2) (Hobbs et al. 1992) is not discussed in this work as the model *S. coelicolor* A3(2) M145 strain is deficient in both SCP1 and SCP2 plasmids. Actinorhodin, undecylprodigiosin and calcium-dependent antibiotic are characterized in this section while coelimycin, the main focus of this work, is the subject of a separate chapter (1.4).

1.2.3.1. **Actinorhodin (ACT)**

Actinorhodin (Fig. 4) is a type II polyketide, redox-active antibiotic (Mak and Nodwell 2017), blue at basic pH and red at acidic pH (Bystrykh et al. 1996). It is produced in the late stationary growth-phase of *S. coelicolor* A3(2), generally after around 50 hours, depending on the medium. The precursors for ACT synthesis are acetyl-CoA, malonyl-CoA and its derivative methylmalonyl-CoA (Hopwood and Sherman 1990). They are supplied by degradation of branched-chain aminoacids and the storage material triacylglycerols (TAGs) (Stirrett et al. 2009; Wang et al. 2020). Actinorhodin production is positively influenced by S-

adenosylmethionine (SAM), however the mechanism is unknown. Interestingly, the direct activator of ACT synthesis – SARP protein ActII-orf4 has a putative SAM binding motif (Kim et al. 2003). Actinorhodin is both excreted and accumulated intracellularly (Bystrykh et al. 1996). Its biosynthetic gene cluster (*act* cluster) spans over 22 kbp - 22 genes (*SCO5071-SCO5092*) (Okamoto et al. 2009). Despite many discoveries in the field of regulation of its synthesis, the chemical properties and function of actinorhodin are poorly understood. It is involved in redox-cycling reactions (Mak and Nodwell 2017) as well as being an organocatalyst for oxidative reactions (Nishiyama et al. 2014). Its proposed mode of action is killing bacteria by catalyzing the production of high levels of H_2O_2 (Nishiyama et al. 2014). Because of its high reactivity and the resulting low specificity of action, actinorhodin is not a good clinical trial antibiotic candidate (Baell and Walters 2014). Perhaps, actinorhodin primarily plays another role as a signaling molecule in the regulation of *S. coelicolor* A3(2) development (Dietrich et al. 2008), and its weak antibiotic activity is not-important in the natural habitat of *Streptomyces* – the soil.

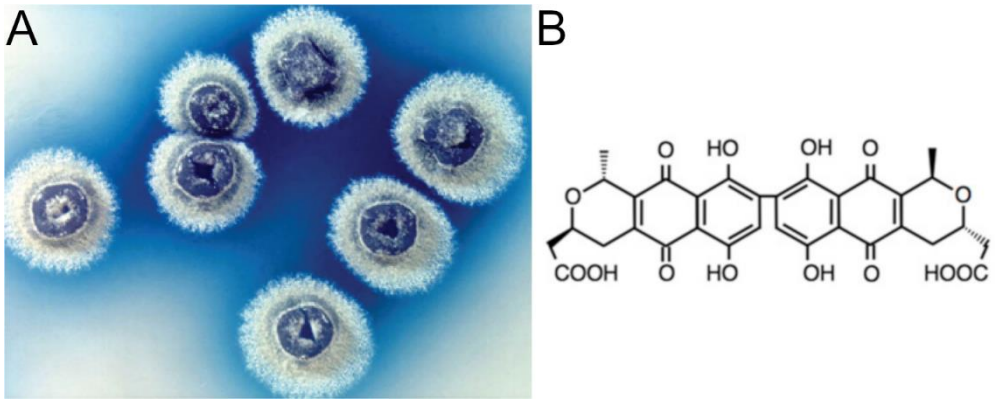

Figure 4. Actinorhodin. A) *S. coelicolor* A3(2) colonies producing the blue pigment actinorhodin (Chater 2016). B) Molecular formula of actinorhodin (Nishiyama et al. 2014).

1.2.3.2. **Undecylprodigiosin (RED)**

Undecylprodigiosin (Fig. 5) is a member of the family of tripyrolle molecules called prodiginines. They are mixed-class molecules, synthesised from precursors also involved in polyketide, fatty acid and nonribosomal peptide synthesis – acetyl-CoA, malonyl-CoA, L-proline, glycine, dodecanoic acid or derivatives (Thomas et al. 2002; Singh et al. 2012). Prodiginines are red-colored immunosuppressive, antimicrobial, anti-helmintic, and anticancer agents (Stankovic et al. 2014). They have a broad range of activity and their cytotoxicity is at least partly a consequence of their DNA-intercalating properties that inhibit topoisomerase

activity (Martinell et al. 2005). The onset of undecylprodigiosin production at ~35 h coincides with the transition from exponential to stationary growth phase of *S. coelicolor* A3(2), while the maximum amount of the compound is accumulated at ~50 h of growth (Tenconi et al. 2018). Interestingly, in *S. coelicolor* A3(2) the compound is accumulated intracellularly despite the lack of any resistance genes in this organism. This effect, taken together with the timing of its production and coinciding with cellular death round before aerial hyphae formation, led scientist to speculate that undecylprodigiosin may be the self-damaging agent necessary for vegetative to aerial hyphae transition. However, data suggest that the production of undecylprodigiosin is the consequence rather than the reason, for this hyphae rearrangement (Tenconi et al. 2018). RED synthesis is positively influenced by S-adenosylmethionine, possibly by a similar manner to actinorhodin production – RedD, the direct undecyloprodigiosin synthesis SARP activator has a putative SAM binding motif (Kim et al. 2003). Undecylprodigiosin biosynthetic gene cluster (*red* cluster) is ~31 kbp and spans over 23 genes (*SCO5877-SCO5898*) (Cerdeño et al. 2001).

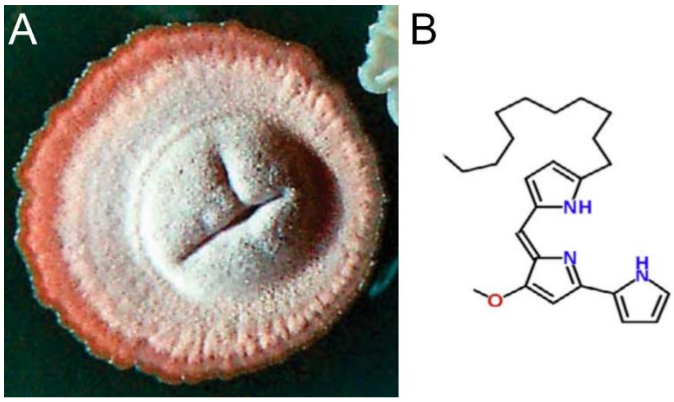

Figure 5. Undecylprodigiosin. A) A colony of *S. celicolor* A3(2) producing the red pigment undecylprodigiosin (Chater 2006). B) Molecular formula of undecylprodigiosin (van Keulen and Dyson 2014).

1.2.3.3. **Calcium-dependent antibiotic (CDA)**

Calcium-dependent antibiotic (CDA, Fig. 6) is a cyclic, acidic lipopeptide belonging to the family of nonribosomal peptides (NRPs), produced by enzymes called NRP synthetases. Interestingly, these enzymes are not dependent on mRNA, and a given NRP synthetase produces only one type of peptide. NRPs can contain proteinogenic as well as unusual amino acids, can have branched and cyclic structures, and undergo a plethora of post-production modifications (Alberto et al. 2016). Precursors for CDA synthesis include acetyl-CoA,

malonyl-CoA and aminoacids tyrosine, aspartate, asparagine, tryptophan, threonine, glycine, serine, glutamate and oxoglutarate (Kim et al. 2004). It was proposed that the mode of action of CDA may be similar to that of structurally-related daptomycin, which disrupts membrane function in multiple ways (Kim et al. 2004). The proteins involved in synthesis of calcium-dependent antibiotic are encoded within the 82 kbp *cda* cluster, spanning 40 genes (Bentley et al. 2002; Micklefield 2009).

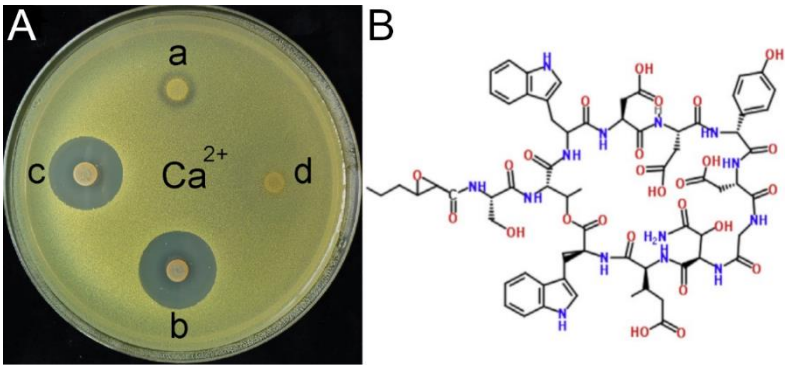

Figure 6. Calcium-dependent antibiotic. A) Calcium-dependent antibiotic bioassay plate. *S. coelicolor* A3(2) strains designated "b" and "c" are potent CDA producers as reflected by the translucent *Bacillus mycoides* growth inhibition zones. "a" is a weak CDA producer, while "d" does not produce the antibiotic. Antimicrobial properties of CDA are dependent on the presence of Ca^{2+} ions. (Lewis et al. 2019). B) The molecular structure of CDA (van Keulen and Dyson 2014).

1.3. Regulation of secondary metabolism in *Streptomyces*.

As mentioned earlier, *S. coelicolor* A3(2) genome encodes an enormous regulatory machinery of proteins, categorized as: two-component systems (TCSs), sigma-factors, serine/threonine kinases, LacI-, IclR-, ROK-, GntR-, WhiB- and TetR-like family proteins along with *Streptomyces* antibiotic regulatory proteins (SARPs) and others. In *Streptomyces*, generally, antibiotic synthesis is regulated on two levels - by the so called "pleiotropic regulators", that control multiple different processes in the cell, as well as "cluster-situated/specific regulators" (CSRs), encoded within the respective BGC and specifically controlling the transcription of its genes. Pleiotropic transcription factors may modulate biosynthetic genes directly or act indirectly through CSRs (van der Heul et al. 2018). Hence, multitude of proteins belonging to different families are associated with the control of each BGC. Commonly, TetR-like and SARP proteins are both located within one biosynthetic gene cluster (Wietzorrek 1997; Cuthbertson and Nodwell 2013). TetR-like proteins generally

constitute a positive feedback loop for specialized metabolite synthesis by binding the end-product of the cluster and derepressing cluster's genes in response, further enhancing production (Cuthbertson and Nodwell 2013), while SARPs are considered to be the direct activators of biosynthetic genes (Wietzorrek 1997). Interestingly, emerging evidence shows that the opposite may also be true - SARPs were shown to affect the expression of pleiotropic regulators and distant biosynthetic gene clusters, however little is known about the nature of such interactions (Huang et al. 2005). Consequently, the paradigm of cluster specific/situated vs. pleiotropic regulators is shifting. This work provides further support to this changing notion.

This chapter is focused on functional characterization of the chosen, dominant, regulatory protein families involved in secondary metabolism modulation in *Streptomyces*.

1.3.1. **Sigma factors**

Sigma factors are dissociable components of RNA polymerase complexes that determine their promoter specificity. Almost all of *S. coelicolor* spp. sigma factors belong to the σ^{70} family, named after the housekeeping σ^{70} of *Escherichia coli* (Sun et al. 2017).

The major houskeeping *Streptomyces* σ factor is σ^{HrdB}, which is present in every studied *Streptomyces* species so far and was shown to be necessary for the cell viability (Buttner et al. 1990). σ^{HrdB} directly controls the transcription of 1694 genes in *S. coelicolor*, including nearly 50% of all energy metabolism-related genes, genes involved in precursor flux, morphological development and also those of other σ factors along with anti-σ factors and their antagonists. On the contrary, secondary metabolism gene transcription was generally shown to be independent of σ^{HrdB} (Zikov et al. 2019). However, more than 60 other σ factors exist in *S. coelicolor* A3(2) that may compete with HrdB and their influence may vary during different stages of growth. Generally, they act as pleiotropic regulators. The classical model of σ factor mode of action assumes that the activity of a σ factor is repressed by binding to its cognate anti-σ factor and that, upon signal sensing, the anti-σ factor undergoes conformational changes and dissociates from its partner, rendering it active (Helmann 2002). A well-characterized σ factor acting in this manner in *Streptomyces coelicolor* A3(2) is σ^{R} – the major oxidative stress-responsive regulator, activating the expression of genes encoding disulfide-stress proteins. Interestingly, σ^{R} is subject to regulation itself - oxidative stress in the cell causes intramolecular disulphide bond formation in the anti-σ factor RsrA, which then loses affinity to σ^{R}, activating it and making it functional (Paget et al. 2001).

On the other hand, σ^T represses undecylprodigiosin and actinorhodin production as well as morphological development on rich media in *S. coelicolor* A3(2) (Mao et al. 2009). The stability of σ^T is completely dependent on binding its anti-σ factor RstA. RstA protects σ^T from ClpP protease-dependent degradation during primary metabolism, itself not being susceptible to this degradation pathway. During secondary metabolism, degradation of RstA is followed by that of σ^T. Diminishing levels of σ^T, which is also a direct repressor of *clpP1/P2*, further enhances the process itself. Interestingly, antibiotics undecylprodigiosin and actinorhodin, but not others, prevent σ^T-*clpP1/P2* promoter binding, providing yet another positive feedback loop to σ^T degradation and further transition from primary to secondary metabolism (Mao et al. 2013).

Although most of the σ factors characterized so far come from the model organism, other notable examples include σ^{25} from *S. avermitilis* and σ^{AntA} from *S. albus*. σ^{25} controls the synthesis of antibiotics oligomycin and avermectin while σ^{AntA} is a CSR involved in the regulation of antimycin biosynthetic gene cluster – a mechanism that was shown to be associated with different antimycin BGCs in *Streptomyces* (Joynt and Seipke 2018).

1.3.2. **Two-component systems (TCSs)**

Two-component systems (TCSs) are among the most common signal transduction systems in *S. coelicolor* A3(2). They sense environmental condition changes and respond by modulating transcription. These functions lie in their membrane-bound histidine kinases (HKs) and cytoplasmic response regulators (RRs), respectively. After receiving a signal, HK autophosphorylates itself and transfers a phosphoryl group to its cognate RR. *S. coelicolor* A3(2) genome encodes 67 typical TCSs (RR with a cognate HK), 17 unpaired HKs and 13 orphan RRs, some of which have been shown to directly bind promoters of cluster-situated regulators (CSRs) and biosynthetic genes from the respective secondary metabolite biosynthetic gene clusters (Hutchings et al. 2004).

An interesting example of regulation by a TCS, is that of the well-studied AfsQ1/Q2 (RR/HK) system. Deletion of *afsQ1-Q2* in *S. coelicolor* A3(2) results in a strong reduction in ACT, RED and CDA synthesis and faster aerial mycelium formation, however these phenotypic effects are present only in a defined minimal medium MM supplemented with glutamate, suggesting that AfsQ1/Q2 responds to a nutritional signal such as C/N/P ratio or a nitrogen metabolism intermediate (Shu et al. 2009; Rodríguez et al. 2013). What is more, AfsQ1/Q2

activates the transcription of an adjacent σ factor gene *sigQ*. Deletion of *sigQ* led to the opposite phenotypic effects to that of *afsQ1-Q2* deletion – precocious ACT, RED and CDA production along with delayed aerial mycelium formation on MM medium with glutamate, and it was proposed that *afsQ1-Q2-sigQ* constitute a pleiotropic system that modulates morphological differentiation and secondary metabolism in specific environmental conditions (Shu et al. 2009). Later, effects of AfsQ1/Q2 on *sigQ* and secondary metabolite production were confirmed to be a consequence of direct AfsQ1 binding to the respective promoters. In the same work, a connection between AfsQ1/Q2 system and nitrogen assimilation repression in the conditions of high glutamate levels was drawn (Wang et al. 2013). In subsequent studies, deletion of *afsQ1/Q2* resulted in strong downregulation of *cpk* cluster expression and lack of CPK production in the conditions of growth on minimal medium supplemented with glutamate. AfsQ1 was shown to exclusively bind to the promoter of *cpkA* biosynthetic gene within the cluster. It was proposed that this binding may facilitate RNA polymerase recruitment and activation of *cpkA/B/C* transcription (Chen et al. 2016).

1.3.3. **TetR-like regulators**

Functionally, TetR-like regulators can be considered as a subfamily of one-component systems, the most abundant regulatory elements in prokaryota, in which the same protein molecule is the receiver of a signal and an effector. As (mostly) pleiotropic regulators, TetR-like regulators control both primary- and secondary metabolism genes by binding to DNA and activating or repressing respective promoters upon ligand (i.e. a metabolite, an ion, antibiotic or a quorum-sensing molecule) binding (Cuthbertson and Nodwell 2013). Structurally, TetR-like proteins bind to DNA by a helix-turn-helix (HTH) N-terminal domain and interact with the ligand through the larger, ligand-binding C-terminal domain. The first identified member of the family, TetR from *Escherichia coli*, provides a typical mechanism of action of such a regulator in antibiotic (tetracycline) resistance. TetR binds to an intergenic region between its own gene *tetR* (autorepression) and the tetracycline efflux pump gene *tetA* as a pair of dimers. When present, tetracycline binds to TetR, changing its conformation so that it can no longer bind to DNA, thus activating transcription of *tetR* and *tetA*, which confers resistance to the antibotic (Kisker et al. 1995). TetR is an example of a regulator in a non-producing strain, since *E. coli* is not a tetracycline producer. Other TetR-like proteins may be involved in self-resistance and multidrug resistance (Cuthbertson and Nodwell 2013). TetR-like proteins, together with SARP

regulators, play a crucial role in controling coelimycin synthesis in *S. coelicolor* A3(2) (discussed later).

1.3.4. *Streptomyces* Antibiotic Regulatory Proteins (SARPs)

Streptomyces antibiotic regulatory proteins (SARPs) are only found in actinomycetes, mostly *Streptomyces*, and are considered to be the „lower-level" regulators (activators) that directly control transcription of secondary metabolite biosynthetic genes. They are subject to transcriptional regulation by „upper-level" pleiotropic regulators associated with multiple mechanisms of primary and secondary metabolism as i.e. σ factors, histidine kinases and TetR-like regulators (Bibb 2005). On N-terminus they contain a winged helix-turn-helix DNA-binding domain (DBD) resembling that of *Escherichia coli* OmpR protein C-terminus. It binds to the heptameric repeats with 4 bp spacers, usually localized between -35 and -10 promoter element, in the major groove of the double helix (Wietzorrek 1997). In small SARPs, DBD is only accompanied by the bacterial transcription activation domain (BTAD) that is responsible for RNA polymerase recruitment to the promoter and transcription initiation. Large SARPs may additionally contain a P-loop NTPase family domain of an unknown function and tetratricopeptide repeat motifs involved in protein-protein interactions (Alderwick et al. 2006, Lu et al. 2020). The DNA binding site of SARPs often overlaps the -35 promoter region, a sequence that is usually a target for repressors and hence it was speculated that SARP-mediated transcription may present a novel activation mechanism. SARPs are expected to bind to the opposite face of DNA than RNA polymerase that they recruit (Wietzorrek 1997; Tanaka et al. 2007). Only a handful of SARPs have been discovered in *S. coelicolor* A3(2).

Pathway-specific SARPs are encoded within each antibiotic BGC in *S. coelicolor* A3(2) - ActII-orf4 in *act* cluster, RedZ and RedD in *red* cluster, CdaR in *cda* cluster and CpkO and CpkN in *cpk* cluster. Examples from other *Streptomyces* species include DnrI (daunorubicin BGC) from *S. peuceticus*, CcaR (clavulanic acid-cephamycin BGC) from *S. clavuligerus* and MtmR (mithramycin BGC) from *S. argillaceus* (Liu et al. 2013). Characterized SARPs are activatory proteins and their gene mRNA levels are good predictors of the respective antibiotic synthesis levels (Takano et al. 1992; Gramajo et al. 2014). Despite being associated with their respective BGCs and being regarded as the „lower-level" regulators, evidence of SARPs' involvement in other BGC regulatory processes is accumulating (McLean et al. 2019). Distant genes on the chromosome of *S. coelicolor* A3(2) have been identified that show expression

profiles coordinated with biosynthetic gene clusters, namely *eca* (expression coordinated with *act*) and *ecr* (expression coordinated with *red*). What is more, the proposed ActII-orf4 binding sequence TCGAG was identified in *eca* promoters. In the same work, it was shown that RedZ and RedD SARPs downregulated, directly or indirectly, *act* cluster transcription while ActII-orf4 downregulated *red* cluster transcription (Huang et al. 2001). In a later publication, *cdaR*, *actII-orf4* and *redD* overexpression downregulated *cpk* cluster transcription (Huang et al. 2005). In the same work it was demonstrated that overexpression of *redZ* activated the transcription of a pleiotropic regulator *afsS* (discussed later in this section).

In addition to BGC-associated SARPs, there are also SARPs located in apparently random sites on the chromosome, and it is one of these, AfsR, that serves as the best characterized model of the family. AfsR was shown to be a pleiotropic regulator that constitutes a TCS together with more than one serine-threonine kinase: AfsK, AfsL and PkaG (Matsumoto et al. 1994; Sawai et al. 2004). At least for AfsK, the trigger for signal transduction seems to be S-adenosyl-L-methionine (Lee et al. 2007). By amino acid sequence, AfsR is only weakly similar to OmpR, however it bears close similarity to ActII-orf4, CdaR, RedD, SCO6633, SCO5433, SCO4116 and SCO2259 (Stutzman-Engwall et al. 1992; Sawai et al. 2004). What differentiates AfsR from other SARPs in general is that the protein contains not only a helix-turn-helix DBD sequence in the N-terminal region, but also an ATPase domain in the middle portion of the molecule and a tetratricopeptide repeat (TPR) domain at the C-terminus (Altschul et al. 1990; Tanaka et al. 2007). Phosphorylation of AfsR by AfsK enhances both its DNA binding affinity and ATPase activity, while TPR domain is dispensable for recruitment of RNA polymerase (Tanaka et al. 2007). Disruption of *afsR* gene caused significant reduction in ACT, RED and CDA synthesis under specific nutritional conditions (Floriano and Bibb 1996). Primary target for activation by AfsR is *afsS*, a pleiotropic modulator gene of antibiotic biosynthesis and nutritional stress response (Lian et al. 2008). It was shown that AfsR mutated in the ATPase domain is not able to activate transcription of *afsS*, despite being able to bind to its promoter (Lee et al. 2002). It was also demonstrated that AfsR competes for *afsS* promoter binding with another activator, PhoP – the phosphate starvation response modulator (Santos-beneit et al. 2011). Other AfsR DNA binding sites are in the promoters of *pstS* (phosphate transport system protein) and *phoR/P* where the protein is a transcriptional inhibitor – a hindrance for RNA polymerase and/or transcription-activator binding (Santos-beneit et al. 2009). These results are indicating that the competition for a promoter between different transcription factors may be a regulatory mechanism serving integration of multiple signals in

the cell. The mechanism by which AfsR affects biosynthetic gene clusters is, however, unknown. Putatively, it indirectly (i.e. through the action of AfsS and other regulators) affects respective cluster specific regulatory genes rather than controls any biosynthetic genes itself. Two monomers of AfsR cooperatively bind to the region of two 9 bp direct repeats localized in the *afsS* promoter and they are necessary for the recruitment of RNA polymerase, with which they form a complex on DNA. AfsR putatively forms a closed complex with RNA polymerase holoenzyme around the transcription start site and utilizes ATP/GTP to transform the complex into an open state, in which DNA is partially denatured and the spacing between -35 and -10 promoter elements is optimized (Lee et al. 2002).

1.4. Coelimycin

Kuczek first identified coelimycin type I polyketide synthase (PKS I) gene in 1997 by a DNA probe that hybridized to acyltransferase domain specific for malonyl- CoA (Kuczek et al. 1997). *cpk* cluster was annotated by Pawlik in 2007 (Pawlik et al. 2007) after the publication of *S. coelicolor* A3(2) genome sequence (Bentley et al. 2002). In 2010, the product of the cluster was observed to be a yellow pigment excreted from the cells into the medium (yCPK) (Gottelt et al. 2010; Pawlik et al. 2010). Its constituents were later identified as coelimycins P1 and P2 (Gomez-Escribano et al. 2012). Moreover, the colorless, antimicrobial compound abCPK was found to be associated with the mycelium (Gottelt et al. 2010). As a matter of fact, the observation of the yellow pigment production was made by Rudd and described in his PhD thesis in 1978. Rudd also mapped the genetic locus necessary for the pigment production (Rudd 1978). It was discovered that CPK production depends on the medium composition and requires high density of the inoculum (Gottelt et al. 2010; Pawlik et al. 2010), which can be attributed to regulation by quorum sensing and possibly by carbon catabolite repression. *cpk* gene expression starts at the early transition phase of growth and coincides with the switch from primary to secondary metabolism (Nieselt et al. 2010).

The term „coelimycin" (CPK) refers to several chemically distinct molecules: the yellow-pigmented coelimycins P1 and P2, and their precursor, the translucent abCPK, which exhibits antimicrobial activity (Gottelt et al. 2010). At the moment, there is no scientific consensus on whether abCPK or CPK P1/P2 is the natural „effector" molecule. Although methods of detection have been developed for CPK P1/P2 (Pawlik et al. 2010; Gomez-

Escribano et al. 2012), it is impossible to determine the growth conditions in which abCPK is the only coelimycin produced, therefore the ambiguity of the term „coelimycin".

1.4.1. **The *cpk* gene cluster**

First annotation of *cpk* cluster (Fig. 7) included only genes *SCO6269–SCO6288* (Pawlik et al. 2007). Later, the butanolide system genes *SCO6265–SCO6268* were discovered to be tightly associated with the cluster and included in it. *cpk* cluster spans over 58 kb and contains 24 genes that encode proteins of 5 functional groups: core biosynthetic (*cpkA, cpkB, cpkC, scoT*), post-polyketide tailoring (*scF, cpkD, cpkE, cpkG, cpkH, cpkI*), precursor supply (*cpkPα, cpkPβ, accA1, cpkK*), regulatory (*scbR, scbA, scbB, orfB, cpkO, scbR2, cpkN*) and export (*cpkF*) (Pawlik et al. 2007; Gomez-Escribano et al. 2012). The functions of *cpkJ* and *cpkL* are unknown. In coelimycin biosynthetic gene cluster, eight transcriptional units have been identified (*cpkPβ/cpkPα/accA1, scF, cpkA/cpkB/cpkC, cpkD/cpkE/cpkF/cpkG/cpkO/cpkH, cpkI, cpkJ/cpkK/cpkL, scbR2, scoT/cpkN*) (Chen et al. 2016) along with 10 promoter regions (*pscbR, pscbA, porfB, paccA1/pscF, pcpkA/pcpkD, pcpkO, pcpkI/ pcpkJ, pscbR2/pscoT, pcpkN*) (Takano et al. 2001; Takano et al. 2005; Gottelt et al. 2010; Li et al. 2015). Transcription start sites have been determined for the transcripts of *scbR, scbA, cpkA, cpkC, cpkD, cpkI, cpkO, cpkH,* and *scbR2* genes (Takano et al. 2001; Romero et al. 2014; Jeong et al. 2016).

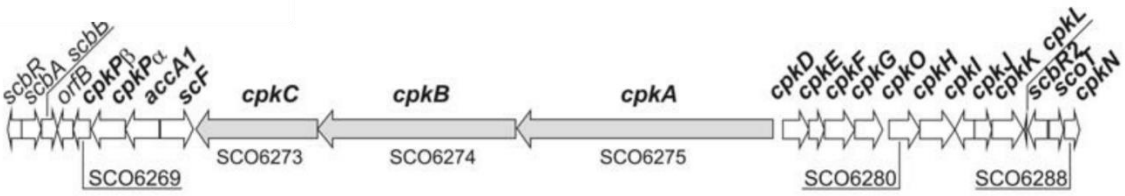

Figure 7. Coelimycin synthesis *cpk* cluster organization (Pawlik et al. 2007).

The main subunits of the modular polyketide synthase - CpkA, CpkB, and CpkC - assemble the core polyketide chain of coelimycin (Gomez-Escribano et al. 2012), while type II thioesterase ScoT removes non-reactive acyl residues blocking the synthase, maintaining PKS activity. ScoT was shown to be necessary for CPK production (Kotowska et al. 2014). The intermediate is released from PKS as a hydroxyaldehyde, transformed by post-PKS tailoring enzymes and presumably transported outside of the cell by membrane efflux protein CpkF. There it undergoes epoxidation to abCPK harbouring weak antibiotic activity that is attributed

to two reactive epoxide rings. The epoxides spontaneously react with N-acetylcysteine or glutamate in the medium to form the yellow-pigmented coelimycins P1 or P2, respectively (Gottelt et al. 2010; Gomez-Escribano et al. 2012). Other colorless coelimycins are probably formed when epoxide rings react with other substrates.

1.4.2. **Coelimycin synthesis pathway**

Polyketides are organic compounds with a carbon chain being a polymer of acyl residues. The synthesis of polyketides is similar to fatty acid biosynthesis, in which carboxylic acid units (derived from acyl-CoA) are successively added to the linear carbon chain, incrementing two carbon atoms at a time. The building (extender) units for polyketides may be acetate, propionate, butyrate, as well as more complex residues. The β-carbons of the extender units carry a keto group that may be reduced to hydroxyl, double bond or removed. It is the presence of these keto groups at multiple carbon atoms in the chain that the name „polyketide" is derived from. Several features contribute to the diversity of polyketides: i) the keto group fate, ii) the extender unit side chain composition, iii) the overall length of the polyketide chain and iv) the optional chirality at carbon atoms (Hopwood and Sherman 1990).

Polyketides are synthesized by a multi-enzymatic complexes called polyketide synthases. They are responsible for substrate selection and stereospecificity of the reduction (along with its degree) in every biosynthetic step and chain cyclization. They operate together with the so-called „post-polyketide tailoring enzymes" that introduce additional chain modifications such as hydroxylation, methylation or glycosylation. Three types of polyketide synthases have been distinguished, however it is necessary to note that examples of enzymes have been discovered that transcend the borders of this classification. Type I synthases produce long chain- and mostly linear polyketides such as amphotericin or coelimycin. Their inherent characteristic is that the enzymatic domains are joined covalently. They can operate in a modular or an iterative way. Type II synthases produce polycyclic aromatic polyketides (such as actinorhodin) and operate in an iterative way – each enzyme is active multiple times during the synthesis of one molecule of the product. These synthases often generate highly reactive and soluble intermediates. In type I and II synthases, the growing polyketide chain is covalently attached to the synthase. Type III synthases are often associated with chalcone synthesis by plants. They work in an iterative manner but, contrary to type I and II synthases, do not contain the acyl carrier protein (ACP, discussed in the next paragraph) (Pawlik and Kotowska 2005).

CPK synthase – a typical member of modular type I polyketide synthases, is a complex of three large proteins, functionally divided into the so-called „modules". Each module is responsible for one chain-extension step. Within the modules there is another level of organization – domains (Fig. 8). Each domain performs a specific step in condensation and modification of every added monomer. A module is comprised of three domains necessary to perform chain extension: i) an acyl carrier protein domain (ACP) containing 4'-phospho-pantetheine linker with a thiol, by which the growing chain is always covalently attached to the synthase as a thioester, ii) acyltransferase domain (AT) that selects the extender unit residue and attaches it to ACP and iii) ketosynthase domain (KS) that condensates the extender unit with the growing chain from the previous module in a Claisen condensation reaction, and a differing set of reducing domains: i) ketoreductase domain (KR) that reduces the keto group to an alcohol, also selecting which stereoisomer is produced, ii) dehydratase domain (DH) that eliminates water from the alcohol to make an alkene and iii) enoyl reductase (ER) that removes the double bond. All modules of CPK synthase contain only KR and DH domains, however DH in module 4 is non-functional. At the N terminus of the synthase there is the loading module and at the C terminus – thioester reductase (TR). TR is unusual, since in polyketide synthases the polyketide chain is typically released by a thioesterase domain. The loading module is responsible for choosing which carboxylic acid starter unit initiates the polymer. The TR domain releases the polyketide chain from the synthase by breakage of the thioester bond (Pawlik and Kotowska 2005; Gomez-Escribano et al. 2012).

The structure of coelimycin P1 and its synthesis pathway has been experimentally determined by Gomez-Escribano et al. (Gomez-Escribano et al. 2012) and is presented in the Fig. 8. From six molecules of malonyl-CoA (synthesised by the action of CpkPα, CpkPβ, AccA1 and CpkK) and using 5 molecules of NADPH (Pawlik et al. 2007; Gomez-Escribano et al. 2012), CPK synthase (encoded by *cpkABC*) produces the aldehyde **2**. Its 2,3-double bond undergoes isomerization (potentially by the action of α,β-hydrolase CpkE) to give **3**. Next, CpkG (a predicted pyridoxal-dependent amino transferase) catalyzes its reductive amination to give amine **4**. **4** is exported out of the cytoplasm by CpkF and its C-6/C-7 and C-8/C-9 double bonds undergo epoxidation (by flavin-dependent epoxidases/dehydrogenases ScF, CpkD or CpkH) to yield **5** or **6**, respectively. This double epoxidation gives rise to a bis-epoxide **7**, C-9 hydroxyl group of which is oxidized to give a ketone that cyclizes spontaneously or by the action of ScF, CpkD or CpkH to **8**. Dehydratation of **8** gives **9** that is most likely the antimicrobial product of *cpk* cluster. Coelimycin P1 results from the nucleophillic attack of

N-acetylcysteine (**10**) thiol- and carboxylic groups on C-6 and C-8 of **9**, giving **11** and **12**, respectively. **12** undergoes dehydratation and oxidation to give **13**, which tautomerizes to **1**. Coelimycin P2 is most likely a glutamate adduct of the double epoxide **8** (Gomez-Escribano et al. 2012). Addition of glutamate to the minimal bacteria culturing medium drives transformation of the bis-epoxide to form coelimycin P2, further supporting this notion (Kotowska et al. 2014).

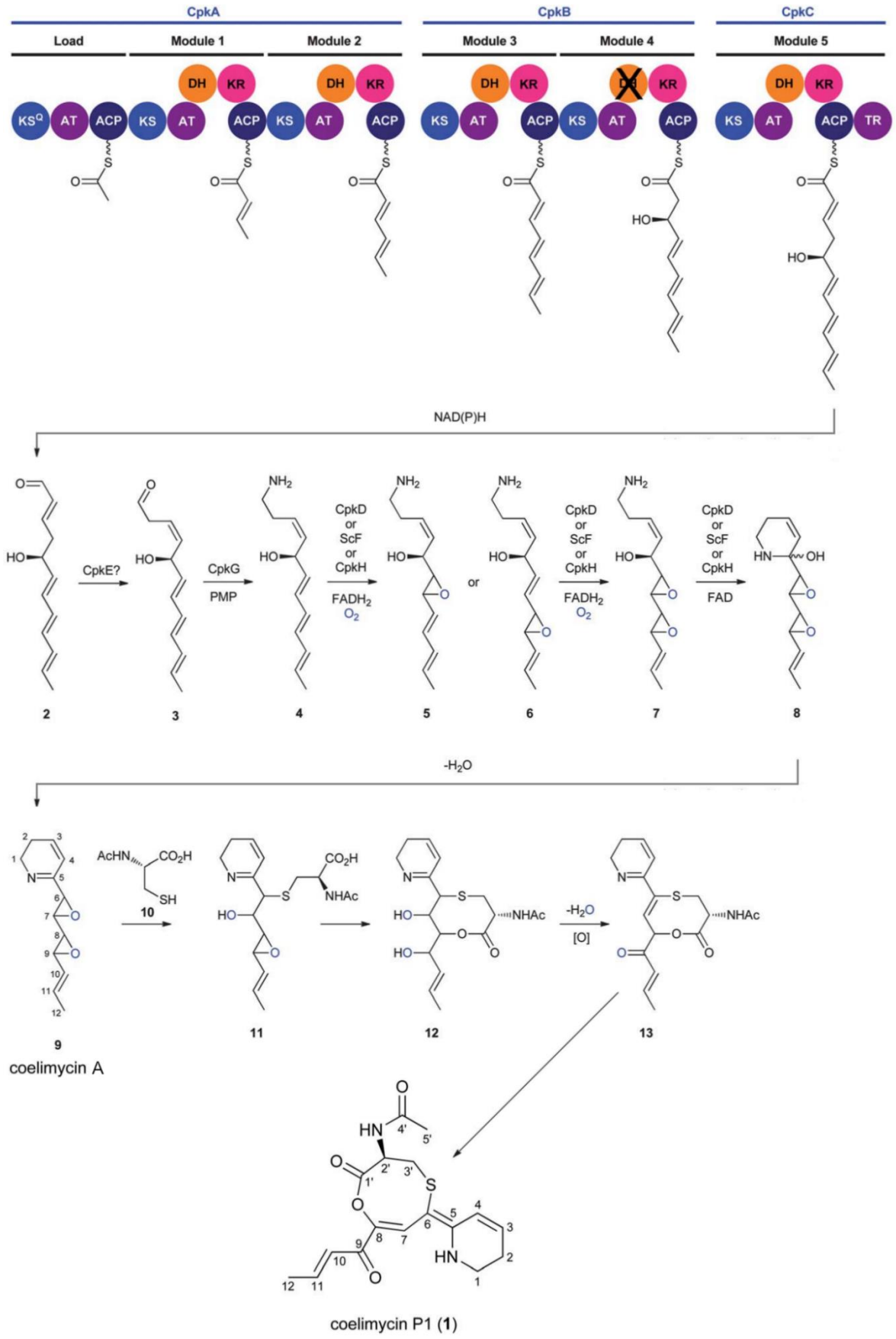

Figure 8. Coelimycin P1 synthesis pathway. Modified from (Gomez-Escribano et al. 2012). The crossed DH in module 4 is non-functional.

1.4.3. **Coelimycin synthesis regulation**

cpk cluster encodes 7 regulatory proteins. While some of them are well-characterized, the functions of others remain to be elucidated. ScbA is a γ-butyrolactone (GBL) synthase that participates in GBL synthesis together with ScbB (Hsiao et al. 2007; Sidda et al. 2016). ScbR is a γ-butyrolactone receptor, belonging to the TetR-like family of proteins. ScbR2, an ScbR homologue, does not bind GBLs but instead binds RED, ACT, and other antibiotics (Xu et al. 2010). ScbA, ScbB, ScbR and ScbR2 together constitute the so called butanolide system. OrfB is a histidine kinase, however its response regulator (target for phosphorylation) is unknown (Takano et al. 2005). CpkO and CpkN are SARP proteins, for which the DNA binding sites are not known. CpkO activates the *cpk* gene cluster as shown by qRT-PCR analysis of *cpkO* null mutant (Takano et al. 2005; Gottelt et al. 2010). CpkN protein has not been studied, however it is predicted to be an activator like other SARP proteins.

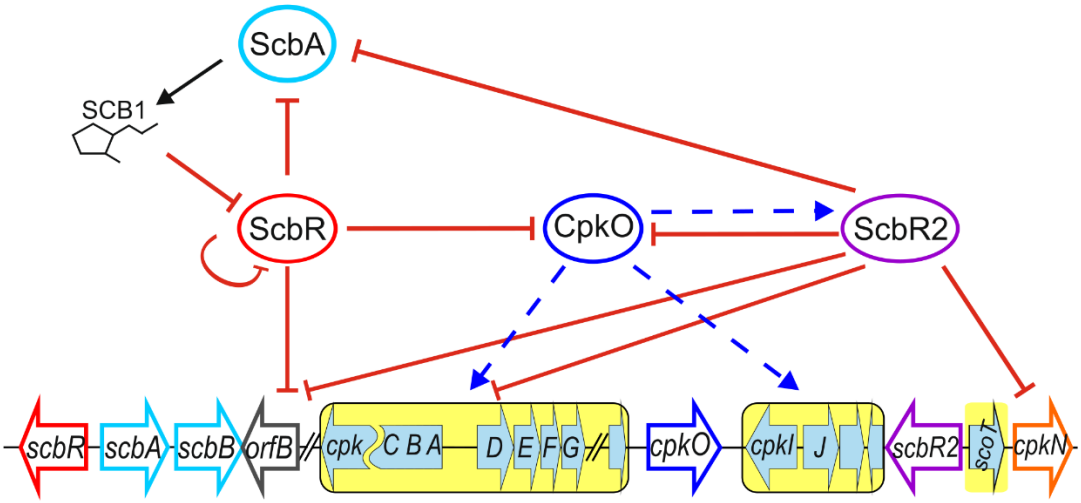

Figure 9. Coelimycin synthesis regulation mechanism (Bednarz et al. 2019).

In favorable conditions, the synthesis of the yellow coelimycin is observed 24 h earlier than the production of other colored metabolites (Gottelt et al. 2010; Pawlik et al. 2010). In the fermenter-grown *S. coelicolor* A3(2) culture, all *cpk* cluster genes showed a strong transient expression peak around 22–24 h. Afterwards, many of them remained at elevated levels (Nieselt et al. 2010). Transcription of regulatory genes *scbR*, *scbA*, *scbB*, and *cpkO* (22 h) peaked first to other *cpk* genes. Next peaked *orfB* (23 h time point) followed by the rest of the *cpk* cluster (including regulators *scbR2* and *cpkN* at 24 h). *scoT* transcription was increased 1 h after that of core biosynthetic genes (Nieselt et al. 2010). ScoT is a type II thioesterase needed to maintain the enzymatic activity of coelimycin polyketide synthase (Kotowska et al. 2014). After *cpk*

cluster activation, BGCs of undecylprodigiosin and actinorhodin were activated at 38 h and 43 h, respectively (Nieselt et al. 2010).

The sharp peak and decline of transcription of *cpk* cluster regulatory genes is controlled by the butanolide system. In the early growth phase of *S. coelicolor* A3(2), the synthesis of γ-butyrolactone SCB1 (by ScbA and ScbB proteins) and its receptor protein ScbR is on the minimal level. ScbR exists mainly as a DNA-protein complex, bound to *scbR*, *scbA*, *cpkO* and *orfB* promoter regions, inhibiting transcription (Takano et al. 2001; Takano et al. 2005; Li et al. 2015). The level of γ-butyrolactone SCB1 rises together with the number of dividing bacterial cells. After SCB1 concentration exceeds the threshold, its binding to ScbR results in ScbR dissociation from target promoter sequences and derepression of *scbR*, *scbA* and *cpkO* gene expression (Takano et al. 2005). CpkO activates (directly or indirectly) the transcription of *cpk* genes, including that of *scbR2*. ScbR2 binds to *scbA* promoter and blocks SCB1 biosynthesis. ScbR2 has been proposed to serve as a switch turning off coelimycin synthesis because it binds to and blocks *cpkO*, *cpkN*, and *orfB* promoters (Fig. 9)(Gottelt et al. 2010; Li et al. 2015).

2. THE AIM OF THIS WORK

Coelimycin is a polyketide secondary metabolite of an unknown function that is produced by *Streptomyces coelicolor* A3(2). The genes required for its synthesis are grouped together on the chromosome in the *cpk* cluster. The production of coelimycin is turned on in the transition growth phase, at the specific time (~24 h), only in very dense bacterial cultures (starting $OD_{600} > 0.1$). Therefore, the mechanism must be tightly controlled on the genetic level. Research of other teams on the topic focused mainly on the cluster regulation by the butanolide system proteins ScbR, ScbA, ScbR2.

Studies on the *cpk* cluster in the Laboratory of Molecular Biology of Microorganisms, Institute of Immunology and Experimental Therapy were initiated by Katarzyna Kuczek who discovered a polyketide synthase-homologous DNA sequence in the genome of *S. coelicolor* A3(2) (Kuczek et al. 1997). Further studies by Krzysztof Pawlik and Magdalena Kotowska resulted in the discovery of the yellow pigment coelimycin (CPK) – the product of the *cpk* cluster (Pawlik et al. 2010) along with elucidation of the function of *cpk* cluster-encoded type II thioesterase ScoT (Kotowska et al. 2014).

The aim of this work was to understand how the production of coelimycin is regulated by cluster-encoded CpkO and CpkN SARP transcription factors and update the present state of knowledge on coelimycin synthesis regulation, recently reviewed by the author (Bednarz et al. 2019). SARP proteins are mainly associated with regulation of biosynthetic gene clusters by which they are encoded but growing evidence suggests that they may also control other, distant BGCs. Therefore, the aim of this research was also to determine the influence of CpkO and CpkN on the secondary metabolism of *S. coelicolor* A3(2) as a whole.

In order to characterize CpkO and CpkN regulatory proteins, the following tasks were undertaken:

1) Analysis of CpkO and CpkN amino acid sequences
2) Generation of *cpkO* and *cpkN* deletion mutants and their derivatives.
3) Phenotypic characterization of *cpkO*, *cpkN* and derivative mutants in the context of coelimycin, actinorhodin and undecylprdigiosin synthesis.
4) Proteomic analysis of *cpkO* and *cpkN* mutant strains in order to elucidate the actions of CpkO and CpkN on coelimycin and other secondary metabolite synthesis pathways.
5) Expression profiling of chosen *cpk* cluster genes using a dense time-point reporter system measurements in *cpkO* and *cpkN* mutant strains.

3. MATERIALS AND METHODS

3.1. Reagents and commercial kits

Table 1. List of chemical reagents and commercial kits used in this work.

Reagent	Source
4 x Laemmli sample buffer	Bio-Rad, USA
6 x DNA loading dye	Thermo Scientific, USA
acetic acid (glacial)	POCH, Poland
acetonitrile (ACN)	VWR Chemicals, USA
30% acrylamide-bisacrylamide (37,5:1) solution	Roth, Germany
agar	Difco, USA
agarose	Maximus, Polska
ampicillin	Polfa, Poland
ammonium persulfate (APS)	Sigma, USA
Amylose resin	New England Biolabs, USA
apramycin	Sigma, USA
arabinose	Roth, Germany
boric acid	Roth, Germany
Bradford assay reagent (5 x concentrated)	Roth, Germany
casein hydrolysate (acidic)	Difco, USA
chloroform	POCH, Polska
dimethyl sulfoxide	Roth, Germany
dNTPs	Thermo Scientific, USA
DreamTaq polymerase	Thermo Scientific, USA
DTT (dithiothreitol)	Sigma, USA
EDTA	Roth, Germany
Gene Ruler 1 kb/1 kb Plus	Thermo Scientific, USA
glucose	POCH, Poland
Glutathione Sepharose	GE Healthcare, USA
glycerol	POCH, Poland
HCl	POCH, Poland
iodoacetamide	VWR Chemicals, USA
IPTG	Roth, Germany
lysyl endopeptidase LysC	Wako, Japan
magnesium chloride (hexahydrate)	POCH, Poland
mannitol	POCH, Poland
maltose	POCH, Poland
nalidixic acid	Polfa, Poland
NaOH	Roth, Germany
Ni-NTA HIS-Select Affinity Gel	Sigma, USA
PEG 4000	Sigma, USA
PEG 6000	Sigma, USA
PEG 20000	Thermo Scientific, USA

peptone	Difco, USA
Phusion polymerase	Thermo Scientific, USA
porcine trypsin	Promega, USA
potassium chloride	POCH, Poland
protease inhibitor cocktail	Sigma, USA
RapiGest	Waters, USA
RNase A	Roth, Germany
SDS (sodium dodecyl sulfate)	Sigma, USA
sodium chloride	POCH, Poland
soya flour	BioRaj, Poland
TEMED	Sigma, USA
tobacco etch virus (TEV) protease	New England Biolabs, USA
thiourea	Roth, Germany
trifluoroacetic acid	Thermo Scientific, USA
tris	Roth, Germany
tryptone	Difco, USA
Tryptone soya broth powder	Oxoid (Thermo Scientific), USA
tween-20	Sigma, USA
urea	VWR Chemicals, USA
X-gal	Roth, Germany
yeast extract	Difco, USA
Commercial kits	**Source**
GeneJET Gel Extraction Kit	Thermo Scientific, USA
GeneJET Plasmid Miniprep Kit	Thermo Scientific, USA
Genomic Mini AX *Streptomyces*	A&A Biotechnology, Poland
Protein concentration determination 2-D Quant Kit	GE Healthcare, USA
Steriflip 41µm nylon net NY41 RS	Sigma, USA

3.2. Microorganisms

Table 2. List of microorganisms used in this work.

Strain	Relevant genotype or description	Source or reference
Escherichia coli		
DH5α	F$^-$ *endA1 glnV44 thi-1 recA1 relA1 gyrA96 deoR nupG Φ80dlacZΔM15 Δ(lacZYA-argF)U169, hsdR17*(r_K^- m_K^+), λ^-	Promega
BL21(DE3)pLysS	F-, *ompT, hsdSB* (rB-, mB-), *gal, dcm* (DE3), pLysS (Cam^R)	Promega
BL21(DE3)pLysS/ pET28a-cpkO/cpkN$_{OE}$	6xHis-*cpkO/cpkN* overexpression *E. coli* strains	This work
BL21(DE3)pLysS/ pGEX-6P-1-cpkO/cpkN$_{OE}$	GST-*cpkO/cpkN* overexpression *E. coli* strains	This work

BL21(DE3)pLysS/pMAL-c2TEV-cpkO/cpkN$_{OE}$	MBP-*cpkO/cpkN* overexpression *E. coli* strains	This work
BL21(DE3)pLysS/pMAL-c2TEV-cpkO/cpkN$_{DBD}$	MBP-*cpkO/cpkN* DNA binding domain (DBD) overexpression *E. coli* strains	This work
ArcticExpress(DE3)	*E. coli* B F$^{–}$ *ompT hsdS*(r_{B}– m_{B}–) *dcm*$^{+}$Tet^{R} *gal*λ(DE3) *endA* Hte [*cpn10 cpn60* GentR]	Agilent Technologies
ArcticExpress(DE3)/cpkO/cpkN$_{OE}$	6xHis-*cpkO/cpkN* overexpression *E. coli* strain	This work
ArcticExpress(DE3)/ pGEX-6P-1-cpkO/cpkN$_{OE}$	GST-*cpkO/cpkN* overexpression *E. coli* strain	This work
ArcticExpress(DE3)/pMAL-c2TEV- cpkO/cpkN$_{OE}$	MBP-*cpkO/cpkN* overexpression *E. coli* strain	This work
BW25113/pIJ790	*lacI*$^{+}$*rrnB*$_{T14}$ Δ*lacZ*$_{WJ16}$ *hsdR*514 Δ*araBAD*$_{AH33}$ Δ*rhaBAD*$_{LD78}$ *rph-1* Δ*(araB–D)567* Δ*(rhaD–B)568* Δ*lacZ4787*(::*rrnB-3*) *hsdR514 rph-1* pIJ790 Recombineering strain harbouring arabinose-inducible RED genes on the plasmid pIJ790.	(Gust et al. 2003)
ET12567/pUZ8002	strain for conjugal transfer of DNA from *E. coli* to *Streptomyces* (*dam dcm hsdS* Cam^{R} Tet^{R} on the bacterial chromosome; *tra* Kan^{R} RP4 23 on pUZ8002)	(Kieser et al. 2000)
***Streptomyces coelicolor* A3(2)**		
M145	wild type strain, *S. coelicolor* A3(2) (SCP1^{-} SCP2^{-})	(Bentley et al. 2002)
P183	SCP1^{-} SCP2^{-} pCJW93-cpkO$_{OE}$	This work
P186	SCP1^{-} SCP2^{-} pCJW93-cpkN$_{OE}$	This work
Δ*cpkO* (P193)	SCP1^{-} SCP2^{-} *cpkO::aac3(IV)*	This work
Δ*cpkO-φ* (P194)	SCP1^{-} SCP2^{-} *cpkO::aac3(IV)* pIJ10257	This work
cpkO$_{CO}$ (P195)	SCP1^{-} SCP2^{-} *cpkO::aac3(IV)* pIJ10257-cpkO$_{CO}$	This work
Δ*cpkN* (P196)	SCP1^{-} SCP2^{-} *cpkN*::Tn5062	This work
Δ*cpkN-φ* (P197)	SCP1^{-} SCP2^{-} *cpkN*::Tn5062 pIJ10257	This work
cpkN$_{CO}$ (P198)	SCP1^{-} SCP2^{-} *cpkN*::Tn5062 pIJ10257-cpkN$_{CO}$	This work
Δ*cpkN-scoT$_{OE}$* (P199)	SCP1^{-} SCP2^{-} *cpkN*::Tn5062 pIJ10257-scoT$_{OE}$	This work
M145, Δ*cpkO* and Δ*cpkN*-derivatives for luciferase reporter assay	The strains listed above harbouring pFLUXH derivatives containing sequences of different *cpk* promoters: pcpkA, pcpkD, pcpkO, pscoT, pcpkN, pscF, pscbA, pscbR and pscbR2	M145 and Δ*cpkO*-derivatives - Marlena Korczyńska (master's degree thesis) Δ*cpkN*-derivatives – this work

3.3. Plasmids/constructs

Table 3. List of genetic constructs used in this work. * BamHI cloning site in inserts for cloning into pFLUXH plasmid, was derived from pTZ57R/T vector sequence.

Name	Relevant genotype or description	Source or reference
pTZ57R/T	T-vector from InstT/A Cloning kit for direct cloning of PCR products (Amp^R)	Thermo Scientific
pET28a	*E. coli* expression vector (Kan^R). Produces proteins with 6xHis tag at N-terminus.	(Novagen)
pET28a-$cpkO_{OE}$	6xHis-*cpkO* overexpression vector for *E. coli*.	This work
pET28a- $cpkN_{OE}$	6xHis-*cpkN* overexpression vector for *E. coli*.	This work
pMAL-c2TEV	*E. coli* expression vector pMAL-c2X derivative (Amp^R) in which a DNA sequence was added upstream of multiple cloning site encoding aminoacid sequence for TEV protease digestion. Produced proteins with MBP tag at N-terminus.	New England Biolabs, Magdalena Kotowska (unpublished)
pMAL-c2TEV-$cpkO_{OE}$	MBP-*cpkO* overexpression vector for *E. coli*.	This work
pMAL-c2TEV-$cpkN_{OE}$	MBP-*cpkN* overexpression vector for *E. coli*.	This work
pMAL-c2TEV-$cpkO_{DBD}$	MBP-$cpkO_{DBD}$ overexpression vector for *E. coli*	This work
pMAL-c2TEV-$cpkN_{DBD}$	MBP-$cpkN_{DBD}$ overexpression vector for *E. coli*.	This work
pGEX-6P-1	*E. coli* expression vector pMAL-c2X derivative (Amp^R). Produces proteins with GST tag at N-terminus.	GE Healthcare
pGEX-6P-1-$cpkO_{OE}$	GST-*cpkO* overexpression vector for *E. coli*.	This work
pGEX-6P-1-$cpkN_{OE}$	GST-*cpkN* overexpression vector for *E. coli*.	This work
pCJW93	*Streptomyces* expression vector ($Apra^R$) with thiostrepton-inducible *tipA* promoter.	(Wilkinson et al. 2002)
pCJW93- $cpkO_{OE}$	6xHis-*cpkO* overexpression vector for *Streptomyces*	This work
pCJW93- $cpkN_{OE}$	6xHis-*cpkO* overexpression vector for *Streptomyces*	This work
pIJ773	A plasmid for amplification of apramycin *aac(3)IV* resistance casette for gene deletion using PCR-targeting	(Gust et al. 2003)
St1G7	SuperCos1 cosmid carrying fragment of *S. coelicolor* A3(2) chromosome encompassing part of *cpk* gene cluster (bp 6905834 to 6947687)	http://www.strepdb.streptomyces.org.uk

St1G7-cpkO$_{DM}$	St1G7 cosmid, in which *cpkO* gene sequence was replaced (by means of PCR-targeting) with an apramycin resistance gene *aac(3)IV* amplified using primers CpkODM-Fw, CpkODM-Rv. Recombineering was performed by PCR-targeting in *E.coli* BW25113/pIJ790	This work
11B05.1.G04	Transposon-mutagenized cosmid in which *cpkN* sequence was disrupted with Tn5062 transposon containing *aac(3)IV* casette. Tn5062 is inserted in codon 114 of *cpkN*	(Fernandez-Martinez et al. 2011)
pIJ10257	ΦBT1 integrating overexpression plasmid containing strong constitutive promoter *ermEp**.	(Hong et al. 2005)
pIJ10257XermEp	pIJ10257 derivative lacking *ermEp** promoter. pIJ10257 was cut with KpnI, HindIII, its ends were blunted with polymerase T4 and autoligated.	This work
pIJ10257-cpkO$_{CO}$	pIJ10257XermEp containing sequence of *cpkO* gene with its native promoter (amplified with primers CpkO_c257_RED_Eco105I_F, CpkO_c257_RED_Eco105I_R) digested with Eco105I and cloned into PvuII site of the plasmid.	This work
pIJ10257-cpkN$_{CO}$ (pKH3prom)	pIJ10257 containing sequence of *cpkN* gene with its native promoter (amplified with primers CPKN_KHp, CPKN_KHR) cloned into KpnI, XhoI sites.	Magdalena Kotowska (unpublished)
pIJ10257-scoT$_{OE}$	pIJ10257 containing sequence of *scoT* gene (amplified with primers TE-K-Hind, TE-P-Nde) cloned under the strong constitutive promoter *ermEp** - sites NdeI, HindIII	This work
pFLUXH	ΦBT1 integrating reporter plasmid with a promoterless luciferase operon *luxCDAEB* and hygromycin resistance cassette	(Craney et al. 2007, Szafran et al. 2016)
pFLUXH-pcpkA pFLUXH-pcpkD	pFLUXH-derivatives containing promoter sequence pcpkA/pcpkD (amplified with primers p6275_Nde, p6276_Nde) cloned into NdeI site and selected for desired insert direction using luxout primer.	Marlena Korczyńska/ Nikola Nowrot (master's thesis)
pFLUXH-pcpkO	pFLUXH-derivative containing *cpkO* promoter sequence pcpkO (amplified with primers p6280_Nde, KSO-FW) cloned into NdeI, BamHI* sites.	
pFLUXH-pcpkN	pFLUXH-derivative containing *cpkN* promoter sequence pcpkN (amplified with primers p6288_Nde, CPKN_KHp) cloned into NdeI, BamHI* sites.	
pFLUXH-pscF	pFLUXH-derivative containing *scF* promoter sequence pscF (amplified with primers accA1-Rv, p6272_Nde) cloned into NdeI, BamHI* sites.	

pFLUXH-pscoT pFLUXH-pscbR2	pFLUXH-derivatives containing promoter sequence pscoT/pscbR2 (amplified with primers p6287_Nde, p6286_Nde) cloned into NdeI site and selected for desired insert direction using luxout primer.	
pFLUXH-pscbA	pFLUXH-derivative containing *scbA* promoter sequence pscbA (amplified with primers scbA_lux, p6266_Nde) cloned into NdeI, BamHI* sites.	
pFLUXH-pscbR	pFLUXH-derivative containing *scbR* promoter sequence pscbR (amplified with primers SCBA-FW, p6265_Nde) cloned into NdeI, BamHI* sites.	

3.4. Oligonucleotides

Table 4. List of oligonucleotides used in this work. Restriction sites are in bold.

Name	Sequence 5'-3'	Restriction sites	Application/amplified fragment
cpkN_Val_Nde	TTTTTT**GGATCCCATATG**GTGCGGTTCAATCTC ATGGGCC	BamHI, NdeI	pET28a-cpkN$_{OE}$ pGEX-6P-1-cpkN$_{OE}$ pMAL-c2TEV-cpkN$_{OE}$
CPKN_KHR	**CTCGAGAAGCTTCTAGA**CCGGCCGGGTCGAG ATCG	XhoI, HindIII, XbaI	pIJ10257-cpkN$_{CO}$ pET28a-cpkN$_{OE}$ pGEX-6P-1-cpkN$_{OE}$ pMAL-c2TEV-cpkN$_{OE}$
CpkOEXFW	**GGATCCCATATG**CGCTTTCGGATGCTC	BamHI, NdeI	pMAL-c2TEV-cpkO$_{OE}$ pET28a-cpkO$_{OE}$ pGEX-6P-1- cpkO$_{OE}$
KSORew	TTTTTT**AAGCTT**GAGCAGCGGGGGTCAGAT	HindIII	
CpkO_c257_RED_Eco105I_F	GATAATTTATCACCGCAGATGGTTACCTCGCCT CTGACC**TACGTA**CCGTCCCGGCGGTCGCCGGA	Eco105I	pIJ10257-cpkO$_{CO}$
CpkO_c257_RED_Eco105I_R	ACTCTAGTTAATTAATCACTCGAGATCTCATAT GGGGCC**TACGTA**TCAGATCGCCCCGCCTCCG	Eco105I	
CpkN_BamNde_F	**GGATCCCATATG**GGCCCGTTCGAGATCG	BamHI, NdeI	pMAL-c2TEV-cpkN$_{DBD}$
CpkN_XhoSTOPHind_R	**AAGCTT**TCA**CTCGAG**CTCCTCGTCGGCGACC	XhoI, HindIII	
CpkO_BamNde_F	**GGATCCCATATG**CGCTTTCGGATGCTC	BamHI, NdeI	pMAL-c2TEV-cpkO$_{DBD}$
CpkO_SalSTOPHind_R	**AAGCTT**TCA**GTCGAC**CCGGATCATGTA	SalI, HindIII	
TE-K-Hind	TTTTTTT**AAGCTT**GTCGTACGTACACGGA	HindIII	pIJ10257-scoT$_{OE}$
TE-P-Nde	TTTTTTTTT**CATATG**GGAAGTGACTGGTT	NdeI	
CpkODM-Fw	TTTCGGATGCTCGGTCCACTCGAGGTGTTGTCC GGCGAGATTCCGGGGATCCGTCGACC	-	St1G7-cpkO$_{DM}$
CpkODM-Rv	GACGGCGGACCGCGGGCGGGCTCGGAGCAGCG GGGGTCATGTAGGCTGGAGCTGCTTC	-	
p6275_Nde	**CATATG**CGGCTGCCCTTTCCTGGCTGT	NdeI	pFLUXH-pcpkA
p6276_Nde	**CATATG**GATTTACTCTCCTTCGACAAG	NdeI	pFLUXH-pcpkD
p6280_Nde	**CATATG**TCCCCCAGTCCTGCACGCTGT	NdeI	pFLUXH-pcpkO
KSO-FW	ATCATCCGGGACACCGACGGA	-	pFLUXH-pcpkO, screening for ΔcpkO recombinant
kasFR	CGACGGCACCGTGTCTGATGA	-	screening for *cpkO* deletion
pcpkNup1C	CGGTGAGTCCCGCGTTC	-	screening for *cpkN* disruption
CPKN_ZARV	AGCGGGTGAGCAATCGAC	-	
p6288_Nde	**CATATG**CTCACACTCCTGTCCCGGCAC	NdeI	pFLUXH-pcpkN
CPKN_KHp	**AGATCTGGTACC**GTGGCGCGAGCACACCAC	BglII, KpnI	pIJ10257-cpkN$_{CO}$ pFLUXH-pcpkN
accA1-Rv	GGCGATGAGCACCTTGCGCA	-	pFLUXH-pscF
p6272_Nde	**CATATG**CGAACCTCCGTGAGAACAAGA	NdeI	
p6287_Nde	**CATATG**CTTTTCCCCTTACCGTTCGAC	NdeI	pFLUXH-pscoT pFLUXH-pscbR2
p6286_Nde	**CATATG**GTGCTCCGTGGTCGCGATCGT	NdeI	
scbA_Lux	CAAGCGGTGACAGAACAACA	-	pFLUXH-pscbA
p6266_Nde	**CATATG**TCCCCCCCAGGAATCATGTGA	NdeI	
SCBA-FW	TATCCAGCTGACCGGGAACGC	-	pFLUXH-pscbR
p6265_Nde	**CATATG**TGCCTCCTTGTTCATGTCTCC	NdeI	
luxout	GCTCTCGGGGAAGATCTCGAC	-	verification of insert orientation in pFLUXH

3.5. Buffers and solutions (1 L formulations in ddH_2O – double-distilled water)

0.5 x TBE

Tris	5.4 g
yeast extract	2.75 g
EDTA 0.5 M	2 ml
pH 8.3	

DUTT

Tris	12.1 g
urea	480.5 g
thiourea	152,24 g
DTT	0.77 g
pH 8	

P1

Tris	6.06 g
EDTA 0.5 M	20 ml
ddH_2O	adjust to 1000 ml
HCl	adjust pH to 8
RNase A	100 mg
pH 8	

P2

NaOH	8.09 g
SDS	10 g
ddH_2O	adjust to 1000 ml

P3

potassium acetate	294.5 g
glacial acetic acid	adjust pH to 5.5

TSS

LB medium	850 ml
PEG (polyethylene glycol) 20000	100 g
After autoclaving:	
2 M $MgCl_2$ (sterile)	25 ml
DMSO (dimethyl sulfoxide)	50 ml

Lysis buffer

Tris	6.057 g
NaCl	17.532 g
DTT	0.15 g
imidazole (only 6xHis-tagged proteins)	1.36 g
pH 8	

MBP-Elution buffer

Tris	6.057 g
NaCl	17.532 g
DTT	0.15 g
maltose	3.42 g
pH 8	

GST-Elution buffer

Tris	6.057 g
NaCl	17.532 g
DTT	0.15 g
reduced glutathione	3.07 g
pH 8	

6xHis-Elution buffer

Tris	6.057 g
NaCl	17.532 g
DTT	0.15 g
imidazole	3.07 g/6.8 g/10.2 g/13.6 g/17 g
(for 50/100/150/200/250 mM final conc.)	
pH 8	

Denaturing S buffer

Tris	6.057 g
DTT	0.15 g
urea	480.5 g
pH 8	

Denaturing W buffer

Tris	6.057 g
DTT	0.15 g
urea	480.5 g
pH 6.3	

Denaturing E buffer

Tris	6.057 g
DTT	0.15 g
urea	480.5 g
pH 4.5	

SDS-PAGE running buffer

Tris	3 g
glycine	14.4 g
SDS	1 g
pH 8.3	

Renaturing O buffer

Tris	6.057 g
NaCl	17.532 g
DTT	0.15 g
L-glutamic acid	7.35 g
L-arginine	8,71 g
pH 8	

Renaturing N buffer

Tris	6.057 g
NaCl	17.532 g
DTT	0.15 g
L-arginine	87.1 g
pH 8	

3.6. Culturing media (1 L formulations in ddH_2O)

Lysogeny broth (LB)

tryptone	10 g
yeast extract	5 g
NaCl	10 g
pH 7.5	

Super optimal broth (SOB)

tryptone	20 g
yeast extract	5 g
NaCl	0.5 g
KCl	0.186 g
ddH_2O	adjust to 1000 ml
pH 7	
After autoclaving:	
$MgCl_2$ 2 M (sterile)	5 ml

Soya flour-mannitol (SFM)*

soya flour	20 g
mannitol	20 g
tap water	1000 ml

Super optimal broth with catabolite repression (SOC)

SOB medium (sterile)	1000 ml
glucose 1 M (sterile)	20 ml

2 x YT

tryptone	16 g
yeast extract	10 g
NaCl	5 g

79 medium without glucose (79 NG)

peptone	10 g
casein hydrolysate (acid)	2 g
yeast extract	2 g
NaCl	6 g
pH 7.2	

Tryptone soya broth – polyethylene glycol (TSB-PEG)

TSB powder (Oxoid)	30 g
PEG 6000	50 g

For preparation of solid media, agar was added to the respective mixtures to the final concentration of 2% before autoclaving. *SFM is used only as a solid medium.

3.7. DNA manipulation techniques

3.7.1. Agarose gel electrophoresis

DNA was separated on 0.5 x TBE (tris-borate-EDTA) gels with 1% or 0.5% content of agarose for fragments < 2000 bp and > 2000 bp, respectively. Before a run, the DNA samples were mixed with an appropriate volume of 6 X LD (loading dye) solution to the final concentration of 1 X. During a separation run, the gel was immersed in 0.5 x TBE buffer and the voltage of 10 V/cm was applied for 20 min. DNA was visualized in GelDoc XR+ (BioRad).

3.7.2. Spectrophotometric DNA concentration measurement

2 µl of a sample was used in order to measure the concentration and purity of DNA in the NanoDrop Lite Spectrophotometer (Thermo Scientific). Absorbance was measured at 230, 260 and 280 nm wavelengths. DNA concentration was calculated based on A260 (for a 50 µg/ml DNA solution A260 = 1). The purity was assayed based on A260/A280 and A260/A230 ratios. A sample was considered free from residual protein when A260/A280 ≥ 1.8.

3.7.3. Cosmid DNA minipreparation by phenol:chloroform extraction

DNA phenol:chloroform extraction was used for cosmid DNA preparation. 1 ml of bacterial culture was centrifuged for 2 min. at 7000 x g, the supernatant was discarded and the pellet was resuspended in 100 µl of solution P1. Immediately, 200 µl of solution P2 was added and mixed by inverting the tube several times. Then, 150 µl of solution P3 was added, followed by inverting the tube several times and centrifuging the sample at 16000 x g for 5 min. The

pellet was discarded and 400 µl of phenol:chloroform:isoamyl alcohol (25:24:1) mixture was added to the supernatant, vortexed for 2 min. and centrifuged at 16000 x g for 5 min. The upper phase was transferred to a new tube and 600 µl of isopropanol was added. The sample was mixed by inverting several times, left on ice for 10 min. and centrifuged at 16000 x g for 5 min. The DNA pellet was washed with 200 µl of 70% ethanol followed by centrifugation at 16000 x g for 5 min. The supernatant was discarded and the pellet was dried at room temperature. Finally, the pellet was resuspended in 50 µl of ddH2O.

3.7.4. **DNA extraction and purification from agarose gel**

After agarose gel electrophoresis the gel slab containing DNA of the respective length was cut out using a scalpel. DNA extraction from the gel and its purification was performed using GeneJET Gel Extraction Kit (Thermo Scientific) according to the producer's instructions.

3.7.5. **DNA purification after enzymatic reactions**

A uniform DNA sample (for example after specific amplification by PCR or after restriction digest) was purified from the reaction constituents using GeneJET Gel Extraction Kit (Thermo Scientific) according to the manufacturer's instructions.

3.7.6. **Plasmid DNA minipreparation**

Small-scale plasmid DNA preparation was performed from 2 ml of liquid *E. coli* cultures using GeneJET Plasmid Miniprep Kit (Thermo Scientific) according to the manufacturer's instructions.

3.7.7. ***S. coelicolor* A3(2) genomic DNA preparation**

The genomic DNA of the wild-type and the mutant *S. coelicolor* A3(2) strains was isolated using the Genomic Mini AX *Streptomyces* kit (A&A Biotechnology).

3.7.8. **Blunting of 5' or 3' DNA ends**

Blunting of DNA ends was performed with T4 DNA polymerase (Thermo Scientific) by fill-in of 5'-overhangs or/and removal of 3' overhangs. The reaction was set up as follows:

Component	**Quantity (for 20 µl reaction)**
5 x reaction buffer	4 µl
Linear DNA	1 µg
dNTP Mix (10 mM each)	0.2 µl
H_2O	Adjust to 20 µl
T4 DNA polymerase (1 U/µl)	0.2 µl

The sample was incubated at 11°C for 20 min. and the reaction was stopped by heating at 75°C for 10 min. Afterwards, the DNA was purified from the reaction with GeneJET Gel Extraction Kit (Thermo Scientific)

3.7.9. **Dephosphorylation of 5' DNA ends**

Whenever a vector was cut with an enzyme/enzymes generating compatible ends, the 5' ends of the digested DNA were dephosphorylated with SAP (shrimp alkaline phosphatase, Thermo Scientific) to prevent vector autoligation. The 20 µl reaction was set up as follows:

Component	**Quantity (for 20 µl reaction)**
DNA	≤ 1 pmol of 5'-termini
10 x Buffer SAP	2 µl
H_2O	Adjust to 20 µl
SAP (1 U/µl)	2 µl

The sample was incubated at 37°C for 60 min. and then the enzyme was inactivated at 65°C for 15 min. Dephosphorylated DNA was used directly for the next cloning steps.

3.7.10. **Phosphorylation of 5' DNA ends**

In order to ligate an insert into the dephosphorylated vector, the 5' ends of the insert DNA were phosphorylated using T4 PNK (T4 polynucleotide kinase, Thermo Scientific). The 40 µl reaction was set up as follows:

Component	**Quantity (for 40 µl reaction)**
DNA	1-40 pmol of 5'-termini
10 x Buffer A PNK	4 µl
10 mM ATP	4 µl
H_2O	Adjust to 40 µl
T4 PNK	4 U

The sample was incubated at 37°C for 20 min. and then the enzyme was inactivated at 75°C for 10 min. Phosphorylated DNA was used directly for the next cloning steps.

3.7.11. **Restriction digest**

In order to generate the desired DNA ends, respective restriction enzymes (with the appropriate reaction buffers) were used according to the manufacturer's instructions (Thermo Scientific). By definition, 1 U of a given restriction enzyme digests 1 µg of DNA in 1 hour. However, the enzymes were used in excess and for a prolonged time in order to ensure complete digestion. The 20 µl reaction was set up as follows:

Component	**Quantity (for 20 µl reaction)**
DNA	~1 µg for preparative reaction ~500 ng for diagnostic reaction
10 x appropriate restriction buffer	To 1X or 2X concentrated, enzyme-dependent
H_2O	Adjust to 20 µl
Restriction enzyme	5 U for preparative 2.5 U for diagnostic

The sample was incubated at the optimal temperature for 2 h. Before resolving a sample on an agarose gel, the enzymes were inactivated according to the manufacturer's instructions in order to prevent protein-DNA interactions.

3.7.12. **Ligation**

Depending on the type of DNA ends (blunt or sticky) to be joined, the 20 µl ligation reactions were set up with Thermo Scientific T4 ligase as follows:

Sticky-end ligation

Component	**Quantity (for 20 µl reaction)**
Vector DNA	25 ng
Insert DNA	3:1 molar ratio over vector DNA
10 x T4 ligase buffer	2 µl
H_2O	Adjust to 20 µl
T4 ligase	1 U

Blunt-end ligation

Component	**Quantity (for 20 µl reaction)**
Vector DNA	25 ng
Insert DNA	3:1 molar ratio over vector DNA
50 % PEG 4000	2 µl
10 x T4 ligase buffer	2 µl
H_2O	Adjust to 20 µl
T4 ligase	5 U

Sticky-end ligation reactions were incubated at 22°C for 10 min. while blunt-end ligation reactions were incubated at the same temperature for 1 h. The whole reactions were directly used for competent *E. coli* cell transformation.

3.7.13. **PCR (polymerase chain reaction)**

Polymerase chain reaction was performed with Phusion and DreamTaq (Thermo Scientific) polymerases for preparative and diagnostic purposes, respectively. 50 µl reactions were set up for DNA preparations while 10 µl reactions were set up for diagnostics. Optimal primer annealing temperature was experimentally chosen for each primer pair. 1 – 10 ng of plasmid DNA or ~50 ng of genomic DNA was added as a template DNA to 10 µl reactions and these amounts were not increased when scaling the volume up. For colony PCR, the minimal visible amount of cell biomass was added to the reaction tube as a DNA template. The reaction constituents and reaction conditions for both polymerases are listed below.

Phusion polymerase

Component	Quantity (10 µl reaction)
5 x HF/GC Buffer	2 µl
dNTPs (10 mM each)	0.2 µl
Primer 1 (10 mM)	0.5 µl
Primer 2 (10 mM)	0.5 µl
DMSO (100%)	0.5 µl
H_2O	X µl
Phusion (2 U/µl)	0.2 µl

Cycle step	Temp.	Time
Initial denaturation	98ºC	30 s
Denaturation	98 ºC	10 s
Annealing	50 - 70 ºC	30 s
Elongation	72 ºC	30 s/1 kb
GO TO STEP 2	-	34X
Final elongation	72 ºC	5 min.
Denaturation	98 ºC	10 s

DreamTaq polymerase

Component	Quantity (10 µl reaction)
10 x DreamTaq Buffer	1 µl
dNTPs (10 mM each)	0.2 µl
Primer 1 (10 mM)	0.25 µl
Primer 2 (10 mM)	0.25 µl
DMSO (100%)	0.5 µl
H_2O	X µl
DreamTaq (5 U/µl)	0.2 µl

Cycle step	Temp.	Time
Initial denaturation	95ºC	5 min.
Denaturation	95 ºC	30 s
Annealing	50 - 70 ºC	30 s
Elongation	72 ºC	30 s/1 kb (product ≤ 2 kb) + 1 min./1 kb for every additional kb
GO TO STEP 2	-	24X
Final elongation	72 ºC	5 min.

For DNA preparation, PCR products were purified directly from the mixtures (when the product was specific) or after resolution on an agarose gel (when PCR specificity was low) by GeneJET Gel Extraction Kit (Thermo Scientific).

3.8. Microorganisms manipulation techniques

3.8.1. *Escherichia coli* culturing

For DNA-preparation techniques, *E. coli* were grown as liquid cultures in 4 ml of LB medium in glass cell culture tubes, or as single colonies after streaking on Petri dishes with 20 ml solid LB medium. If not stated otherwise, the bacteria were incubated in 37^{O}C in a rotary shaker (180 rpm) or an incubator, respectively, for ~20 h. Antibiotics were used as selective genetic markers in the following final concentrations:

ampicillin – 100 μg/ml
apramycin – 50 μg/ml
chloramphenicol – 25 μg/ml
gentamycin – 20 μg/ml
hygromycin B – 200 μg/ml
kanamycin – 30 μg/ml

For blue-white selection, 40 μl of 2 % X-gal (5-bromo-4-chloro-3-indolyl-β-D-galactopyranoside) and 10 μl of 1 M IPTG (isopropyl β-d-1-thiogalactopyranoside) were additionally included in 20 ml of the solid LB medium, to the final concentrations of 0.5 mM and 0.004%, respectively.

For preparation of glycerol stocks, 1 ml of *E. coli* culture was mixed with 500 μl of 60% glycerol and stored in -70°C.

3.8.2. **Preparation of *S. coelicolor* A3(2) spore glycerol stocks**

Crude spore material, scraped off of the top of solid SFM-grown *S. coelicolor* A3(2) colony/biomass with an inoculation loop, was suspended in 1 ml of ddH_2O. Next, 200 μl aliquots of the suspension were streaked over 5 Petri dishes with 20 ml of solid SFM medium supplemented with the proper selective antibiotics. After 5 day incubation, 5 ml of ddH_2O was added on the surface of biomass of each plate. Then, spores were scraped off of the surface of the biomass into ddH_2O with a swab stick and the solution was collected and filtered through a SteriFlip filter (40 μm pore diameter). Spore chains were disrupted by vortexing the solution for 1 min. and then the spores were centrifuged for 10 min. in 4000 x g. The pellet was resuspended in 20 ml ddH_2O, centrifuged again for 10 min. in 4000 x g and the supernatant was discarded. The pellet was suspended in 2-4 ml of 20% glycerol, depending on the pellet size, and stored in -70°C.

3.8.3. **Intergenic conjugation between *E. coli* and *S. coelicolor* A3(2)**

The respective genetic constructs were introduced to the non-methylating *E. coli* strain ET12567/pUZ8002 by heat-shock transformation. Proper clones were selected on plates with solid LB medium, kanamycin (30 μg/ml), chloramphenicol (25 μg/ml) and the suitable selection antibiotic for the construct. In a glass vial, 4 ml of liquid LB medium (supplemented with suitable antibiotics) was inoculated with a single bacterial colony and incubated overnight at 37°C (shaking 180 rpm). The next day, 10 ml of LB medium with antibiotics was inoculated

with 200 µl of the overnight culture and incubated in 37ºC (shaking 180 rpm) until the OD_{600} reached 0.4. The bacteria were collected by centrifugation (4ºC, 4000 x g, 10 min.), washed twice with 10 ml LB medium, resuspended in 500 µl LB and left on ice. ~10^8 of *S. coelicolor* A3(2) spores were added to 500 µl of 2xYT medium and incubated for 10 min. in 50ºC in order to induce germination. The volume of spores to be added was calculated based on the observation that 1 ml of 0.1 OD_{600} spore suspension contains approx. 2*10^7 colony forming units – cfu. After the suspension has cooled down for at least 10 min., it was mixed with 500 µl of previously prepared *E. coli* cell suspension and incubated at room-temperature for 5 min. Then, 200 µl and the rest of the mixture (after centrifugation at 4ºC, 4000 x g for 2 min and discarding most of the supernatant) was streaked on a Petri dish containing 20 ml of SFM with 10 mM $MgCl_2$. The plates were incubated at 30ºC for 20 h and then flooded with 1 ml of ddH_2O supplemented with 20 µl of 25 mg/ml nalidixic acid to kill *E. coli* and the selective antibiotic marker for the construct. After the medium dried, the plates were incubated at 30ºC for the next 4 days.

3.8.4. **Construction of *S. coelicolor* A3(2) deletion mutants and their derivatives**

St1G7-cpkO$_{DM}$ construct was generated by PCR targeting-mediated replacement (Gust et al. 2003) of *cpkO* gene sequence in St1G7 cosmid with PCR-amplified apramycin resistance casette *aac(3)IV* (primers: CpkODM-Fw + CpkODM-Rv, product: 1447 bp, template DNA: pIJ773, see chapter 3.8.8). Cosmid 11B05.G04, in which *cpkN* gene sequence was disrupted with Tn5062 transposon (also containing *aac(3)IV* casette), was obtained thanks to P.J. Dyson (Fernandez-Martinez et al. 2011). Complementation construct pIJ10257-cpkN$_{CO}$ was obtained as a courtesy of Magdalena Kotowska (Institute of Immunology and Experimental Therapy) and was generated by cloning *cpkN* promoter-gene sequence (primers: CPKN_KHp + CPKN_KHR, PCR product: 1234 bp, template: M145 gDNA) digested with KpnI and HindIII, into KpnI-HindIII sites of pIJ10257 (Hong et al. 2005) (Appendix Fig. 1). Complementation construct pIJ10257-cpkO$_{CO}$ was generated by cloning *cpkO* promoter-gene sequence (primers: CpkO_c257_RED_Eco105I_F + CpkO_c257_RED_Eco105I_R, PCR product: 2028 bp, template: St1G7 cosmid) digested with Eco105I, into PvuII site of pIJ10257XermEp plasmid. *scoT* overexpression construct pIJ10257-scoT$_{OE}$ was generated by cloning *scoT* gene sequence (primers: TE-K-Hind + TE-P-Nde, PCR product: 932 bp, template: St1G7 cosmid) digested with NdeI and HindIII, into NdeI-HindIII sites of pIJ10257. The pFLUXH-based constructs for luciferase reporter assay were obtained as a courtesy of Marlena Korczyńska and Nikola

Nowrot (Institute of Immunology and Experimental Therapy). The information on the design of all of the constructs is in Table 3. The constructs were introduced into the genomes of the respective *S. coelicolor* A3(2) strains by *E. coli* ET12567/pUZ8002-mediated conjugation. In the case of deletion mutants, the exconjugants that underwent a double crossing-over event were selected for growth in the presence of apramycin and loss of resistance to kanamycin on SFM agar medium. The deletion and disruption, respectively, were confirmed by PCR on genomic DNA of the mutants with primers KSO-FW + kasFR (Δ*cpkO* = 2077 bp, WT = 2292 bp) and pcpkNup1C + CPKN_ZARV (Δ*cpkN* = 4448 bp, WT = 1006 bp). All of the derivative mutants (complementation, control and reporter strains) were selected for growth in the presence of hygromycin (50 μg/ml) on SFM-agar.

3.8.5. **Construction of CpkO and CpkN protein-overproducing strains**

Constructs pET28a-cpkN$_{OE}$ and pET28a-cpkO$_{OE}$ were generated by cloning the *cpkN* and *cpkO* genes (amplified with primers cpkN_VAL_Nde + CPKN_KHR and CpkOEXFW + KSORew, respectively, template: M145 gDNA, products: 899 bp and 1665 bp, respectively) into NdeI-HindIII sites of plasmid pET28a (Appendix Fig. 2). The same amplified fragments were cloned, respectively, into pGEX-6P-1 (Appendix Fig. 3) BamHI-XhoI sites (to generate construct pGEX-6P-1-cpkN$_{OE}$) and BamHI-SmaI sites (to generate construct pGEX-6P-1-cpkO$_{OE}$). Morover, the *cpkN* fragment was also cloned into BamHI-HindIII sites of pMAL-c2TEV (Appendix Fig. 4) to generate construct pMAL-c2TEV-cpkN$_{OE}$. To generate construct pMAL-c2TEV-cpkO$_{OE}$, *cpkO* was amplified with primers CpkOEXFW + KSORew (template: M145 gDNA, product: 1665 bp) and introduced into BamHI-HindIII sites of pMAL-c2TEV. To generate constructs pMAL-c2TEV-cpkN$_{DBD}$ and pMAL-c2TEV-cpkO$_{DBD,}$ *cpkN* was amplified using primers CpkN_BamNde_F + CpkN_XhoSTOPHind_R (product: 315 bp, template M145 gDNA) and *cpkO* was amplified with primers CpkO_BamNde_F + CpkO_SalSTOPHind_R (product: 315 bp, template: M145 DNA), then both inserts were cloned into BamHI-HindIII restriction sites of pMAL-c2TEV plasmid. The generated constructs were introduced into *E. coli* expression strains BL21(DE3)pLysS and ArcticExpress(DE3) by heat shock transformation (see chapter 3.8.7).

For the construction of plasmids pCJW93-cpkN$_{OE}$ and pCJW93-cpkO$_{OE}$, *cpkN* gene was amplified with primers cpkN_Val_Nde + CPKN_KHR (product: 905 bp, template: M145 gDNA) and *cpkO* gene was amplified with primers CpkOEXFW + KSORew (product: 1665 bp, template: M145 gDNA). Next, the inserts were cloned into NdeI-HindIII sites of plasmid

pCJW93 (Wilkinson et al. 2002, Appendix Fig. 5). The constructs were introduced into *E. coli* ET12567/pUZ8002 cells by heat shock transformation. ET12567/pUZ8002 were used to introduce the constructs into *S. coelicolor* A3(2) M145 strain (see chapter 3.8.3), generating mutants P183 (*cpkO* overexpression) and P186 (*cpkN* overexpression).

3.8.6. **Preparation of competent *E. coli* for heat-shock transformation**

200 ml of LB medium was inoculated with 4 ml of overnight *E. coli* culture and shaken in 37ºC until OD_{600} reached 0.3 – 0.4. The culture was cooled on ice and centrifuged at 2500 x g for 10 min. in 4ºC. The pellet was resuspended in 10 ml of cold TSS solution and 100 µl aliquots were prepared in pre-chilled eppendorf tubes. The aliquots were frozen in liquid nitrogen and stored in -70ºC. The competent cells were prepared fresh every 6 months.

3.8.7. **Competent *E. coli* cell transformation by heat-shock**

The 100 µl aliquots of frozen, TSS-competent *E. coli* cells were thawed on ice and 1-50 ng of plasmid DNA or a whole ligation reaction mixture was added to the respective samples, followed by gentle mixing. The cells were incubated with DNA for 20 min. on ice, transferred to 42°C water bath for 90 s and placed back on ice for additional 2 min. Next, 1 ml of SOC medium was added to the cells and the samples were incubated at 37°C (orbital shaker) for 1 h for the respective antibiotic resistance gene expression. Afterwards, 200 µl of the mixture was spread on LB agar plates containing the appropriate selective antibiotic(s) with a glass spreader. The remaining portion of cells was spread after centrifugation for 2 min. at 4000 x g, and resuspension in 100 µl of SOC medium.

3.8.8. ***E. coli* cell transformation by electroporation**

Electroporation was used in order to introduce cosmid St1G7 DNA into *E. coli* BW25113 harbouring the recombineering plasmid pIJ790 (Gust et al. 2003) (Appendix Fig. 6) and then for introduction of PCR-derived linear apramycin resistance casette DNA into *E. coli* BW25113/pIJ790/St1G7 for homologous recombination with the *cpkO* gene on the cosmid (PCR-targeting).

For the introduction of St1G7, an overnight 3 ml culture of *E. coli* BW25113/pIJ790 was grown in LB medium with chloramphenicol (25 µg/ml) at 30ºC in a rotary shaker. In the

morning, 10 ml of SOB medium with the addition of 20 mM $MgSO_4$ and 25 μg/ml chloramphenicol were inoculated with 200 μl of the overnight culture and grown at 30°C in a rotary shaker until the OD_{600} reached 0.4. Bacteria were centrifuged at 4000 x g for 5 min. at 4°C, the supernatant was discarded and the pellet was resuspended in 10 ml of cold 10% glycerol. The washing step was repeated once again and afterwards the bacterial pellet was resuspended in 100 μl of 10% glycerol. 100 ng of cosmid DNA or ddH_2O was added to 50 μl of prepared bacteria and the suspensions were transferred to chilled electroporation cuvettes. Electroporation was performed at 200 Ω, 25 μF and 2,5 kV using Gene Pulser II (BioRad) system. Afterwards, 1 ml of warm SOC medium was added to the cuvettes, the suspensions were recovered into eppendorf tubes and the bacteria were incubated at 30°C with shaking for 1 h. The bacteria were spread on a Petri dish with LB agar supplemented with ampicillin (100 μg/ml) and chloramphenicol (25 μg/ml) and incubated overnight at 30°C for selection of a desired clone.

For PCR-targeting, an overnight culture of *E. coli* BW25113/pIJ790/St1G7 was grown in LB medium with chloramphenicol (25 μg/ml) and ampicillin (100 μg/ml) at 30°C. In the morning, 15 ml of LB medium with the same antibiotics were inoculated with 150 μl of the overnight culture and grown at 30°C until the OD_{600} reached 0.2. Then, 180 μl of 1 M arabinose was added and the culture was further incubated in the same conditions until the OD_{600} reached 0.4. Afterwards, the bacteria were centrifuged at 4000 x g for 5 min. at 4°C, the supernatant was discarded and the pellet was resuspended in 15 ml of cold 10% glycerol. The washing step was repeated again and afterwards the bacterial pellet was resuspended in 350 μl of 10% glycerol. The competent bacteria were divided into two 100 μl aliquots and 500 ng of purified linear PCR product (primers: CpkODM-Fw + CpkODM-Rv, product: 1447 bp, template DNA: pIJ773) in a total volume of 4 μl was added to one of them while the equal volume of ddH_2O was added to the negative control aliquot. The suspensions were incubated 15 min. on ice and transferred to pre-chilled electroporation cuvettes and electroporation was performed at 600 Ω, 25 μF i 2,5 kV. Afterwards, 1 ml of warm SOC medium was added to the cuvettes, the suspensions were recovered into eppendorf tubes and the bacteria were incubated at 37°C with shaking for 1 h. The bacteria were spread on a Petri dishes with LB agar supplemented with ampicillin (100 μg/ml) and apramycin (50 μg/ml) and incubated overnight at 37°C to cure the bacteria from the temperature sensitive plasmid pIJ790. The desired clone was identified by the ability to grow on apramycin, cPCR (primers KSO-FW + ksFR, St1G7 = 2292 bp, St1G7-$cpkO_{DM}$ = 2077 bp) and inability to grow in the presence of chloramphenicol.

3.8.9. **Phenotypic characterization of *S. coelicolor* A3(2) strains**

For visual imaging of strain phenotypes, 20 µl of respective *S. coelicolor* A3(2) spore suspensions in ddH_2O (OD_{600} = 0.3) were spotted on solid medium 79NG and grown at 30^{o}C for 114 hours. Bacteria were photographed at 18, 21, 25, 41, 48, 70, 96 and 114 h timepoints.

3.8.10. **Transcriptional profiling of *cpk* cluster genes**

pFLUXH derivatives with *cpk* promoters were generated and introduced into *S. coelicolor* A3(2) M145 and Δ*cpkO* strains by means of intergenic conjugation by Marlena Korczyńska (Institute of Immunology and Experimental Therapy) with the help of the author. The pFLUXH derivatives were introduced into Δ*cpkN* by the author. The generated constructs and the derivative strains are listed in Tables 3 and 2, respectively. The reporter measurements in this work were performed as follows. 200 µl of solid medium 79NG was poured into thevwells of an optical-bottom, white 96-well plate (Thermo Scientific). 10 µl of spore suspensions in ddH_2O (OD_{600} = 0.3) of reporter *S. coelicolor* A3(2) strains were inoculated into the wells and grown in ClarioStar microplate reader (BMG Labtech) for 110 h at 30^{o}C. Luminescence was measured automatically every 30 minutes, the focal height was set to 15 mm and gain was set to 3600. Each strain containing a reporter construct was plated as 3 biological and 3 technical replicates.

3.9. Protein manipulation techniques

3.9.1. **Protein overproduction**

For protein overproduction in *E. coli*, 20 ml of liquid LB medium with the appropriate antibiotic was inoculated with *E. coli* BL21(DE3)pLysS or ArcticExpress(DE3) cells, containing the expression plasmid with the *cpkO* or *cpkN* gene, and cultured overnight at 37°C (BL21(DE3)pLysS) or 30°C (ArcticExpress(DE3)) with shaking 180 rpm/min. The next day, 1 L of LB medium was inoculated with 10 ml of overnight culture and cultured in the same conditions until the OD_{600} reached 0.6. Next, IPTG (isopropyl β-D-1-thiogalactopyranoside) was added to the cultures to the final concentration of 0.1 - 1 mM, the incubation temperature was changed to 10°C (ArcticExpress(DE3)) or 30°C (BL21(DE3)pLysS) and the bacteria were cultured for additional 4 hours (see summary in Table 5). After this time, the bacterial cultures

were centrifuged (4800 x g, 10 min. 4°C) and the pellets were frozen at -20°C for further purification steps.

For protein overproduction in *S. coelicolor* A3(2) cells, the spores were inoculated into 50 ml TSB-PEG medium with apramycin to the OD_{600} of 0.1. and the overproduction inducer thiostrepton was added to the cultures to the final concentrations of 1 – 10 μg/ml. Next, the bacteria were grown in an orbital shaker (30ºC, 220 rpm) for 24 or 48 hours (see summary in Table 5). After this time, the cultures were centrifuged (4800 x g, 4ºC, 10 min.) and frozen at -20ºC for further purification steps (next chapter).

3.9.2. **Protein purification by affinity chromatography**

The cell pellet was thawed on ice and resuspended in 20 ml (for *E. coli* cells) or 5 ml (for *S. coelicolor* A3(2) cells) of the Lysis buffer. Cell disintegration was performed in One Shot Cell Disruptor (Constant Systems Ltd.) at the pressure of 20 kPsi and the suspension was centrifuged (30,000 x g, 30 min, 4°C). Next, the supernatant was incubated with 1 ml (for *E. coli* lysate supernatant) or 100 μl (for *S. coelicolor* A3(2) lysate supernatant) of the apropriate affinity chromatography bed (previously equilibrated with the lysis buffers) for 1 h at room temperature. For MBP (maltose binding protein)-tagged proteins the used bed was Amylose resin (New England Biolabs), for 6xHis-tagged proteins – Ni-NTA HIS Select Nickel Affinity Gel (Sigma), for GST (glutathione S-transferse)-tagged proteins – Glutathione Sepharose resin (GE Healthcare). Next the chromatography bed was transferred to a gravity flow column and washed with 20 volumes of lysis buffer. The bound protein was eluted with 1 bed volume fractions of the respective elution buffer until the protein was completely eluted from the bed as indicated by Bradford assay. For Amylose resin, MBP-Elution buffer was used, for Glutathione Sepharose – GST-Elution buffer, for Ni-NTA HIS-Select Affinity Gel resin – 6xHis-Elution buffer fractions with the addition of 50, 100, 150, 200 and 250 mM imidazole. When needed, MBP tag was cleaved off by incubation of 100 μg of MBP-tagged protein with 2 μg of TEV protease (New England Biolabs) at 4ºC overnight. Then, MBP tag was eliminated from the sample by incubation of the sample with Amylose resin.

For purification of 6xHis-CpkN in denaturing conditions, the insoluble lysate fraction (inclusion bodies) was solubilised in 20 ml of Denaturing S buffer overnight. Next, 1 ml of the equilibrated Ni-NTA HIS-Select Affinity Gel bed was added to the lysate and incubated at room temperature for 1 h. Washing of the bed and protein elution were performed on a gravity flow

column with the buffers Denaturing W and Denaturing E, respectively. 6xHis-CpkN was dialysed to Renaturing N buffer while CpkO was dialysed to Renaturing O buffer.

The purity of the preparations was analysed by SDS-PAGE (sodium dodecyl sulfate - polyacrylamide gel electrophoresis, see chapter 3.9.3.), and their concentrations were determined by the Bradford method (next chapter). For the storage of samples at -20°C, glycerol was added to the preparations to the final concentration of 50%.

3.9.3. **Bradford assay**

Protein concentration was determined using the method of Bradford (Bradford 1976). For this purpose, 10 µl of a protein sample was added to 1 ml of 1 X concentrated Bradford reagent (Roth), followed by mixing and 5 min. incubation. Next, the absorbance value was measured at a wavelength of 595 nm. Protein concentration was determined from a standard curve based on BSA (bovine serum albumin).

3.9.4. **SDS-PAGE**

Proteins were separated according to their molecular weight in a polyacrylamide gel by electrophoresis under denaturing conditions according to (Laemmli 1970). The 8x10x0.1 cm two-part gel consisted of a 5% stacking gel and a 12.5% resolving gel. The finished gel was placed in a Mini-PROTEAN Tetra Cell electrophoresis apparatus (Bio-Rad).

Before applying the samples to the gel, they were mixed with 4 x Laemmli sample loading buffer (ratio 3:1), and then incubated at 95°C for 5 min. To determine the size of the separated proteins, molecular weight standards (Protein Molecular Weight Marker, Thermo Scientific) were applied in parallel. Separation was performed at 30 mA/gel in Tris-Gly-SDS buffer until the blue dye (bromophenol blue) had flown out of the gel. After the separation was completed, the gels were washed with tap water and stained by zinc-imidazole method. For this purpose, they were incubated (with shaking) for 12 min. in 0.2 M solution of imidazole, transferred to 0.2 M solution of $ZnCl_2$ and shaken until the protein bands appeared. Gel formulations are presented below.

Stacking gel (5%)		**Resolving gel (12,5%)**	
Acrylamide solution (30% acrylamide, 0,8% bisacrylamide)	0.33 ml	Acrylamide solution (30% acrylamide, 0,8% bisacrylamide)	2.5 ml
0.625 M Tris–HCl, pH 8.8	0.4 ml	1,88 M Tris–HCl, pH 8.8	1.2 ml
0.5% SDS	0.4 ml	0.5% SDS	1.2 ml
H_2O	0.87 ml	H_2O	1.1 ml
10% APS(ammonium persulfate)	10 µl	10% APS(ammonium persulfate)	30 µl
TEMED	2 µl	TEMED	5 µl

3.10. Proteomics

3.10.1. **Sample preparation**

200 µl of spore suspensions (OD_{600} = 0.3) of strains M145, Δ*cpkO* and Δ*cpkN* were streaked on top of a perforated cellophane disk on solid medium 79NG. Four biological replicates were prepared for each strain. After 27 hours of growth in 30ºC, all biomass was scraped off from the surface with a scalpel, washed two times with 50 mM Tris-HCl pH 7.8 and frozen at -80ºC. Proteins were extracted and digested as described in (Millan-Oropeza et al. 2017) with small modifications. The pellets were thawed on ice, suspended in 3 ml of DUTT buffer and 150 µl of protease inhibitor cocktail (Sigma Aldrich) was added to each sample. Samples were then processed in One Shot Cell Disruptor (Constant Systems LTD) by two disruption shots at 40 kPsi, cell debris was removed by centrifugation (4500 x g, 15 min, 4°C) and soluble proteins were recovered. Protein concentration in the samples was measured using the 2D Quant Kit (GE Healthcare). Aliquots of 50 µg of each protein extract were supplemented with RapiGest™ (Waters) and iodoacetamide (VWR Chemicals) to a final concentration of 0.1% and 50 mM, respectively. The samples were then incubated in the dark at room temperature for 45 min (alkylation). Subsequently, 1 µg of lysyl endopeptidase LysC (Wako) was added to each sample, followed by incubation at 37ºC for 3 h. Next, samples were diluted 6 X with deionized H_2O and 1 µg of modified porcine trypsin (Promega) was added, followed by overnight incubation at 37ºC. Trifluoroacetic acid (Thermo Scientific) was added to adjust pH to 2, to quench the digestion reaction. Peptides were pre-cleaned using Strata-X columns (Phenomenex) by washing with 1.5 ml of washing buffer (3% acetonitrile (ACN, VWR Chemicals), 0.06% glacial acetic acid). Peptides were recovered using 600 µl of elution buffer (40% ACN and 0.06% glacial acetic acid). Samples were then dried under vacuum and resuspended in 320 µl of loading buffer (0.1% trifluoroacetic acid, 2% ACN).

3.10.2. **LC-MS/MS analysis**

4 µl of each sample (1 µg of peptides) was injected into a Dionex Ultimate 3000 RSLC system coupled to an Orbitrap Fusion Lumos Tribrid mass spectrometer (Thermo Scientific). Peptides were separated in an Acclaim PepMap 75 µm (diameter) x 500 mm (length) column packed with 3 µm diameter superficially porous particles (Thermo Scientific). The separation was performed at the flow of 0.3 µl/min. with a linear gradient 1-35% (0.1% formic acid and

80% ACN) for 160 min and 35-50% for 10 min. A complete run including regeneration (98% buffer) was 215 min. Nanospray ionization was performed by applying 1.6 kV in a positive mode. Capillary transfer was performed at 275^{o}C using a capillary probe SilicaTip Emitter 10 µm.

The mass spectrometer was operated in data-dependent acquisition mode. Full MS scan occurred in Orbitrap (scan range 400-1600 m/z) with a resolution of 120000 (automatic gain control (AGC) target of 5 x 10^5, maximum injection time of 100 ms and data type of centroid). Analyzed charge states were set to 2-5 with a top speed cycle of 3 s for the most intense double or multiple charged precursor ions. The dynamic exclusion was set to 10 ppm, duration of 60 s, and the intensity threshold was fixed at 5 x 10^4. MS2 was performed using High Collision Dissociation (HCD) in Orbitrap with the resolution of 15 000 (collision energy of 30 %, AGC target of 5.0 x 10^4, max. injection time of 150 ms). Polysiloxane ions (m/z 445.12002, 519.13882, 593.15761 and 667.1764) were used for internal calibration.

3.10.3. **Protein identification and quantification**

Mass spectrometry output was analysed as described before (Millan-Oropeza et al. 2017). Protein identification was performed with X!TandemPipeline C++ 0.2.24 (Langella et al. 2017) using X!Tandem algorithm (version Alanine 2017.02.01, http://www.thegpm.org/TANDEM/) and the *Streptomyces coelicolor* A3(2) database obtained from UniProt (http://www.uniprot.org, 17.10.2018). Protein cleavage sites were defined for trypsin, with a maximum of 1 missed cleavage site. Carboxyamidomethylation of cysteine residues and oxidation of methionine residues were set to „fixed" and „potential" modifications, respectively. Precursor mass tolerance and fragment mass tolerance were set to 10 ppm. Data filtering was achieved according to a peptide E-value < 0.01, protein log (E-value) < –4 and to a minimum of two identified peptides per protein. Peptide and protein false discovery rates (FDR) were estimated at 0.03% and 0.17%, respectively. MS1 peaks were detected and aligned using MassChroQ 2.2.12 (Valot et al. 2011).

Relative quantification of protein abundances was performed using three complementary methods: spectral counting (SC) defined as the number of MS2 spectra assigned to a protein (Liu et al. 2004), extracted ion chromatograms (XIC) defined as the sum of MS1 intensities of all peptides associated to a protein and peak counting (PC) defined as the number of MS1 chromatogram peaks (peptides) attributed to each protein. Data post-processing and

statistical analysis were performed by using the R package MCQR 0.4.3 (http://pappso.inra.fr/en/bioinfo/mcqr/). Different bioinformatic pipelines were applied as indicated. For SC it involved: i) removal of proteins having < 5 spectra in all samples, and ii) removal of proteins with < 1.5 variation between strains. For XIC it included: i) removal of peptides with high retention time variation >20 s and peak width > 200 s, ii) normalization of peptide intensities based on a reference sample, iii) removal of shared peptides, iv) removal of peptides with >5% of missing values in the whole experiment, v) peptides correlated to a reference peptide with a coefficient of correlation ($r^2 < 0.75$) were kept for further analysis, vi) missing values of peptide intensities were imputed by replacing them with the minimum abundance obtained for this protein in the whole experiment, and vii) removal of peptides showing abundance variation < 1.5 between strains. For PC: i) removal of peptides with high retention time variation 20 s and peak width 200 s, ii) removal of proteins showing < 5 peaks in all samples, and iii) removal of proteins with < 1.5 variation between conditions. Protein abundance changes were detected by ANOVA tests for all methods (SC, XIC and PC), the obtained p values were adjusted by the Benjamini-Hochberg approach (Benjamini and Hochberg 1995). The abundance of a protein was considered significantly variable when the adjusted p value was < 0.01. Descriptive analysis of protein abundances was performed based on heatmap representations and calculated relative protein abundance ratios. Heatmaps were constructed using hierarchical clustering based on Euclidean distances. MS data are available via ProteomeXchange (Perez-Riverol et al. 2019) with the identifier PXD012672. In order to annotate the functions of proteins with detected abundance changes (adjusted p value <0.01), the BioCyc database (https://biocyc.org) and The Gene Ontology Resource (https://geneontology.org) were used along with literature searches.

The bioinformatic tools used for proteomics analysis (X!TandemPipeline C++, MassChroQ, MCQR) are open and free resources available in the following repository : https://forgemia.inra.fr/pappso.

4. RESULTS

4.1. Analysis of CpkO and CpkN amino acid sequences

Coelimycin synthesis SARP regulators CpkN and CpkO are comprised of 281 and 543 amino acids, respectively. It needs to be noted that the automatic *cpkN* annotation on *S. coelicolor* A3(2) genome corresponds to a 276 bp protein (Bentley et al. 2002), however, a more recent annotation of *S. lividans* TK24 genome, containing a gene of 99.88% sequence identity (differing by only one nucleotide), includes 15 additional nucleotides on the 5' end of the gene, encoding 5 additional amino acids (Rückert et al. 2015). These 15 nucleotides were therefore included in the annotation of *cpkN* on *S. coelicolor* A3(2) genome in this work. Both CpkO and CpkN are similar in their winged HTH and BTAD domains (a feature of SARPs), however, being two times larger, CpkO has an uncharacterized amino acid sequence stretching from the middle to the C-terminus of the protein (Fig. 10). The N-terminus winged HTH domains are responsible for binding within the major groove of DNA while BTAD domains recruit RNA polymerase to the respective promoter to initiate transcription (Tanaka et al. 2007). BTAD domains are found mainly in streptomycetes and mycobacteria, which are closely related. The domains are located in regulatory proteins connected to antibiotic synthesis. 11 pathway-specific regulators, along with the pleiotropic regulator AfsR in *S. coelicolor* A3(2), harbour BTAD domains (Yeats et al. 2003). Within BTAD domain, the TPR (tetratricopeptide repeat) motifs form a protein-protein interaction module. This motif contains 34 hydrophobic amino acids and multiple (usually 5 or 6) tandem repeats of the motif constitute a right-handed helical structure with an amphipathic channel that accommodates an alpha-helix of a partner protein (Zeytuni and Zarivach 2012).

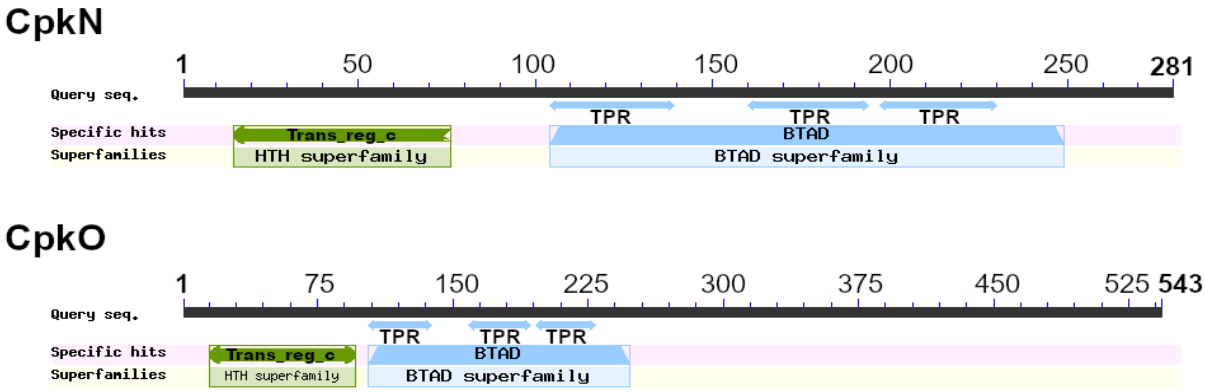

Figure 10. Common domains identified in CpkN and CpkO proteins using CDD/SPARCLE algorithm integrated into BLAST (Lu et al. 2020). TPR – tetratricopeptide repeat.

The C-terminal domain of CpkO protein could not be automatically assigned by BLAST (basic local alignment search tool) with certainty, however, it was observed that CpkO sequence from amino acid 345 to 527 resembles partial AAA family ATPase sequence. The most similar BLAST hit to such a protein type was that of amino acids 335 – 509 from an uncharacterized *Streptomyces* sp. KM273126 AAA ATPase (45% identity, 55% similarity, E value = 4e-29, accession: WP_131568959.1). This sequence is predicted to contain a class III nucleotidyl cyclase (mononucleotidyl cyclase) homology domain. The products of such cyclases are cyclic guanyl and adenyl nucleotides that play signaling roles in signal transduction systems (Lu et al. 2020).

4.2. CpkO and CpkN protein overproduction and DNA binding site determination

The initial approach to studying the functions of CpkO and CpkN regulators required protein overpoduction in *Escherichia coli* host, protein purification and determination of CpkO and CpkN DNA binding sites using electrophoretic mobility shift assays (EMSAs). *cpkO* and *cpkN* gene sequences were amplified in PCR reactions and cloned into the appropriate restriction sites of the vectors pET28a, pMAL-c2TEV and pGEX-6P-1 (Table 3). CpkO and CpkN were overproduced in two different *E. coli* hosts (BL21(DE3)pLysS and ArcticExpress(DE3)), with a set of different tags (6xHis, MBP, GST) (Table 5). The only obtained soluble fractions - MBP-CpkN and GST-CpkN were tested for DNA binding activity in EMSAs with a set of chosen *cpk* cluster gene promoters: pcpkA/D, pscbR/A, pscbR2/pscoT, pcpkO and pcpkN, however no protein-DNA interaction was detected.

Another approach was to overproduce DNA binding domains (DBDs) of CpkO and CpkN as fusion proteins with MBP tag in *E. coli*. In the strain BL21(DE3)pLysS, it was possible to obtain soluble form of MBP-CpkN$_{DBD}$ but not that of MBP-CpkO$_{DBD}$. What is more, after release of the MBP tag, CpkN$_{DBD}$ was still soluble. However, neither MBP-CpkN$_{DBD}$ nor CpkN$_{DBD}$ was able to bind any of the *cpk* promoters tested in EMSAs.

In the next approach, resolubilization of 6xHis-tagged CpkN and CpkO inclusion bodies was attempted in a buffer containing urea. Next, a screening for appropriate refolding buffers was performed. Despite the successful resolubilization and stabilization of soluble forms, proteins were non-functional in DNA binding EMSAs with the same set of promoters (Table 5). It was concluded that despite being soluble, the proteins did not regain their native conformations or that they lacked ligands that could be potentially necessary for their DNA-binding activities.

Another task was undertaken in order to obtain functional CpkO and CpkN proteins – their overproduction was performed in the native host *S. coelicolor* A3(2). However, despite overexpression of *6xHis-cpkO* and *6xHis-cpkN* genes under thiostrepton-inducible promoter ptipA, from a multicopy plasmid pCJW93 (Wilkinson et al. 2002), the protein production levels were only minimal and not enough to proceed with the protein purification (Table 5).

Since none of the attempts at obtaining functional CpkO and CpkN proteins and determining their DNA binding sites were successful, they were only summarized in the form of a table (Table 5). Due to those difficulties, studying the functions of CpkO and CpkN regulators in this work was performed *in vivo*.

Table 5. Summary of the attempts at obtaining functional CpkO and CpkN proteins.

Host	Vector	Tag/ terminus	Overexpression conditions (inducer conc./ temp. after induction)	Outcome
BL21(DE3)pLysS	pET28a	6xHis/N	0.1, 0.5, 1 mM IPTG/ 10 °C, 30 °C	In native conditions, 6xHis-CpkO and 6xHis-CpkN could not be obtained in soluble forms. In the next approach, re-solubilization of 6xHis-tagged CpkN and CpkO inclusion bodies was attempted in a buffer containing 8 M urea and screening for appropriate refolding buffers was performed. The soluble form of 6xHis-CpkO was only stable in a Tris-based buffer containing 50 mM L-arginine and 50 mM L-glutamic acid as additives, and soluble form of 6xHis-CpkN - in a Tris-based buffer containing 500 mM L-arginine. ~ 1 ml of 0.1 mg/ml fractions were obtained for 6xHis-CpkO and 6xHis-CpkN.
	pMAL-c2TEV	MBP/N	0.3 mM IPTG/30°C	Soluble but impure MBP-CpkN and GST-CpkN fractions were obtained (~ 2 ml of 0.25 mg/ml fractions). Neither MBP- nor GST-CpkO could be obtained in a soluble form. After excision of MBP tag with TEV protease, CpkN protein precipitated. In another approach, CpkO and CpkN DNA binding domains were overproduced as fusions with MBP tag. Only MBP-$CpkN_{DBD}$ was obtained in a soluble form. After excision of MBP tag, $CpkN_{DBD}$ remained soluble.
	pGEX-6P-1	GST/N	0.3 mM IPTG/30°C	
Arctic Express	pET28a	6xHis/N	0.3 mM IPTG/10°C	In native conditions, 6xHis-CpkO and 6xHis-CpkN could not be obtained in soluble forms. Soluble but impure MBP-CpkN and GST-CpkN fractions were obtained (~ 2 ml of 0.25 mg/ml fractions). Neither MBP- nor GST-CpkO could be obtained in a soluble form. After excision of MBP tag with TEV protease CpkN protein precipitated.
	pMAL-c2TEV	MBP/N	0.3 mM IPTG/10°C	
	pGEX-6P-1	GST/N	0.3 mM IPTG/10°C	
S. coeli-color	pCJW93	6xHis/N	1 – 10 µg/ml thiostrepton/30°C	Protein production levels were minimal – not suitable for proceeding with protein purification.

4.3. Generation of *cpkO* and *cpkN* deletion mutants and their derivatives

In order to study the functions of CpkO and CpkN proteins, two *S. coelicolor* A3(2) mutants were prepared in which *cpkO* and *cpkN* genes were deleted and disrupted, respectively:

1) Δ*cpkO* – *cpkO* deletion mutant in which *cpkO* gene was replaced with an apramycin resistance casette *aac(3)IV*.
2) Δ*cpkN* – *cpkN* disruption mutant in which *cpkN* gene was disrupted with transposon Tn5062, containing apramycin casette *aac(3)IV*, rendering *cpkN* inactive. Tn5062 is inserted 141 bp downstream of *cpkN* translation starting point.

Deletion and disruption were generated by introducing cosmid constructs St1G7-cpkO$_{DM}$ and 11B05.1.G04 (for Δ*cpkO* and Δ*cpkN*, respectively) into the wild-type *S. coelicolor* A3(2) strain M145 by intergenic conjugation with *E. coli* ET12567/pUZ8002 (Fig. 11). The transformants were selected for growth on solid SFM medium with apramycin (screening for the resistance casette and the whole construct integration into the genome – a single crossing over). In the next step, the colonies were streaked on both SFM plates with apramycin and plates with kanamycin. Double crossing-over exconjugants were selected on the basis of growth on apramycin and lack of growth on kanamycin. These exconjugants had the apramycin casette integrated in the place of *cpkO* or within *cpkN* gene, respectively, but lacked the core of the deletion constructs in the genome. In order to confirm gene deletions, genomic DNA of the mutants was extracted and tested by PCR with primers KSO-FW + kasFR (Δ*cpkO* = 2077 bp, WT = 2292 bp) and pcpkNup1C + CPKN_ZARV (Δ*cpkN* = 4448 bp, WT = 1006 bp), respectively (Fig. 12). Spore glycerol stocks were prepared for the generated mutants.

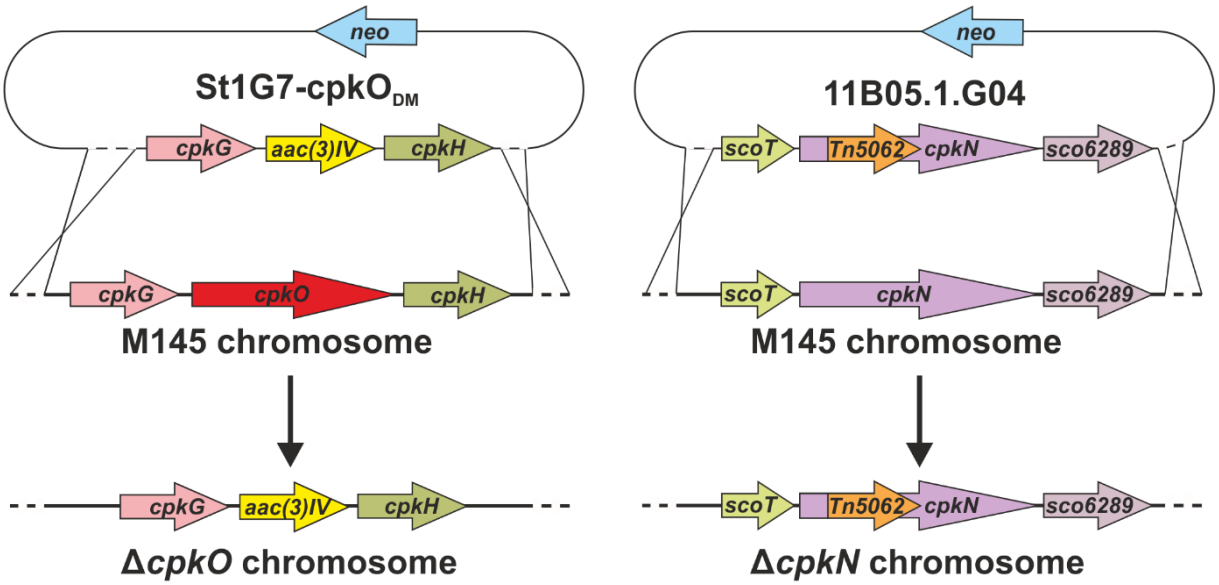

Figure 11. Schematic representation of *cpkO* and *cpkN* gene deletion/disruption in *S. coelicolor* A3(2).

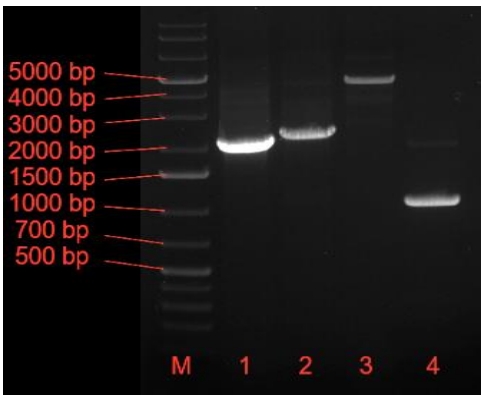

Figure 12. Confirmation of *cpkO* and *cpkN* gene deletion/disruption in *S. coelicolor* A3(2). Marker: GeneRuler 1kb Plus, lanes 1 and 2) primers KSO-FW + kasFR (Δ*cpkO* and M145 genomic DNA, respectively), lanes 3 and 4) primers pcpkNup1C + CPKN_ZARV (Δ*cpkN* and M145 genomic DNA, respectively).

In the next step, *cpkO* and *cpkN* deletions were complemented with the respective constructs by means of intergenic conjugation with *E. coli* ET12567/pUZ8002. Along with the complementation strains, their respective control strains were generated:

3) Δ*cpkO*$_{CO}$ – *cpkO* complementation strain, derived from Δ*cpkO* mutant, into which *cpkO* gene sequence, under the native promoter, was introduced on a ΦBT1 integrating plasmid pIJ10257 (construct pIJ10257-cpkO$_{CO}$). Generated to prove that the phenotype of Δ*cpkO* was caused by the lack of *cpkO* gene and not by any polar/random effects associated with the deletion.
4) Δ*cpkO*-φ – a control strain for *cpkO* complementation mutant *cpkO*$_{CO}$, generated to asses if the integration of "empty" pIJ10257 into the genome of Δ*cpkO* affects its phenotype.
5) Δ*cpkN*$_{CO}$ – *cpkN* complementation strain, derived from Δ*cpkN* mutant into which *cpkN* gene sequence, under the native promoter, was introduced on a ΦBT1 integrating plasmid pIJ10257 (construct pIJ10257-cpkN$_{CO}$). Generated to prove that the phenotype of Δ*cpkN* was caused by the lack of *cpkN* gene and not any polar/random effects associated with the deletion.
6) Δ*cpkN*-φ - a control strain for *cpkN* complementation mutant *cpkN*$_{CO}$, generated to asses if the integration of "empty" pIJ10257 into the genome of Δ*cpkN* affects its phenotype.

The complementation and the control strains were selected based on their growth on SFM plates with hygromycin (50 μg/ml). Next, their spore glycerol stocks were prepared.

After obtaining results of proteomic analysis and transcriptional profiling (chapters 4.5 and 4.6) of the above-mentioned strains, an additional Δ*cpkN*-derivative strain was generated to test the hypothesis that CpkN is only required in the cell for *scoT* gene expression activation:

7) Δ*cpkN*-*scoT*$_{OE}$ - ΔcpkN derivative, into which *scoT* gene sequence, under the strong, constitutive promoter *ermEp**, was introduced on a ΦBT1 integrating plasmid pIJ10257 (construct pIJ10257-scoT$_{OE}$).

The strain was selected for growth on SFM plate with the addition of hygromycin (50 μg/ml) and its spore glycerol stock was prepared.

Finally, for *cpk* cluster gene expression profiling studies, a set of 9 ΦBT1-integrating pFLUXH plasmids was used, with chosen *cpk* cluster promoters cloned directly upstream of *luxCDABE* reporter operon (Table 3). The operon is derived from *Photorhabdus luminescens* and encodes both the luciferase and enzymes that produce its substrate. It enables to assess relative gene transcription levels by measuring luminescence intensity *in vivo* (Craney et al. 2007). The following strains with chosen *cpk* cluster promoters were generated by the author of this work and Marlena Korczyńska (Institute of Immunology and Experimental Therapy) (Table 2) by means of intergenic conjugation with *E. coli* ET12567/pUZ8002:

1) M145-pcpkA
2) M145-pcpkD
3) M145-pscF
4) M145-pcpkO
5) M145-pcpkN
6) M145-pscoT
7) M145-pscbR2
8) M145-pscbA
9) M145-pscbR
10) Δ*cpkO*-pcpkA
11) Δ*cpkO*-pcpkD
12) Δ*cpkO*-pscF
13) Δ*cpkO*-pcpkO
14) Δ*cpkO*-pcpkN
15) Δ*cpkO*-pscoT
16) Δ*cpkO*-pscbR2
17) Δ*cpkO*-pscbA
18) Δ*cpkO*-pscbR
19) Δ*cpkN*-pcpkA
20) Δ*cpkN*-pcpkD
21) Δ*cpkN*-pscF
22) Δ*cpkN*-pcpkO
23) Δ*cpkN*-pcpkN
24) Δ*cpkN*-pscoT
25) Δ*cpkN*-pscbR2
26) Δ*cpkN*-pscbA
27) Δ*cpkN*-pscbR2

The exconjugants were selected by screening for hygromycin resistance (50 μg/ml) on SFM-agar plates and the respective spore glycerol stocks were prepared.

4.4. Phenotypic characterization of Δ*cpkO*, Δ*cpkN* and derivative mutants

Previously, deletion of *cpkO* gene was shown to abolish coelimycin synthesis on rich or minimal media supplemented with glutamate, however no clear additional phenotypic changes were reported (Gottelt et al. 2010). CpkN was so far regarded as a putative activator of *cpk* cluster but no studies on its function were previously published.

In this work, phenotypic studies were performed on solid rich medium without glucose (79NG) because of simple medium formulation and its suitability for the production of 3 antibiotics: coelimycin, undecylprodigiosin and actinorhodin by *S. coelicolor* A3(2). The

bacteria were grown as spots and observed for 114 hours (Fig. 13 A). Simultaneously, phenotypic analysis was performed for 68 h for the wild-type and mutant strains grown in the conditions for biomass collection for proteomic studies (see chapter 4.5) – on a Petri dish with 79NG medium, on top of a porous cellophane disc (Fig 13 B).

It was shown in this work that deletion of either *cpkO* or *cpkN* gene abolishes coelimycin synthesis, regardless of whether bacteria are grown as spots or grown on cellophane disks (Fig. 13 A, B). Complementation of both *cpkO* and *cpkN* deletions with respective genes under their native promoters (strains Δ*cpkO*$_{CO}$ and Δ*cpkN*$_{CO}$) restored CPK production (Fig. 13 A). Because proteomic and transcription profiling studies (see chapters 4.5 and 4.6) indicated that Δ*cpkN* mutant is impaired in transcription of *cpk* cluster gene *scoT*, an additional strain Δ*cpkN-scoT*$_{OE}$ was included in the studies, shown in Fig. 13 A. Δ*cpkN-scoT*$_{OE}$ is a *cpkN* deletion mutant harbouring a construct for constitutive expression of type II thioesterase *scoT* gene from a strong, constitutive promoter *ermEp**. ScoT is an editing enzyme that ensures correct functioning of the polyketide synthase. It was also shown to be necessary for CPK production (Kotowska et al. 2014). Production of CPK was restored in Δ*cpkN-scoT*$_{OE}$ strain, leading to the conclusion that activation of *scoT* transcription is the main function of CpkN in coelimycin synthesis regulation.

Deletion of *cpkO* enhanced undecylprodigiosin (Fig. 13 A, B) and calcium-dependent antibiotic production (Appendix Fig. 7) in comparison to the wild-type strain M145, when bacteria were grown as spots. Actinorhodin production was delayed for around one day and markedly reduced in Δ*cpkO* strain (onset after 70 hours of growth) in these conditions (Fig. 13 A). On the other hand, ACT production was clearly enhanced in Δ*cpkO* in the conditions of growth on a cellophane disk (Fig. 13 B).

When grown as spots, Δ*cpkN* strain showed only slightly reduced ACT synthesis with no apparent changes in RED and CDA synthesis (Fig. 13 A, B and Appendix Fig. 7). When bacteria were grown on a cellophane disk covering the surface of the agar medium, ACT and RED production were not affected in Δ*cpkN* strain (Fig. 13 B). It is worth noting that both Δ*cpkO* and Δ*cpkN* were slightly delayed in white aerial mycelium formation, visible on the tops of the spots (Fig. 13 A). Δ*cpkO-φ* and Δ*cpkN-φ* mutants were control strains for the influence of the plasmid pIJ10257 sequence in complementation strains and the *scoT* overexpression strain. When introduced to Δ*cpkO* and Δ*cpkN*, empty pIJ10257 slightly decreased actinorhodin production but had no effect on undecylproigiosin and coelimycin synthesis (Fig. 13 A).

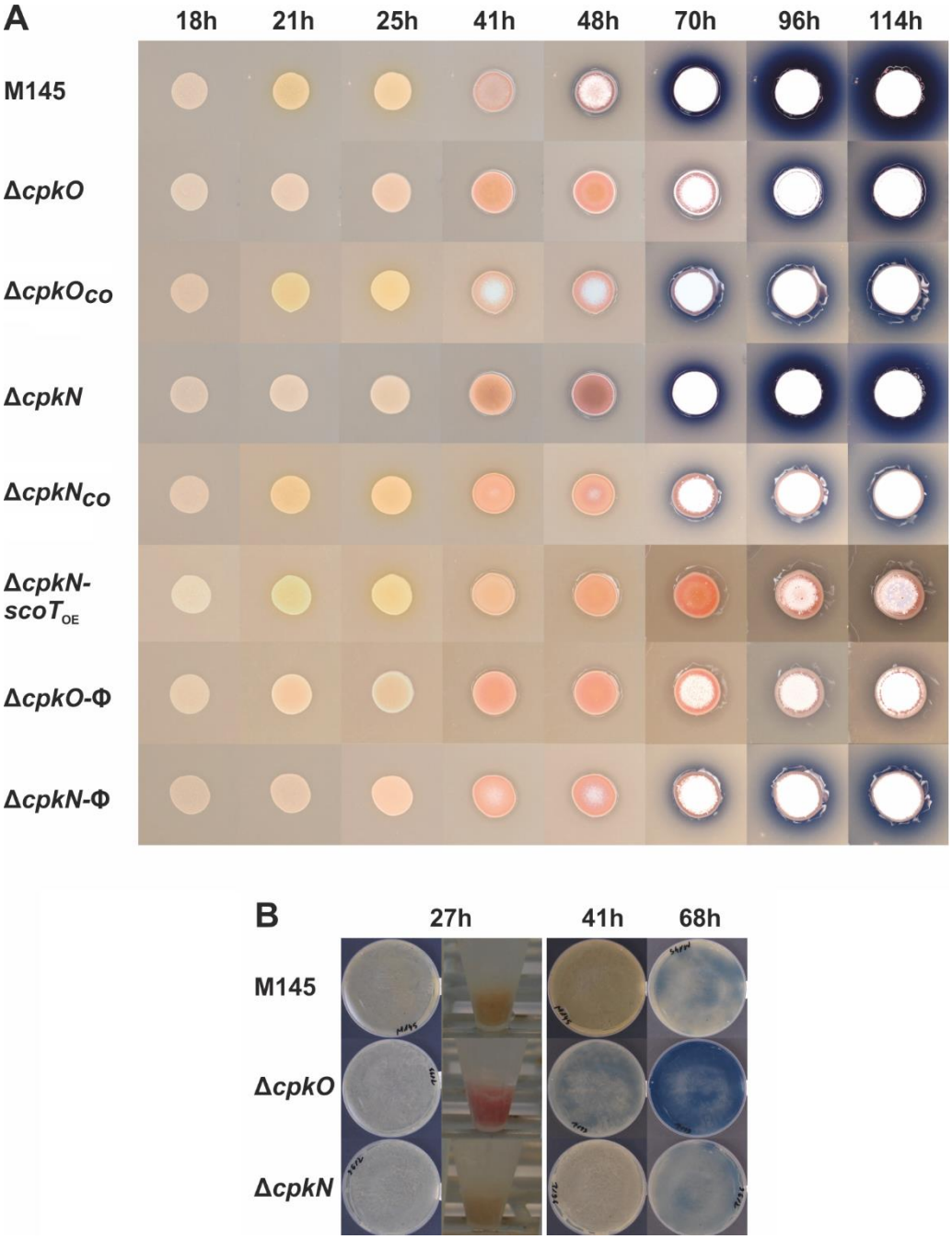

Figure 13. Phenotypes of *S. coelicolor* A3(2) wild-type (M145), Δ*cpkO* and Δ*cpkN* strains cultivated on solid medium 79NG. CPK, RED and ACT are yellow, red and blue pigments, respectively. Aerial mycelium is white. **(A)** *Streptomyces* strains grown as spots; CO – complementation strains; $scoT_{OE}$ – overexpression of *scoT*; φ – strains with empty pIJ10257 plasmid (Table 2). **(B)** Growth on top of cellophane disks on plates and collected biomass samples (in Falcon tubes).

4.5. Proteomic analysis of Δ*cpkO* and Δ*cpkN* mutant strains

For the proteomic analysis of strains, growth conditions and timing optimal for CPK production in *S. coelicolor* A3(2) occurred in the medium 79NG at 27 h (Fig. 13 B). Based on the identified peptides, a total of 2899 proteins (36% of the theoretical proteome) were identified in the studied strains M145, Δ*cpkO* and Δ*cpkN*. The distribution of protein identifications in the strains is shown in Fig. 14 A. During data post-processing, one sample (M145 A) was excluded from data analysis because of its dubious LC-MS/MS results, observed in principal component analysis (PCA) (Appendix Fig. 8).

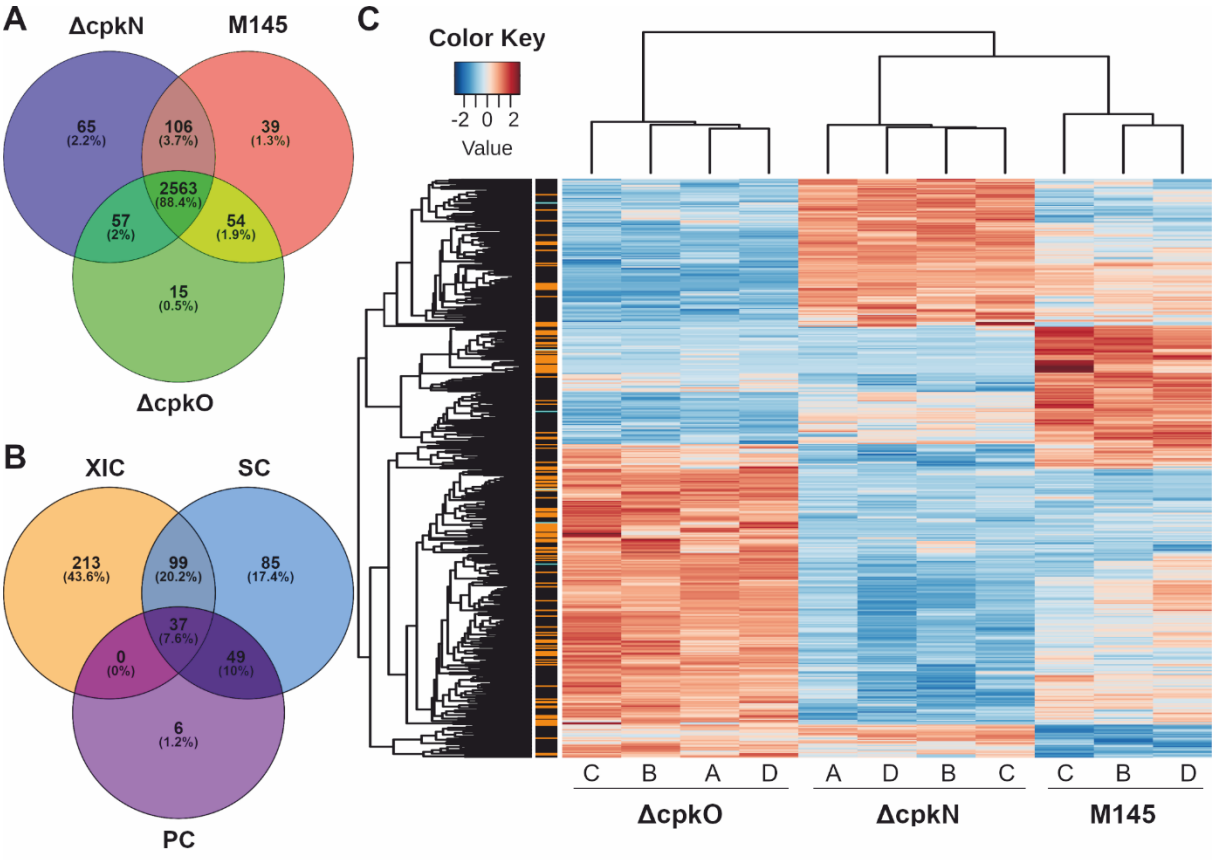

Figure 14. Analysis of the proteomes of *S. coelicolor* A3(2) wild-type (M145), Δ*cpkO* and Δ*cpkN*. **(A)** Number of protein identifications in the strains. **(B)** Quantification of 489 proteins showing significant abundance changes between the strains (ANOVA test, adjusted p value < 0.01); methods: XIC – extracted ion chromatograms, SC – spectral count, PC - peak count. **(C)** Global heatmap representation of protein abundances with significant abundance change in function of the different strains (ANOVA test, adjusted p value < 0.01). The method of quantification of each protein is indicated in colors on the left of the heatmap for extracted ion chromatogram (black), spectral count (orange) or peak count (cyan).

The data treatment resulted in 1862 valid proteins quantified by XIC (extracted ion chromatograms), SC (spectral counting) and/or PC (peak counting) complementary methods (Appendix Table 1). Out of all quantified proteins, 489 showed statistically significant differences in abundance (adjusted p value < 0.01) between at least two of the studied strains (Appendix Table 2). When measurements by multiple methods were available, XIC result was prioritized over SC result, which in turn was prioritized over that of PC. 349 proteins were quantified using XIC, 270 proteins were quantified by SC and 92 were quantified by complementary PC method (Fig. 14 B). The 489 statistically significant proteins (adjusted p value < 0.01) are represented as a heatmap using hierarchical clustering (Fig. 14 C). The most pronounced abundance changes were observed for proteins involved in secondary metabolism, however, unexpected changes in primary metabolism proteins also appeared. The effects of *cpkO* and *cpkN* deletion on the proteome of *S. coelicolor* A3(2) are presented below. The comparison of mean protein abundances for selected antibiotic synthesis pathways is shown in Fig. 15.

Figure 15. Comparison of relative levels of proteins involved in antibiotic (CPK, CDA, RED) biosynthesis and antibiotic precursor flux in *S. coelicolor* A3(2) M145, Δ*cpkO* and Δ*cpkN* strains. The method of quantification of each protein is indicated by the colors on the left of the heatmap - extracted ion chromatogram (black), spectral count (orange) or peak count (cyan).

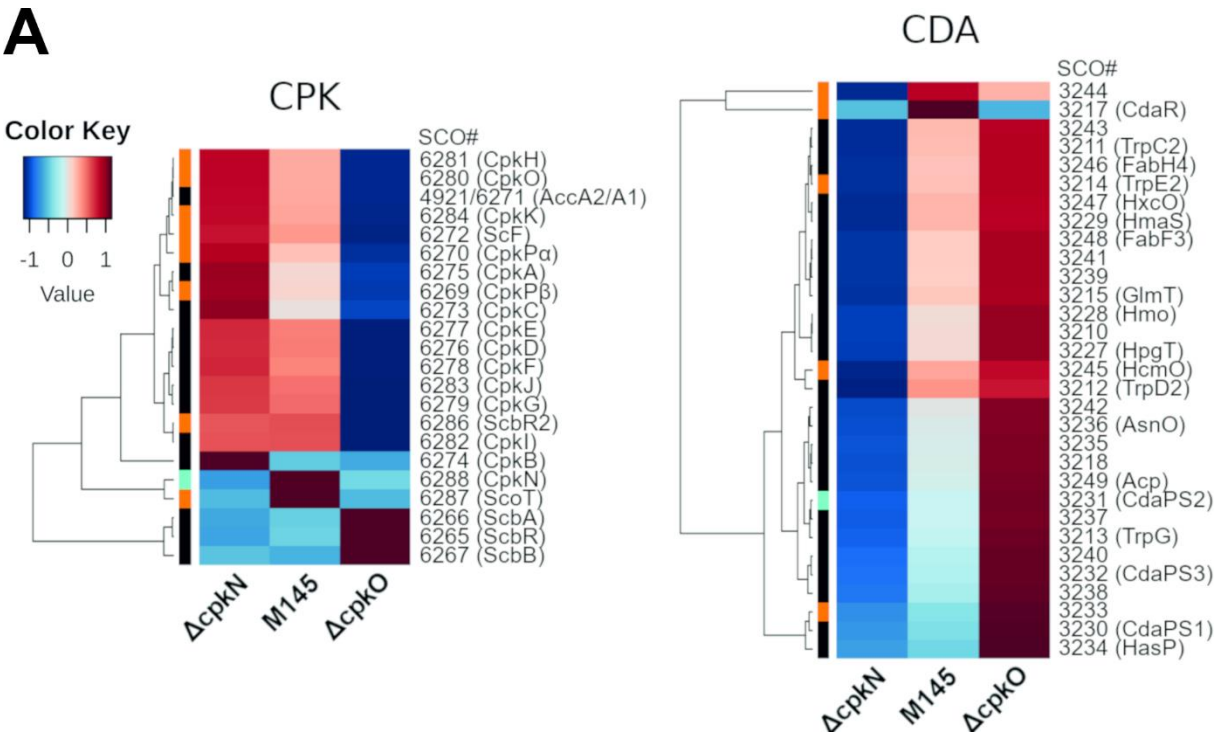

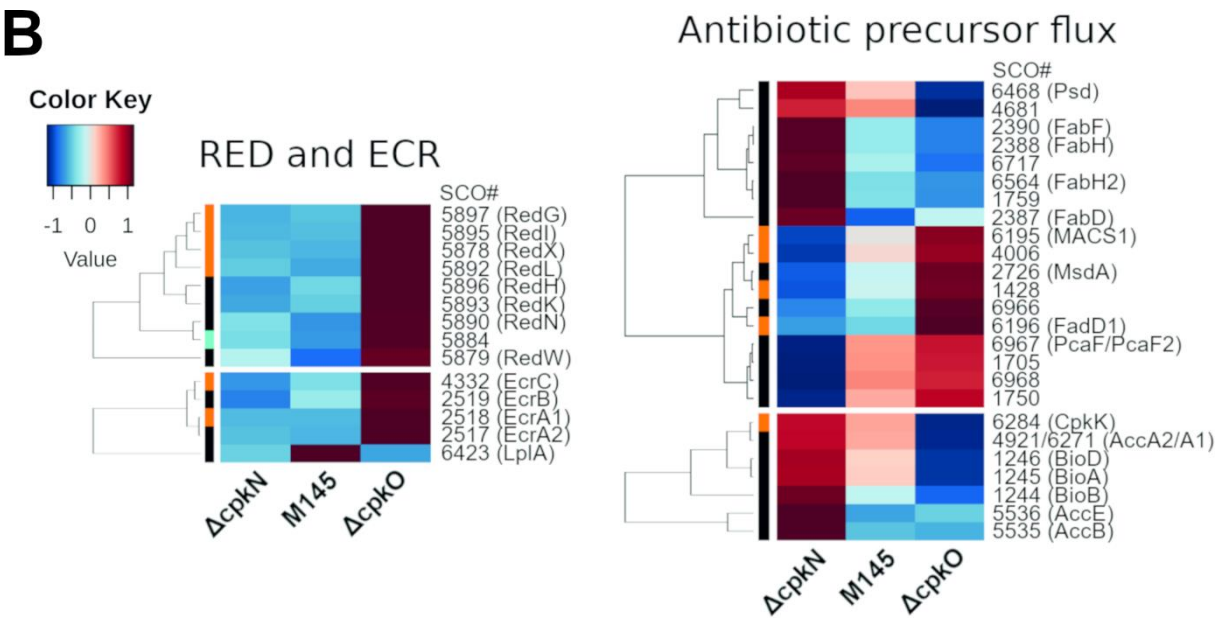

4.5.1. **Coelimycin biosynthetic gene cluster (*cpk*)**

The abundance of nearly all detected *cpk* cluster proteins (including CpkN and ScbR2) was reduced to 0 in Δ*cpkO* as a result of the absence of the cluster activator CpkO (Fig. 15 A). Only butanolide system proteins (ScbA, ScbB, ScbR) were more abundant, presumably as a result of the absence of CpkO-dependent repressor ScbR2. Contrary to this observation, *cpk* cluster biosynthetic proteins were generally more abundant, and those of butanolide system were generally only slightly less abundant in Δ*cpkN* strain (except ScbR2 which was not changed). The exception to this general *cpk* protein increase was ScoT, which was completely absent from Δ*cpkN* strain.

Putative histidine kinase OrfB (SCO6268) and a small uncharacterized protein CpkL (SCO6285) were the only members of the *cpk* cluster which were not detected. AccA1 (SCO6271) differs by only 4 amino acids from AccA2 (SCO4921), therefore it is not possible to distinguish accurately between these two proteins by the shotgun proteomics method. Almost all detected peptides can be attributed to both of them. AccA1 and/or AccA2 proteins were less abundant in Δ*cpkO* and more abundant in Δ*cpkN* strain.

4.5.2. **Undecylprodigiosin biosynthetic gene cluster (*red*) and expression correlated with *red* cluster (*ecr*)**

Perhaps the most striking difference in protein abundance profiles between the mutants and the parent strain involves the undecylprodigiosin biosynthetic gene cluster (Fig. 15 B). At the time-point of 27 hours, all of the detected *red* proteins were drastically more abundant in Δ*cpkO* than in the parent strain, the increase being between 4-fold for the oxidoreductase RedK to 58-fold for the type I PKS protein RedL. In Δ*cpkN* strain, the profile of *red* proteins was heterogeneous.

Proteins encoded by *ecr* (expression coordinated with *red*) genes were also detected. EcrA2/A1/B (SCO2517-SCO2519) and EcrC (SCO4332) were more abundant in Δ*cpkO* strain, which corresponds to its high *red* gene expression, while in Δ*cpkN* they were unchanged or less abundant. The only exception was EcrF, also named LplA (SCO6423), which was less abundant in both mutants. This protein, however, is also subject to different regulatory pathways, such as stress-response pathway controlled by σ^R (see chapter 1.3.1.).

4.5.3. **Calcium-dependent antibiotic biosynthetic gene cluster (*cda*)**

The mutants Δ*cpkN* and Δ*cpkO* presented the opposite *cda* cluster proteomic profiles in comparison to the M145 strain (Fig. 15 A). Deletion of *cpkN* caused a marked decrease in the amount of all 31 detected *cda* proteins, while deletion of *cpkO* led to a strong increase in the amount of 29 of them. Enhancement of CDA production in Δ*cpkO* after 27 h of growth was also reflected in an *in vivo* CDA assay (Appendix Fig. 7). Interestingly, contrary to the general cluster profiles, the putative *cda* cluster-specific activator CdaR, along with uncharacterized protein SCO3244, were less abundant in both Δ*cpkO* and Δ*cpkN* strains.

4.5.4. **Antibiotic precursor flux**

Biosynthesis of both fatty acids and polyketides requires the same building blocks, typically acetyl-CoA as a starter unit and acetyl-CoA-derived malonyl-CoA as the most common extender unit (Hopwood and Sherman 1990). It was shown recently, that the pool of acetyl-CoA for polyketide synthesis, which occurs in the stationary phase of growth, comes from degradation of triacylglycerols accumulated earlier (Wang et al. 2020).

A pattern was observed of lipid biosynthesis proteins being generally more abundant in Δ*cpkN* and less abundant in Δ*cpkO*, while lipid degradation proteins were generally less abundant in Δ*cpkN* and more abundant in Δ*cpkO* (Fig. 15 B). Biosynthesis group consisted of: SCO1759 (a putative transferase), SCO2387 (FabD, malonyl CoA:acyl carrier protein malonyltransferase), SCO2388 (FabH, 3-oxoacyl-[acyl-carrier-protein] synthase 3 protein 1), SCO2390 (FabF, 3-oxoacyl-[acyl-carrier-protein] synthase 2), SCO4681 (a putative short chain dehydrogenase), SCO6468 (a phosphatidylserine decarboxylase proenzyme), SCO6564 (FabH2, 3-oxoacyl-[acyl-carrier-protein] synthase 3 protein 4), SCO6717 (a putative acyl-[acyl-carrier protein] desaturase) and degradation group members were: SCO1428 (an acyl-CoA dehydrogenase), SCO1705 (a putative alcohol dehydrogenase), SCO1750 (a putative acyl-CoA dehydrogenase), SCO4006 (a putative fatty acid-CoA ligase), SCO6195 (MACS1, described below), SCO6196 (FadD1, described below), SCO6966 (a putative lipase) and SCO6968 (a probable long-chain-fatty-acid-CoA ligase) (Kanehisa et al. 2016).

The first step of lipid degradation is the synthesis of fatty acyl-CoA. Two co-transcribed fatty acyl-CoA synthetases MACS1 (SCO6195) and FadD1 (SCO6196) were found: to be less abundant in Δ*cpkN* and more abundant in Δ*cpkO*. FadD1 is produced in the stationary phase of growth, its level was shown to be positively correlated with ACT production (Banchio and Gramajo 2002) and it is the key enzyme for triacylglycerol degradation (Wang et al. 2020). Additional acetyl-CoA could also be supplied by MsdA (SCO2726, a methylmalonic acid semialdehyde dehydrogenase) or SCO6967 (a beta-ketoadipyl-CoA thiolase) (Davis and Sello 2010) with putatively co-transcribed SCO6968 (a probable long-chain-fatty-acid-CoA ligase) and neighboring putative lipase SCO6966 (Kanehisa et al. 2016) - their abundance was generally reduced in Δ*cpkN* and increased in Δ*cpkO*.

Malonyl-CoA biosynthesis occurs through carboxylation of acetyl-CoA by an acetyl-CoA carboxylase (ACCase) (Toh et al. 1993). Acetyl-CoA carboxylase consists of two subunits (α and β chains) and relies on biotin as a cofactor. In *S. coelicolor* A3(2) there are two almost identical α subunits, AccA1 (SCO6271), encoded within *cpk* gene cluster, and the essential AccA2 (SCO4921) (Rodríguez et al. 2001). It was found that ACCase α subunit(s) AccA2 and/or AccA1, β subunits AccB (SCO5535) and CpkK (SCO6284), and a small accesory protein AccE (SCO5536), were more abundant in Δ*cpkN* along with biotin biosynthesis proteins BioA (SCO1245), BioB (SCO1244) and BioD (SCO1246). Δ*cpkO* strain presented a different pattern of deregulation – the amounts of AccA2 (and/or AccA1) and CpkK were reduced and AccB and AccE remained generally unchanged, while BioA, BioB and BioD

were all less abundant. SCO1243 – another biotin synthesis protein, belonging to a different transcriptional unit than the predicted *bioBAD*, remained unchanged in both mutant strains.

Malonyl-CoA is a precursor for CPK, RED and ACT synthesis, hence a feedback loop between their BGCs and malonyl-CoA synthesis possibly exists. Previous results indicated that in the case of *cpk* cluster, it is a negative feedback loop, operating via repression of *accA2* by ScbR and ScbR2. The promoter of *accA1* was also shown to be the target for ScbR2 (Li et al. 2015). Transcription of *cpk* cluster results in high abundance of ScbR2, activated by CpkO. Here, despite drastically reduced level of ScbR2 in Δ*cpkO* strain, the level of AccA2 (and/or AccA1) is not increased, as expected, but reduced, suggesting involvement of another repressor or direct activation by CpkO. The latter hypothesis is in concordance with higher abundance of AccA2 (and/or AccA1) in Δ*cpkN* strain in which ScbR2 level is similar as in the wild type, but the level of CpkO is considerably increased.

The proteomics data presented are available in raw version via The Proteome Xchange Consortium (http://www.proteomexchange.org/) with the Project Accession PXD012672. Additional, electronic representations of the proteomics data can be found on the attached compact disc.

4.6. In *vivo* expression profiling of *cpk* cluster genes in Δ*cpkO* and Δ*cpkN* mutants

Studying detailed *cpk* cluster gene transcription profiles over time was expected to complement the proteomic studies performed in a single time-point. A luciferase reporter system was used to measure expression patterns of chosen *cpk* cluster genes in *S. coelicolor* A3(2) wild-type M145, Δ*cpkO*, and Δ*cpkN* every 30 minutes over 110 hours. For this purpose, bacteria were grown on solid medium 79NG in a white, optical-bottom 96-well plate. Both the incubation (temperature of 30^{o}C) and the measurements were performed in ClarioStar microplate reader (BMG Labtech). For the assay, the derivative strains of M145, Δ*cpkO*, and Δ*cpkN* were used that harboured pFLUXH reporter plasmid with *luxCDABE* genes under the control of chosen *cpk* promoters. Selected promoter regions included those of regulatory genes (pcpkO, pcpkN, pscbR, pscbR2 and pscbA) and structural genes (pcpkA, pcpkD, pscF and pscoT). Fragment pcpkA is located upstream of co-transcribed genes *cpkA/cpkB/cpkC* of the modular polyketide synthase core subunits and pcpkD represents co-transcribed post-polyketide tailoring genes *cpkD/cpkE/cpkF/cpkG/cpkO/cpkH* (Chen et al. 2016). Although it was shown that *cpkO* is a part of *cpkD/cpkE/cpkF/cpkG/cpkO/cpkH*

transcriptional unit, and *cpkN* is co-transcribed with its preceding gene *scoT* (Chen et al. 2016), the preliminary results at Institute of Immunology and Experimental Therapy suggest that the sequences immediately upstream of *cpkO* and *cpkN* are functional promoters. The obtained transcription profiles are shown in Fig. 16.

The effects of *cpkO* and *cpkN* deletion on *cpk* cluster gene transcription are in agreement with the proteomic data. Deletion of *cpkO* gene leads to the most distinct effects. In Δ*cpkO* strain, transcription is silenced for all four analysed biosynthetic pathway genes (*cpkA*, *cpkD*, *scF* and *scoT*), along with two regulatory genes *cpkN* and *scbR2*. These results indicate that CpkO is the higher-level activator of *cpk* cluster – activating other regulatory genes (*cpkN* and *ScbR2*) and possibly biosynthetic pathway genes. At the same time, transcription of the regulatory genes *scbA, scbR* and *cpkO* itself is noticeably upregulated. Since it is unlikely for a SARP to act as a repressor, this effect can be attributed to the lack of ScbR2 – the repressor of *cpkO* and *scbA* (Gottelt et al. 2010; Wang et al. 2011). It is noteworthy that *cpkO* transcription level in Δ*cpkO* mutant is „resistant" to the elevated level of *cpkO* repressor *scbR* transcription, although a slight retardation can be seen that shifts *cpkO* transcription peak at ~60 h (as in M145) to ~75 h. Interestingly ~60 h timepoint is the peaking point of *scbR* transcription. This only partial repression of *cpkO* by ScbR may be because of the latter protein population being mostly complexed with GBL - a consequence of strong transcription of *scbA* in Δ*cpkO*.

On the other hand, Δ*cpkN* strain was characterized by slightly elevated (or slightly precocious, in the case of *cpkA* and *scbR2*) transcription of most of *cpk* cluster genes, with the exception of *scbA*, *scbR* and *scoT*. Lower *scbA* and *scbR* levels can be easily attributed to the precocious *scbR2* transcription in Δ*cpkN*. However, there is no explanation for the strong downregulation of *scoT* gene other than that CpkN is the activator of *scoT*. This statement is reinforced by phenotypic and proteomic analyses (chapters 4.4 and 4.5). Weak transcription from *scoT* promoter was observed in Δ*cpkN* strain after approx. 40 hours of growth, while in Δ*cpkO* strain it was completely abolished. This suggests that CpkO can partly activate transcription of *scoT* independently from CpkN, but this activation is too low to maintain a noticable ScoT protein level and CPK production. As for transcription upregulation of some *cpk* genes (*cpkA, scF, cpkN,* and *scbR2*) in Δ*cpkN*, it is unlikely that CpkN has any inhibitory activity. This effect may potentially be the result of a negative feedback loop driven by lack of coelimycin synthesis that results in *cpkO* upregulation, responsible for all the effects that follow. However, the existence of such a feedback loop between the product and the *cpk* cluster has not been demonstrated as for now (see Discussion).

Figure 16. Transcriptional profiles of *cpk* cluster genes. The charts show luciferase-based reporter system measurements over 110 h of growth with sampling time of 30 min. For clarity, standard deviation was shown for every 10 h time-point. In case of pscbA and pscbR profiles, parts of the graphs were zoomed in to better visualize the differences in earlier time-points.

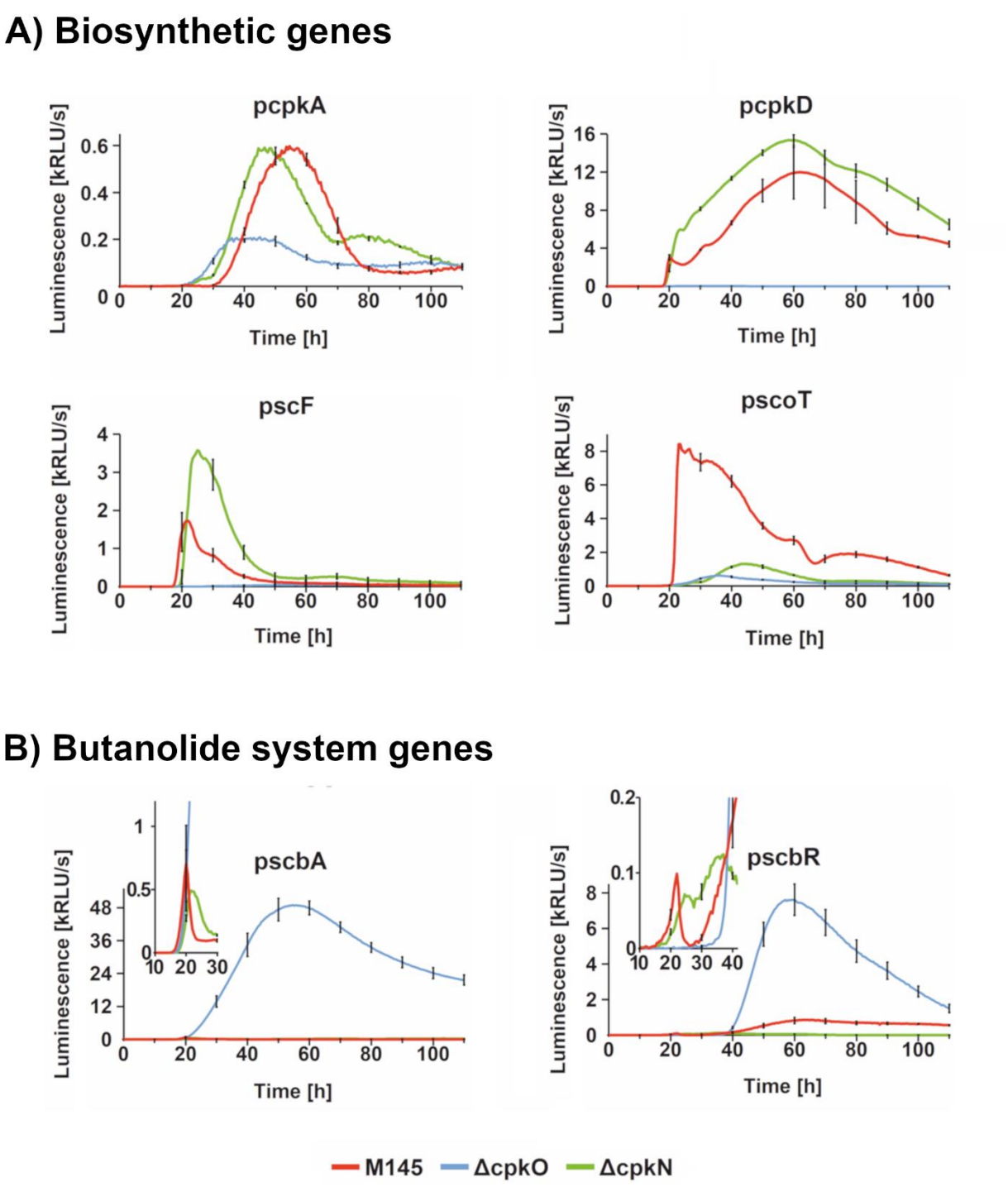

C) Regulatory genes

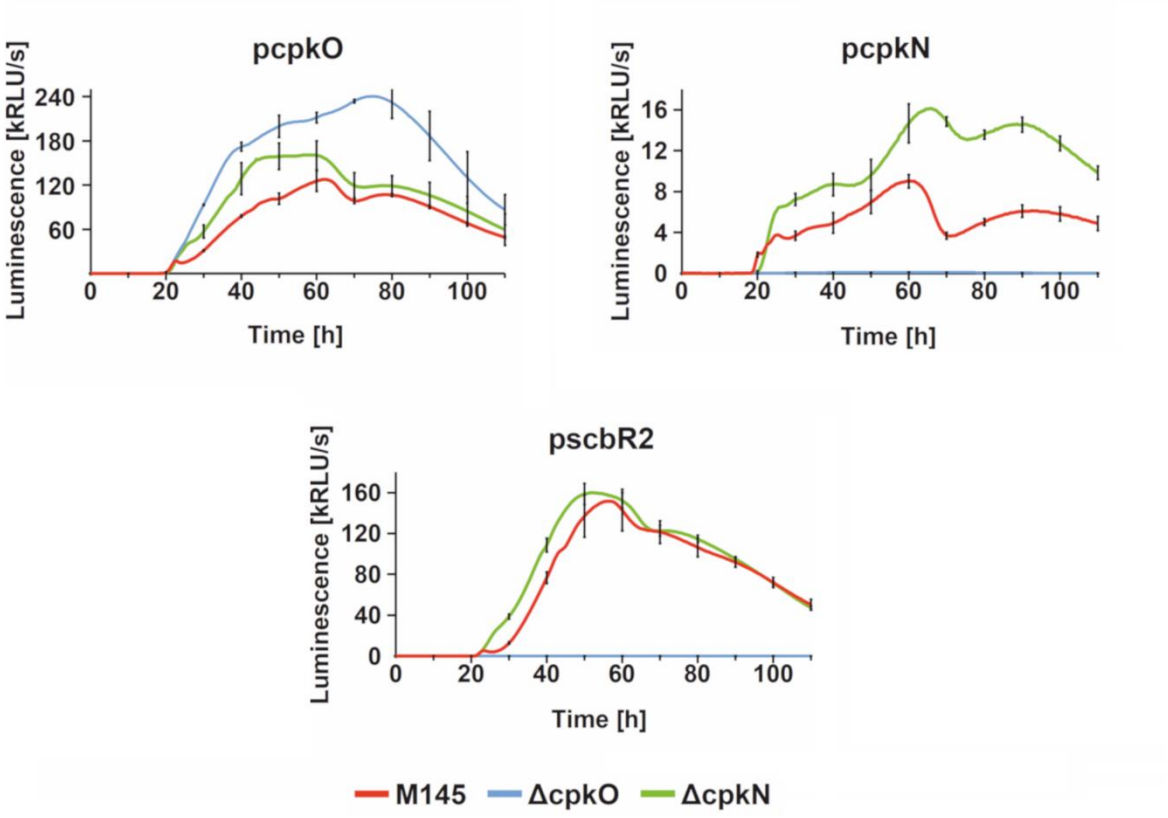

5. DISCUSSION

Specialized antibiotic production by microorganisms is a way of competing, reacting to, and interacting with the changing environmental conditions. The stringent control of biosynthetic gene transcription is therefore necessary for adaptation to complex ecological niches.

In the past, the studies of *cpk* cluster regulation have mainly focused on TetR-like repressors ScbR and ScbR2. It may be attributed to their involvemnent in other secondary metabolite production pathways as pleiotropic regulators and therefore being an attractive possible link in secondary metabolism regulatory networks. However, regulation of coelimycin synthesis by CpkO and CpkN SARP proteins has not received enough interest since this family of proteins is predicted to act mainly as direct activators of genes involved in biosynthesis and being active within their own cluster.

CpkO was previously shown to be the activator necessary for *cpk* cluster gene transcription, as deletion of *cpkO* gene completely abolishes coelimycin production (Gottelt et al. 2010). However, studies on CpkO have not unraveled its DNA binding sites nor presented a comprehensive list of its targets. It is therefore not known which actions of CpkO are direct and indirect. CpkN has not been previously studied, but rather was regarded as a putative activator of *cpk* cluster without any experimental evidence.

In this work, it was demonstrated that both CpkO and CpkN are activators required for CPK biosynthesis and that they act in a cascade regulatory manner. What is more, their actions, direct or indirect, extend to other antibiotic biosynthesis pathways and beyond – to the regulation of primary metabolism that provides the precursor flux for secondary metabolism processes.

5.1. CpkO and CpkN activate coelimycin biosynthetic cluster in a cascade manner

Experimental results presented in this work show that coelimycin synthesis requires not only CpkO, but also CpkN (Fig. 13). CpkO activates most of *cpk* cluster genes i.e. *scbR2* as well as structural genes, but not acting as an autoactivator (Fig. 15 and 16). Because the levels of ScoT and CpkN were drastically decreased in Δ*cpkO* strain and ScoT was also absent from Δ*cpkN* (despite the presence of CpkO in this strain), it suggests that CpkO is the activator of

cpkN and CpkN is the activator of *scoT*. Indeed, complementation of *cpkN* deletion with *scoT* gene, under the constitutive promoter *ermEp**, restored CPK production (Fig. 13 A). ScoT is a type II thioesterase that was previously shown at Institute of Immunology and Experimental Therapy to be required for coelimycin synthesis. It was proposed to maintain PKS activity by removal of non-reactive acyl residues blocking the ”assembly line” (Kotowska et al. 2014). CpkO, which is present in Δ*cpkN* strain, seems to be able to partially activate transcription of *scoT* (Fig. 16, the thin blue arrow indicates this weak activation) but this level is insufficient for high enough ScoT protein synthesis (Fig. 15) and coelimycin production (Fig. 13 A, B).

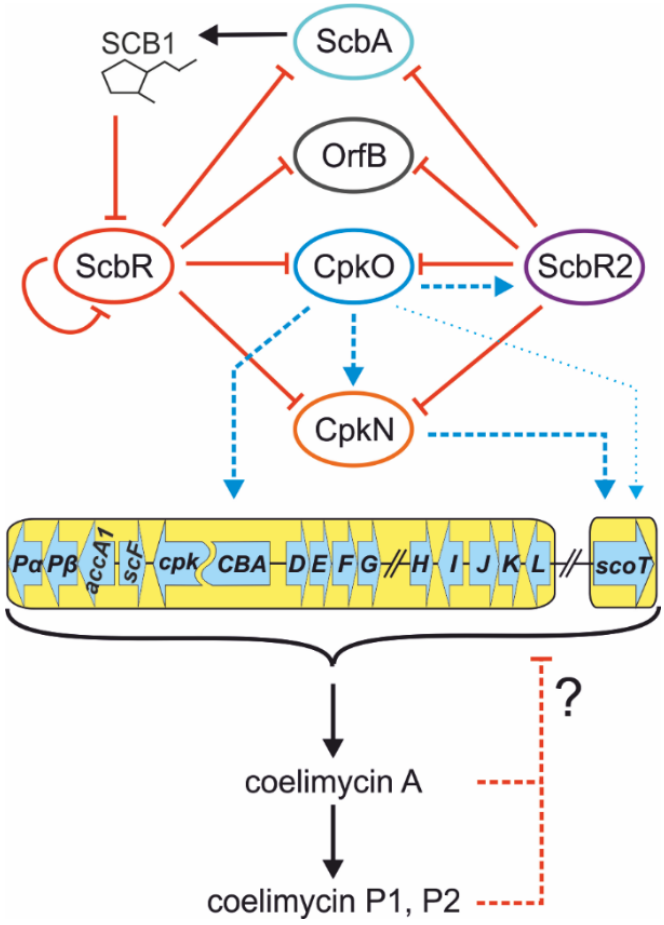

Figure 17**.** Updated mechanism of coelimycin biosynthetic gene cluster regulation by cluster-situated regulators. Black arrows indicate γ-butyrolactone SCB1 and CPK production. Solid red lines ending with bars indicate inhibition of ScbR by SCB1 and direct repression by promoter binding. Dashed red lines indicate putative negative feedback loop exerted by coelimycin. Blue lines ending with arrows denote transcription activation. Thin blue arrow indicates weak activation of *scoT* transcription by CpkO independent from CpkN. Dashed lines imply an indirect or unknown regulatory action (unknown binding site of the activator). CPK biosynthetic/post-polyketide tailoring genes are marked in yellow. Regulatory genes are omitted from the cluster diagram for clarity.

Whether coelimycin itself has a regulatory effect on *cpk* cluster is unknown. However, results obtained using proteomics and luciferase assay in Δ*cpkN* suggest a potential negative feedback loop in cluster regulation by CPK. Further studies should be conducted on *S. coelicolor* A3(2) mutant with a deletion/disruption in Cpk type I PKS genes to answer this question. The next step in such studies would be determination which CPK intermediate is the signaling molecule.

The updated mechanism of coelimycin synthesis regulation is shown in Fig. 17.

5.2. CpkO and CpkN act as pleiotropic regulators of secondary metabolism

Results presented in this work show that deletion of *cpkO* and *cpkN* genes influenced well-studied antibiotic BGCs. In a report by (Gottelt et al. 2010), the expression of *actII-orf4* and *redD* genes was found to be precocious in *cpkO* deletion mutant in comparison to the wild-type strain M145 grown in liquid SMM medium (supplemented minimal medium). This suggests the possibility of an increased actinorhodin and undecylprodigiosin production by the mutant, however the authors did not mention any differences in the pigments production on any of the tested media.

In this study, RED production was indeed increased in Δ*cpkO* strain (Fig. 13 A, B) and this phenotype corresponds well to the proteomic background (Fig. 15 B). The heterogeneous profiles of *red* proteins in Δ*cpkN* mutant resulted in no visible change in RED production by this strain. As anticipated, proteomic profiles of *ecr* proteins matched those of *red* proteins in a given strain, further emphasizing their close co-regulation.

Surprisingly, in contrast to other pigments, actinorhodin production was apparently affected by growth on a porous cellophane disc. Such conditions prevent most of the vegetative mycelium from growing into the medium and enable biomass collection from the agar plate. Δ*cpkO* grown directly on the 79NG medium produced considerably less ACT than the other strains, while on cellophane ACT synthesis was strongly upregulated in this strain (Fig. 13 A, B). This observation underpins the importance of careful consideration of growth conditions when analysing *Streptomyces* metabolism. One possible explanation for this observation is that the perforated cellophane disc spatially separates small signaling molecules, excreted by the bacteria, from the mycelium. These molecules diffuse into the medium and are no longer able to exert their effects on the bacteria. Such an example is the unidentified

repressor molecule of the ACT biosynthesis activator AtrA (Hasan 2015). This factor may be diluted in the medium, not being able to reach high enough concentration to enter the cells and bind to AtrA. As a result, AtrA is stably bound to the *actII-orf4* promoter, driving *actII-orf4* gene transcription and ACT production continously. ACT biosynthesis is activated relatively late in the culture development, therefore proteins from its biosynthetic cluster were not detected in the samples from the 27 h of growth.

Completely opposite protein abundance profiles were observed for the mutants within the calcium-dependent antibiotic BGC (Fig. 15 A). The cluster was upregulated in Δ*cpkO* and downregulated in Δ*cpkN*, with the exception of the SARP activatory protein CdaR, which was less abundant in both mutants. Similar CdaR levels suggest CdaR-independent *cda* cluster regulation by an unknown mechanism, perhaps involving two-component system AbsA1/A2, encoded within the *cda* cluster (McKenzie and Nodwell 2007). Enhanced CDA production by Δ*cpkO* strain was later confirmed in a plate test performed by Magdalena Kotowska (Institute of Immunology and Experimental Therapy) (Appendix Fig. 7).

An increasing amount of evidence is accumulating for the cross-regulation of disparate secondary metabolite biosynthetic pathways by cluster-situated regulators in *Streptomyces*. For example, it was shown that biosynthesis of candicidin and antimycin, which are unrelated natural products, is controlled by a LuxR-family-, candicin cluster-situated regulator FscRI in *S. albidoflavus* S4. Activation of both clusters by FscRI is direct and operates by transcriptional activation of their key biosynthetic genes by this regulator (McLean et al. 2016). On the other hand, in *S. autolyticus* CGMCC0516, the switching between geldanamycin and elaiophylin biosynthesis is regulated by the geldanamycin cluster-situated regulator GdmRIII that belongs to the TetR-like family of proteins. GdmRIII directly regulates the expression of post-PKS tailoring genes from both clusters by binding to their promoter regions, but the effects of these interactions are antagonistic – transcriptional activation of geldanamycin BGC and inhibition of elaiophylin BGC (Jiang et al. 2017). To the author of this work, such different outcomes may imply the existence of an additional mechanism of regulation to that by GdmRIII. Another example of coordinated antimicrobial agent production is dependent on the regulation of the so-called β-lactam supercluster, driving the synthesis of cephamycin C and clavulanic acid in *S. clavuligerus*. The effector molecule in this regulatory cascade is the SARP protein CcaR, which directly activates cephamycin C production genes and, at the same time, indirectly activates clavulanic acid synthesis genes (Santamarta et al. 2002). In *S. venezuelae*, JadR1 – a SARP-type protein directly activates production of the antibiotic jadomycin but, at the same

time, directly represses chloramphenicol synthesis. JadR1 was shown to bind the end-product of the *jad* cluster - jadomycin, which inhibits its binding to DNA (Wang et al. 2009). This mechanism is subject to yet another level of regulation – JadR2, the repressor of *jadR1* transcription, was shown to bind both jadomycin and chloramphenicol which dissociate JadR2 from DNA and inhibit its function (Xu et al. 2010). Cross-regulation of antibiotic production was also studied in *S. coelicolor* A3(2) by overexpression of SARP proteins and assessing the transcriptomic profiles of BGCs by microarrays (see chapter 1.3.4.) but these results may lack reproducibility due to the usage of thiostrepton as the gene expression inducer. Thiostrepton itself was shown to alter antibiotic production profiles in *S. coelicolor* A3(2) (Wang et al. 2017). The above-mentioned examples show that BGC cross-regulation may operate in a multitude of complex mechanisms, involving regulators from different protein families as well as small molecules – their potential ligands. It is also apparent that understanding of those mechanisms may potentially be flawed due to inappropriate experiment design, incomplete data or false-negative/false-positive results of *in vivo,* and *in vitro* procedures such as ChIP-seq (chromatin immunoprecipitation-sequencing) and EMSA (electrophoretic mobility shift assay).

Because of the lack of genome-wide data on binding sites of CpkO and CpkN proteins in *S. coelicolor* A3(2), it is impossible to assess which effects observed in the proteomics data were directly caused by lack of *cpkO* and *cpkN* genes. It is certain, however, that the lack of *cpkO* gene results in the lack of *scbR2* gene transcript, encoding the pleiotropic regulator/pseudo-GBL receptor ScbR2. Because of that, many effects of the lack of ScbR2 protein in Δ*cpkO* could be mistakenly attributed solely to the absence of CpkO. ScbR2 binds promoters of genes associated with *cpk*, *act*, *red* and *cda* clusters and although it represses *cpk* genes, its influence on *act*, *red* and *cda* genes is activatory rather than inhibitory (Li et al. 2015). Proteomic results and their associated phenotypes discussed in this work (ACT, RED and CDA synthesis upregulation in Δ*cpkO* on cellophane disc-overlaid medium 79 NG) are in contrast to transcriptomic and phenotypic results of (Li et al. 2015) with regard to the activity of ScbR2 and taken together, should incline against ScbR2 involvement in *act*, *red* and *cda* regulation. The details of the regulatory cascade that involves CpkO in ACT, RED and CDA production inhibition remains to be elucidated.

Moreover, both Δ*cpkO* and Δ*cpkN* mutants lack coelimycin synthesis and it cannot be excluded that some of the effects observed in the phenotypic/proteomics data were associated with the lack of the effectory/regulatory role (if any) of the coelimycin molecule itself. To elucidate the function of coelimycin and to assess the consequences of its production it will be

necessary to study the phenotype and the proteomic background of a mutant lacking some are all of the Cpk synthase genes.

5.3. Deletion of the major coelimycin synthesis activator directs the precursor flux to the production of other antibiotics

Deletion of *cpkO* gene caused a profound induction of actinorhodin, undecylprodigiosin and calcium-dependent antibiotic production when grown on top of a cellophane disc, on 79NG medium (Fig. 13 A, B and Fig. 15). A very recent discovery linking triacylglycerol (TAG) usage with polyketide synthesis levels (Wang et al. 2020) provides an excellent molecular background enabling ACT overproduction in Δ*cpkO* strain. The proteomic profile of generally decreased fatty acid biosynthetic protein levels and increased fatty acid degradation protein abundance, including that of FadD1 (SCO6196) at 27 h time-point (Fig. 15 B), implies early activation of accumulated cellular TAG pool degradation in Δ*cpkO*. Fatty acyl-CoA synthetase SCO6196 is the key enzyme responsible for TAG mobilization and SCO6196 abundance correlates well with polyketide synthesis levels. TAG degradation provides acetyl-CoA for polyketide production along with reducing power and ATP that inhibit enzymes of tricarboxylic acid cycle, directing even more acetyl-CoA to ACT synthesis (Wang et al. 2020). Δ*cpkN* strain showed the opposite lipid biosynthesis/degradation profile (Fig. 15 B) and hence it did not exceed ACT production capabilities of the wild-type strain (Fig. 13).

It is uncertain why deletion of *cpkO* results in increased calcium-dependent antibiotic and undecylprodigiosin production (Fig. 13 A, B and Appendix Fig. 7). It is worth noting that tryptophan is a precursor for CDA synthesis and this process has to depend on primary metabolism TrpAB synthase (SCO2036 and SCO2037) as *cda* cluster itself does not encode any tryptophan synthases (Hojati et al. 2002). Indeed, TrpAB synthase was overproduced in Δ*cpkO* (Appendix Table 2). Undoubtedly, RED synthesis requires malonyl-CoA, derived from acetyl-CoA, plenty of which should be available in the intracellular environment of the mutant. Perhaps a complementary cause for all of the described antibiotic production phenotypes in Δ*cpkO* is the overproduction of S-adenosylmethionine by the S-adenosylmethionine synthetase MetK, the abundance of which was increased two-fold in the mutant (Appendix Table 2). S-adenosylmethionine is a known ACT, RED and CDA overproduction inducer (Okamoto et al. 2003).

Even the slightest alterations in growth conditions seem to affect antibiotic production. When grown directly on 79NG medium, the strains showed the same CPK and RED production phenotypes as in the case of growth on top of a cellophane disk on 79NG but ACT synthesis levels differed between conditions (discussed in chapter 5.2.)

It is clear that once activated, respective secondary metabolite production is not simply overtaking productive repertoire of the cell by means of competition for available precursors. Biosynthetic gene clusters not only respond to the outside environmental stimuli but also shape the intracellular conditions and thus communicate with each other. The means to this communication are not clear. This cross-talk may be realized by cluster-situated regulators modulating primary metabolism or directly acting on other BGCs or pleiotropic regulators. Even the products of the clusters themselves may have regulatory functions. Coupling metabolic flux analysis with regulatory network models presents an exciting challenge, the outcome of which will profoundly facilitate industrial antibiotic-producing strain engineering.

6. REFERENCES

Alderwick LJ, Molle V, Kremer L, Cozzone AJ, Dafforn TR, Besra GS, Fütterer K (2006) Molecular structure of EmbR, a response element of Ser/Thr kinase signaling in *Mycobacterium tuberculosis*. Proc Natl Acad Sci U S A 103:2558–2563. doi: 10.1073/pnas.0507766103

Altschul SF, Gish W, Miller W, Myers EW, Lipman DJ (1990) Basic Local Alignment Search Tool. J Mol Biol 3:403–410. doi: 10.1016/S0022-2836(05)80360-2

Angert ER (2005) Alternatives to binary fission in bacteria. Nat Rev Microbiol 3:214–224. doi: 10.1038/nrmicro1096

Baell J, Walters MA (2014) Chemical con artists foil drug discovery. Nature 513:481-483. doi: 10.1038/513481a

Banchio C, Gramajo H (2002) A stationary-phase acyl-coenzyme A synthetase of *Streptomyces coelicolor* A3 (2) is necessary for the normal onset of antibiotic production. Appl Environ Microbiol 68:4240–4246. doi: 10.1128/AEM.68.9.4240

Bednarz B, Kotowska M, Pawlik KJ (2019) Multi-level regulation of coelimycin synthesis in *Streptomyces coelicolor* A3 (2). Appl Microbiol Biotechnol 103:6423–6434. doi: 10.1007/s00253-019-09975-w

Benjamini Y, Hochberg Y (1995) Controlling the false discovery rate: a practical and powerful approach to multiple testing. J R Stat Soc Ser B 57:289–300. doi: 10.2307/2346101

Bentley SD, Thomson NR, James KD, Harris DE, Quail MA, Harper D, Bateman A, Brown S, Collins M, Cronin A, Fraser A, Goble A, Hidalgo J, Hornsby T, Howarth S, Larke L, Murphy L, Oliver K, Rabbinowitsch E, Rutherford K, Rutter S, Seeger K, Saunders D, Sharp S, Squares R, Squares S, Taylor K, Warren T, Woodward J, Barrell BG, Parkhill J, Hopwood DA (2002) Complete genome sequence of the model actinomycete *Streptomyces coelicolor* A3(2). Nature 417:141–147. doi: 10.1038/417141a

Bibb MJ (2005) Regulation of secondary metabolism in streptomycetes. Curr Opin Microbiol 8:208–215. doi: 10.1016/j.mib.2005.02.016

Blin K, Wolf T, Chevrette MG, Lu X, Schwalen CJ, Kautsar SA, Suarez Duran HG, De Los Santos ELC, Kim HU, Nave M, Dickschat JS, Mitchell DA, Shelest E, Breitling R, Takano E, Lee SY, Weber T, Medema MH (2017) AntiSMASH 4.0 - improvements in chemistry prediction and gene cluster boundary identification. Nucleic Acids Res 45:W36–W41. doi: 10.1093/nar/gkx319

Bradford MM (1976) A rapid and sensitive method for the quantitation of microgram quantities of protein utilizing the principle of protein-dye binding. Anal Biochem 72:248-54. doi: 10.1006/abio.1976.9999

Buttner MJ, Chater KF, Bibb MJ (1990) Cloning, disruption and transcriptional analysis of three RNA polymerase sigma factor genes of *Streptomyces coelicolor* A3 (2). doi: 172:3367–3378

Bystrykh LV, Fernández-Moreno MA, Herrema JK, Malpartida F, Hopwood DA, Dijkhuizen

L (1996) Production of actinorhodin-related "blue pigments'' by *Streptomyces coelicolor* A3 (2). J Bacteriol 178:2238–2244. doi: 10.1128/jb.178.8.2238-2244.1996

Celler K, Koning RI, Willemse J, Koster AJ, Wezel GP Van (2016) Cross-membranes orchestrate compartmentalization and morphogenesis in *Streptomyces*. Nat Commun 7:ncomms11836. doi: 10.1038/ncomms11836

Cerdeño AM, Bibb MJ, Challis GL (2001) Analysis of the prodiginine biosynthesis gene cluster of *Streptomyces coelicolor* A3 (2): new mechanisms for chain initiation and termination in modular multienzymes. Chem Biol 8:817–829. doi: 10.1016/s1074-5521(01)00054-0

Champness WC (1988) New loci required for *Streptomyces coelicolor* morphological and physiological differentiation. J Bacteriol 170:1168–1174. doi: 10.1128/jb.170.3.1168-1174.1988

Chater KF (2001) Regulation of sporulation in *Streptomyces coelicolor* A3 (2): a checkpoint multiplex ? Curr Opin Microbiol 4:667–673. doi: 10.1016/s1369-5274(01)00267-3

Chater KF (2016) Recent advances in understanding *Streptomyces*. F1000Res 5:2795. doi: 10.12688/f1000research.9534.1

Chater KF (2006) Streptomyces inside-out : a new perspective on the bacteria that provide us with antibiotics. Philos Trans R Soc Lond B Biol Sci 361:761–768. doi: 10.1098/rstb.2005.1758

Chater KF, Lee KJ, Palmer T, Schrempf H, Biro S (2010) The complex extracellular biology of *Streptomyces*. FEMS Microbiol Rev 34:171–198. doi: 10.1111/j.1574-6976.2009.00206.x

Chen S, Zheng G, Zhu H, He H, Chen L, Zhang W, Jiang W, Lu Y (2016) Roles of two-component system AfsQ1/Q2 in regulating biosynthesis of the yellow-pigmented coelimycin P2 in Streptomyces coelicolor. FEMS Microbiol Lett 363:fnw160. doi: 10.1093/femsle/fnw160

Claessen D, Jong W De, Dijkhuizen L, Wösten HAB (2006) Regulation of *Streptomyces* development: reach for the sky! Trends Microbiol 14:313-319. doi: 10.1016/j.tim.2006.05.008

Claessen D, Stokroos I, Deelstra HJ, Penninga NA, Bormann C, Salas JA, Dijkhuizen L, Wösten HAB (2004) The formation of the rodlet layer of streptomycetes is the result of the interplay between rodlins and chaplins. Mol Microbiol 53:433–443. doi: 10.1111/j.1365-2958.2004.04143.x

Craney A, Hohenauer T, Xu Y, Navani NK, Li Y, Nodwell JR (2007) A synthetic *luxCDABE* gene cluster optimized for expression in high-GC bacteria. Nucleic Acids Res 35:e46. doi: 10.1093/nar/gkm086

Cuthbertson L, Nodwell R (2013) The TetR family of regulators. Microbiol Mol Biol Rev 77:440–475. doi: 10.1128/MMBR.00018-13

Davis JR, Sello JK (2010) Regulation of genes in *Streptomyces* bacteria required for catabolism of lignin-derived aromatic compounds. Appl Microbiol Biotechnol 86:921–929. doi: 10.1007/s00253-009-2358-0

Dietrich LEP, Teal TK, Price-Whelan A, Newman DK (2008) Redox-active antibiotics

control gene expression and community behavior in divergent bacteria. Science 321:1203–1206. doi: 10.1126/science.1160619

Fernández-Martínez LT, Del Sol R, Evans MC, Herron PR, Chandra G, Dyson PJ (2011) A transposon insertion single-gene knockout library and new ordered cosmid library for the model organism *Streptomyces coelicolor* A3(2). Antonie Van Leeuwenhoek 99:515–522. doi: 10.1007/s10482-010-9518-1

Flärdh K, Richards DM, Hempel AM, Howard M, Buttner MJ (2012) Regulation of apical growth and hyphal branching in *Streptomyces*. Curr Opin Microbiol 15:737-743. doi: 10.1016/j.mib.2012.10.012

Floriano B, Bibb M (1996) *afsR* is a pleiotropic but conditionally required regulatory gene for antibiotic production in *Streptomyces coelicolor* A3(2). Mol Microbiol 21:385–396. doi: 10.1046/j.1365-2958.1996.6491364.x

Gomez-Escribano JP, Song L, Fox DJ, Yeo V, Bibb MJ, Challis GL (2012) Structure and biosynthesis of the unusual polyketide alkaloid coelimycin P1, a metabolic product of the *cpk* gene cluster of *Streptomyces coelicolor* M145. Chem Sci 3:2716–2720 . doi: 10.1039/c2sc20410j

Gottelt M, Kol S, Gomez-Escribano JP, Bibb MJ, Takano E (2010) Deletion of a regulatory gene within the *cpk* gene cluster reveals novel antibacterial activity in *Streptomyces coelicolor* A3(2). Microbiology 156:2343–2353. doi: 10.1099/mic.0.038281-0

Gramajo HC, Takano E, Bibb MJ (1993) Stationary-phase production of the antibiotic actinorhodin in *Streptomyces coelicolor* A3(2) is transcriptionally regulated. Mol Microbiol 7:837–845. doi: 10.1111/j.1365-2958.1993.tb01174.x

Gust B, Challis GL, Fowler K, Kieser T, Chater KF (2003) PCR-targeted Streptomyces gene replacement identifies a protein domain needed for biosynthesis of the sesquiterpene soil odor geosmin. Proc Natl Acad Sci 100:1541–1546. doi: 10.1073/pnas.0337542100

Hasan AH (2015) Specific and global networks of gene regulation in *Streptomyces coelicolor*. PhD dissertation. The University of Leeds Press, Leeds.

Helmann JD (2002) The extracytoplasmic function (ECF) sigma factors. Adv Microb Physiol 46:47-110. doi: 10.1016/s0065-2911(02)46002-x

Hobbs G, Obanye AI, Petty J, Mason JC, Barratt E, Gardner DC, Flett F, Smith CP, Broda P, Oliver SG (1992) An integrated approach to studying regulation of production of the antibiotic methylenomycin by *Streptomyces coelicolor* A3 (2). J Bacteriol 174:1487–1494. doi: 10.1128/jb.174.5.1487-1494.1992

Hojati Z, Milne C, Harvey B, Gordon L, Borg M, Flett F, Wilkinson B, Sidebottom PJ, Rudd BAM, Hayes MA, Smith CP, Micklefield J (2002) Structure, biosynthetic origin, and engineered biosynthesis of calcium-dependent antibiotics from *Streptomyces coelicolor*. Chemisry Biol 9:1175–1187. doi: 10.1016/s1074-5521(02)00252-1

Hong H, Hutchings MI, Hill LM, Buttner MJ (2005) The role of the novel Fem protein VanK in vancomycin resistance in *Streptomyces coelicolor*. J Biol Chem 280:13055–13061. doi: 10.1074/jbc.M413801200

Hopwood DA (1957) Genetic recombination in *Streptomyces coelicolor*. J Gen Microbiol 16:ii-iii.

Hopwood DA (2007) *Streptomyces* in nature and medicine: the antibiotic makers. Oxford University Press, New York

Hopwood DA, Sherman DH (1990) Molecular genetics of polyketides and its comparison to fatty acid biosynthesis. Annu Rev Genet 24:37–66. doi: 10.1146/annurev.ge.24.120190.000345

Hsiao NH, Söding J, Linke D, Lange C, Hertweck C, Wohlleben W, Takano E (2007) ScbA from *Streptomyces coelicolor* A3(2) has homology to fatty acid synthases and is able to synthesize γ-butyrolactones. Microbiology 153:1394–1404. doi: 10.1099/mic.0.2006/004432-0

Huang J, Lih CJ, Pan KH, Cohen SN (2001) Global analysis of growth phase responsive gene expression and regulation of antibiotic biosynthetic pathways in *Streptomyces coelicolor* using DNA microarrays. Genes Dev 15:3183–3192. doi: 10.1101/gad.943401

Huang J, Shi J, Molle V, Sohlberg B, Weaver D, Bibb MJ, Karoonuthaisiri N, Lih CJ, Kao CM, Buttner MJ, Cohen SN (2005) Cross-regulation among disparate antibiotic biosynthetic pathways of *Streptomyces coelicolor*. Mol Microbiol 58:1276–1287. doi: 10.1111/j.1365-2958.2005.04879.x

Hutchings MI, Hoskisson PA, Chandra G, Buttner MJ (2004) Sensing and responding to diverse extracellular signals? Analysis of the sensor kinases and response regulators of *Streptomyces coelicolor* A3(2). Microbiology 150:2795–2806. doi: 10.1099/mic.0.27181-0

Jeong Y, Kim JN, Kim MW, Bucca G, Cho S, Yoon YJ, Kim BG, Roe JH, Kim SC, Smith CP, Cho BK (2016) The dynamic transcriptional and translational landscape of the model antibiotic producer *Streptomyces coelicolor* A3(2). Nat Commun 7:1–11. doi: 10.1038/ncomms11605

Jiang M, Yin M, Wu S, Han X, Ji K, Wen M, Lu T (2017) GdmRIII, a TetR family transcriptional regulator, controls geldanamycin and elaiophylin biosynthesis in *Streptomyces autolyticus* CGMCC0516. Sci Rep 7:4803. doi:10.1038/s41598-017-05073-x

Jong W De, Wösten HAB, Dijkhuizen L, Claessen D (2009) Attachment of *Streptomyces coelicolor* is mediated by amyloidal fimbriae that are anchored to the cell surface via cellulose. 73:1128–1140. doi: 10.1111/j.1365-2958.2009.06838.x

Joynt R, Seipke RF (2018) A phylogenetic and evolutionary analysis of antimycin biosynthesis. Microbiology 164:28–39. doi: 10.1099/mic.0.000572

Kanehisa M, Sato Y, Kawashima M, Furumichi M, Tanabe M (2016) KEGG as a reference resource for gene and protein annotation. Nucleic Acids Res 44:457–462. doi: 10.1093/nar/gkv1070

Kieser T, Bibb M, Buttner M, Chater K, Hopwood D (2000) Practical *Streptomyces* genetics. John Innes Foundation, Norwich, UK

Kim DJ, Huh JH, Yang YY, Kang CM, Lee IH, Hyun CG, Hong SK, Suh JW (2003) Accumulation of S-adenosyl-L-methionine enhances production of actinorhodin but inhibits sporulation in *Streptomyces lividans* TK23. J Bacteriol 185:592–600. doi: 10.1128/jb.185.2.592-600.2003

Kim HB, Smith CP, Micklefield J, Mavituna F (2004) Metabolic flux analysis for calcium

dependent antibiotic (CDA) production in *Streptomyces coelicolor*. Metab Eng 6:313–325. doi: 10.1016/j.ymben.2004.04.001

Kisker C, Hinrichs W, Tovar K, Hillen W, Saenger W (1995) The complex formed between Tet repressor and tetracycline-Mg^{2+} reveals mechanism of antibiotic resistance. J Mol Biol 247:260–280. doi: 10.1006/jmbi.1994.0138

Kotowska M, Ciekot J, Pawlik K (2014) Type II thioesterase ScoT is required for coelimycin production by the modular polyketide synthase Cpk of *Streptomyces coelicolor* A3(2). Acta Biochim Pol 61:141–147

Kuczek K, Pawlik K, Kotowska M, Mordarski M (1997) *Streptomyces coelicolor* DNA homologous with acyltransferase domains of type I polyketide synthase gene complex. FEMS Microbiol Lett 157:195–200. doi: 10.1016/S0378-1097(97)00476-X

Laemmli UK (1970) Cleavage of structural proteins during the assembly of the head of bacteriophage T4. Nature 227:680-185

Langella O, Valot B, Balliau T, Blein-Nicolas M, Bonhomme L, Zivy M (2017) X!TandemPipeline : a tool to manage sequence redundancy for protein inference and phosphosite identification. J Proteome Res 16:494–503. doi: 10.1021/acs.jproteome.6b00632

Lee PC, Umeyama T, Horinouchi S (2002) *afsS* is a target of AfsR, a transcriptional factor with ATPase activity that globally controls secondary metabolism in *Streptomyces coelicolor* A3 (2). Mol Microbiol 43:1413–1430. doi: 10.1046/j.1365-2958.2002.02840.x

Lee Y, Kim K, Suh JW, Rhee S, Lim Y (2007) Binding study of AfsK, a Ser/Thr kinase from *Streptomyces*. FEMS Microbiol Lett 3:236–240. doi: 10.1111/j.1574-6968.2006.00531.x

Lewis RA, Wahab A, Bucca G, Laing EE, Möller-Levet CS, Kierzek A, Smith CP (2019) Genome-wide analysis of the role of the antibiotic biosynthesis regulator AbsA2 in *Streptomyces coelicolor* A3(2). PloS One 14: e0200673. doi: 10.1371/journal.pone.0200673

Li X, Wang J, Li S, Ji J, Wang W, Yang K (2015) ScbR-and ScbR2-mediated signal transduction networks coordinate complex physiological responses in *Streptomyces coelicolor*. Sci Rep 5:14831. doi: 10.1038/srep14831

Lian W, Jayapal KP, Charaniya S, Mehra S, Glod F, Kyung YS, Sherman DH, Hu WS (2008) Genome-wide transcriptome analysis reveals that a pleiotropic antibiotic regulator, AfsS, modulates nutritional stress response in *Streptomyces coelicolor* A3(2). BMC Genomics 9:56. doi: 10.1186/1471-2164-9-56

Liu G, Chater KF, Chandra G, Niu G, Tan H (2013) Molecular regulation of antibiotic biosynthesis in *Streptomyces*. Microbiol Mol Biol Rev 77:112–143. doi: 10.1128/MMBR.00054-12

Liu H, Sadygov RG, Yates JR (2004) A model for random sampling and estimation of relative protein abundance in shotgun proteomics. Anal Chem 76:4193–4201. doi: 10.1021/ac0498563

Lu S, Wang J, Chitsaz F, Derbyshire MK, Geer RC, Gonzales R, Gwadz M, Hurwitz DI, Marchler GH, Song JS, Thanki N, Yamashita RA, Yang M, Zhang D, Zheng C, Lanczycki CJ, Marchler-bauer A (2020) CDD / SPARCLE: the conserved domain

database in 2020. Nucleic Acids Res 48:265–268. doi: 10.1093/nar/gkz991

Mak S, Nodwell JR (2017) Actinorhodin is a redox-active antibiotic with a complex mode of action against Gram-positive cells. Mol Microbiol 106:597–613. doi: 10.1111/mmi.13837

Manteca A, Sanchez J (2009) Streptomyces development in colonies and soils. App Environ Microbiol 75:2920–2924. doi: 10.1128/AEM.02288-08

Martínez-Núñez MA, López y López VE (2016) Nonribosomal peptides synthetases and their applications in industry. Sustain Chem Process 4:1. doi: 10.1186/s40508-016-0057-6

Mao X, Sun N, Wang F (2013) Dual positive feedback regulation of protein degradation of an extra-cytoplasmic function δ factor for cell differentiation in *Streptomyces coelicolor*. J Biol Chem 288:31217–31228. doi: 10.1074/jbc.M113.491498

Mao X, Zhou Z, Cheng LY, Hou XP, Guan WJ, Li YQ (2009) Involvement of SigT and RstA in the differentiation of *Streptomyces coelicolor*. FEBS Lett 583:3145–3150. doi: 10.1016/j.febslet.2009.09.025

Matsumoto A, Hong SK, Ishizuka H, Horinouchi S, Beppu T (1994) Phosphorylation of the AfsR protein involved in secondary metabolism in *Streptomyces* species by a eukaryotic-type protein kinase. Gene 146:47-56. doi: 10.1016/0378-1119(94)90832-x

McCormick JR (2009) Cell division is dispensable but not irrelevant in *Streptomyces*. Curr Opin Microbiol 12:689-698. doi: 10.1016/j.mib.2009.10.004

McKenzie NL, Nodwell JR (2007) Phosphorylated AbsA2 negatively regulates antibiotic production in *Streptomyces coelicolor* through interactions with pathway-specific regulatory gene promoters. J Bacteriol 189:5284–5292. doi: 10.1128/JB.00305-07

McLean TC, Hoskisson PA, Seipke RF (2016) Coordinate regulation of antimycin and candicidin biosynthesis. mSphere 1:e00305-16. doi:10.1128/mSphere.00305-16

McLean TC, Wilkinson B, Hutchings MI, Devine R (2019) Dissolution of the disparate: co-ordinate regulation in antibiotic biosynthesis. Antibiotics (Basel) 8:83. doi: 10.3390/antibiotics8020083

Merrick MJ (1976) A morphological and genetic mapping study of bald colony mutants of *Streptomyces coelicolor*. J Gen Microbiol 96:299-315. doi: 10.1099/00221287-96-2-299

Micklefield J (2009) Biosynthesis and biosynthetic engineering of calcium-dependent lipopeptide antibiotics. Pure Appl Chem 81:1065–1074. doi: 10.1351/PAC-CON-08-08-29

Millan-Oropeza A, Henry C, Blein-Nicolas M, Moussa F, Bleton J, Virolle MJ (2017) Quantitative proteomic analysis confirmed oxidative metabolism predominates in *Streptomyces coelicolor* versus glycolytic metabolism in *Streptomyces lividans*. J Proteome Res 16:2597–2613

Montaner B, Castillo-Avilla W, Martinell M, Ollinger, Aymami J, Giralt E, Pérez-Tomás R (2005) DNA interaction and dual topoisomerase I and II inhibition properties of the anti-tumor drug prodigiosin. Toxicol Sci 85:870–879. doi: 10.1093/toxsci/kfi149

Nett M, Haruo I, Moore BS (2009) Genomic basis for natural product biosynthetic diversity in the actinomycetes. Nat Prod Rep 26:1362–1384. doi: 10.1039/b817069j

Nieselt K, Battke F, Herbig A, Bruheim P, Wentzel A, Jakobsen ØM, Sletta H, Alam MT, Merlo ME, Moore J, Omara WAM, Morrissey ER, Juarez-Hermosillo MA, Rodríguez-García A, Nentwich M, Thomas L, Iqbal M, Legaie R, Gaze WH, Challis GL, Jansen RC, Dijkhuizen L, Rand DA, Wild DL, Bonin M, Reuther J, Wohlleben W, Smith MCM, Burroughs NJ, Martín JF, Hodgson DA, Takano E, Breitling R, Ellingsen TE, Wellington EMH (2010) The dynamic architecture of the metabolic switch in *Streptomyces coelicolor*. BMC Genomics 11:10. doi: 10.1186/1471-2164-11-10

Nishiyama T, Hashimoto Y, Kusakabe H, Kumano T, Kobayashi M (2014) Natural low-molecular mass organic compounds with oxidase activity as organocatalysts. Proc Natl Acad Sci USA 111:48. doi: 10.1073/pnas.1417941111

Okamoto S, Lezhava A, Hosaka T, Okamoto-Hosoya Y, Ochi K (2003) Enhanced expression of S-adenosylmethionine synthetase causes overproduction of actinorhodin in *Streptomyces coelicolor* A3 (2). J Bacteriol 185:601–609. doi: 10.1128/JB.185.2.601

Okamoto S, Taguchi T, Ochi K, Ichinose K (2009) Biosynthesis of actinorhodin and related antibiotics: discovery of alternative routes for quinone formation encoded in the *act* gene cluster. Chem Biol 16:226–236. doi: 10.1016/j.chembiol.2009.01.015

Paget MSB, Molle V, Cohen G, Aharonowitz Y, Buttner MJ (2001) Defining the disulphide stress response in *Streptomyces coelicolor* A3 (2): identification of the sigma R regulon. Mol Microbiol 42:1007–1020. doi: 10.1046/j.1365-2958.2001.02675.x

Pawlik K, Kotowska M (2005) Od sekwencji DNA do antybiotyku. Biotechnologia 3:57-74.

Pawlik K, Kotowska M, Chater KF, Kuczek K, Takano E (2007) A cryptic type I polyketide synthase (*cpk*) gene cluster in *Streptomyces coelicolor* A3(2). Arch Microbiol 187:87–99. doi: 10.1007/s00203-006-0176-7

Pawlik K, Kotowska M, Kolesiński P (2010) *Streptomyces coelicolor* A3(2) produces a new yellow pigment associated with the polyketide synthase Cpk. J Mol Microbiol Biotechnol 19:147–51 . doi: 10.1159/000321501

Perez-Riverol Y, Csordas A, Bai J, Bernal-llinares M, Hewapathirana S, Kundu DJ, Inuganti A, Griss J, Mayer G, Eisenacher M, Enrique P, Uszkoreit J, Pfeuffer J, Tiwary S, Audain E, Walzer M, Jarnuczak AF, Ternent T, Brazma A, Vizca A (2019) The PRIDE database and related tools and resources in 2019: improving support for quantification data. Nucleic Acids Res 47:442–450. doi: 10.1093/nar/gky1106

Rodríguez E, Banchio C, Diacovich L, Bibb MJ, Gramajo H (2001) Role of an essential acyl coenzyme A carboxylase in the primary and secondary metabolism of *Streptomyces coelicolor* A3 (2). Appl Environ Microbiol 67:4166–4176. doi: 10.1128/AEM.67.9.4166

Rodríguez H, Rico S, Díaz M, Santamaría RI (2013) Two-component systems in *Streptomyces*: key regulators of antibiotic complex pathways. Microb Cell Fact 12:127. doi: 10.1186/1475-2859-12-127

Romero DA, Hasan AH, Lin Y fei, Kime L, Ruiz-Larrabeiti O, Urem M, Bucca G, Mamanova L, Laing EE, van Wezel GP, Smith CP, Kaberdin VR, McDowall KJ (2014) A comparison of key aspects of gene regulation in *Streptomyces coelicolor* and *Escherichia coli* using nucleotide-resolution transcription maps produced in parallel by global and differential RNA sequencing. Mol Microbiol 94:963–987. doi: 10.1111/mmi.12810

Rudd BAM (1978) Genetics of pigmented secondary metabolites in Streptomyces coelicolor. PhD thesis. University of East Anglia, Norwich

Rückert C, Albersmeier A, Busche T, Jaenicke S, Winkler A, Friðjónsson ÓH, Hreggviðsson GÓ, Lambert C, Badcock D, Bernaerts K, Anne J, Economou A, Kalinowski J (2015) Complete genome sequence of *Streptomyces lividans* TK24. J Biotechnol 199:21-2. doi: 10.1016/j.jbiotec.2015.02.004

Santamarta I, Rodríguez-García A, Pérez-Redondo R, Martín JF, Liras P (2002) CcaR is an autoregulatory protein that binds to the *ccaR* and *cefD-cmcI* promoters of the cephamycin C-clavulanic acid cluster in *Streptomyces clavuligerus*. J Bacteriol 184:3106-3113. doi: 10.1128/jb.184.11.3106-3113.2002

Santos-Beneit F, Rodríguez-García A, Martín JF (2011) Complex transcriptional control of the antibiotic regulator *afsS* in *Streptomyces*: PhoP and AfsR are overlapping, competitive activators. J Bacteriol 193:2242–2251. doi: 10.1128/JB.01462-10

Santos-Beneit F, Rodríguez-García A, Sola-Landa A, Martín JF (2009) Cross-talk between two global regulators in *Streptomyces*: PhoP and AfsR interact in the control of *afsS* , *pstS* and *phoRP* transcription. Mol Microbiol 72:53–68. doi: 10.1111/j.1365-2958.2009.06624.x

Sawai R, Suzuki A, Takano Y, Lee PC, Horinouchi S (2004) Phosphorylation of AfsR by multiple serine/threonine kinases in *Streptomyces coelicolor* A3 (2). Gene 334:53–61. doi: 10.1016/j.gene.2004.02.046

Shu D, Chen L, Wang W, Yu Z, Ren C, Zhang W, Yang S, Lu Y, Jiang W (2009) *afsQ1-Q2-sigQ* is a pleiotropic but conditionally required signal transduction system for both secondary metabolism and morphological development in *Streptomyces coelicolor*. Appl Microbiol Biotechnol 81:1149–1160. doi: 10.1007/s00253-008-1738-1

Sidda JD, Poon V, Song L, Wang W, Yang K, Corre C (2016) Overproduction and identification of butyrolactones SCB1-8 in the antibiotic production superhost: *Streptomyces* M1152. Org Biomol Chem 14:6390–6393. doi: 10.1039/c6ob00840b

Singh R, Mo S, Florova G, Reynolds KA (2012) *Streptomyces coelicolor* RedP and FabH enzymes, initiating undecylprodiginine and fatty acid biosynthesis, exhibit distinctacyl-CoA and malonyl-acyl carrier protein substrate specificities. FEMS Microbiol Lett 328:32-38. doi: 10.1111/j.1574-6968.2011.02474.x

Stankovic N, Senerovic L, Ilic-Tomic T, Vasiljevic B, Nikodinovic-Runic J (2014) Properties and applications of undecylprodigiosin and other bacterial prodigiosins. Appl Microbiol Biotechnol 98:3841–3858. doi: 10.1007/s00253-014-5590-1

Stirrett K, Denoya C, Westpheling J (2009) Branched-chain amino acid catabolism provides precursors for the Type II polyketide antibiotic, actinorhodin, via pathways that are nutrient dependent. J Ind Microbiol Biotechnol 36:129–137. doi: 10.1007/s10295-008-0480-0

Stutzman-Engwall KJ, Otten SL, Hutchinson CR (1992) Regulation of secondary metabolism in *Streptomyces* spp. and overproduction of daunorubicin in *Streptomyces peucetius*. J Bacteriol 174:144–154

Sun D, Liu C, Zhu J, Liu W (2017) Connecting metabolic pathways: sigma factors in *Streptomyces* spp. Front Microbiol 8:2546. doi: 10.3389/fmicb.2017.02546

Szafran MJ, Gongerowska M, Gutkowski P, Zakrzewska-Czerwińska J, Jakimowicz D (2016) The coordinated positive regulation of topoisomerase genes maintains topological homeostasis in *Streptomyces coelicolor*. J Bacteriol 198:3016–3028. doi: 10.1128/JB.00530-16

Šmídová K, Ziková, Pospíšil J, Schwarz M, Bobek J, Vohradsky J (2019) DNA mapping and kinetic modeling of the HrdB regulon in Streptomyces coelicolor. Nucleic Acids Res 47:621–633. doi: 10.1093/nar/gky1018

Takano E, Chakraburtty R, Nihira T, Yamada Y, Bibb MJ (2001) A complex role for the γ-butyrolactone SCB1 in regulating antibiotic production in *Streptomyces coelicolor* A3(2). Mol Microbiol 41:1015–1028. doi: 10.1046/j.1365-2958.2001.02562.x

Takano E, Gramajo HC, Strauch E, Andres N, White J, Bibb MJ (1992) Transcriptional regulation of the *redD* transcriptional activator gene accounts for growth-phase-dependent production of the antibiotic undecylprodigiosin in *Streptomyces coelicolor* A3(2). Mol Microbiol 6:2797–2804. doi: 10.1111/j.1365-2958.1992.tb01459.x

Takano E, Kinoshita H, Mersinias V, Bucca G, Hotchkiss G, Nihira T, Smith CP, Bibb M, Wohlleben W, Chater K (2005) A bacterial hormone (the SCB1) directly controls the expression of a pathway-specific regulatory gene in the cryptic type I polyketide biosynthetic gene cluster of *Streptomyces coelicolor*. Mol Microbiol 56:465–79. doi: 10.1111/j.1365-2958.2005.04543.x

Tanaka A, Takano Y, Ohnishi Y, Horinouchi S (2007) AfsR recruits RNA polymerase to the *afsS* promoter: a model for transcriptional activation by SARPs. J Mol Biol 369:322–333. doi: 10.1016/j.jmb.2007.02.096

Tenconi E, Traxler MF, Hoebreck C, van Wezel GP, Rigali S (2018) Production of prodiginines is part of a programmed cell death process in *Streptomyces coelicolor*. Front Microbiol 9:1742. doi: 10.3389/fmicb.2018.01742

Thomas MG, Burkart MD, Walsh CT (2002) Conversion of L-proline to pyrrolyl-2-carboxyl-S-PCP during undecylprodigiosin and pyoluteorin biosynthesis. Chem Biol 9:171–184. doi: 10.1016/s1074-5521(02)00100-x

Toh H, Kondo H, Tanabe T (1993) Molecular evolution of biotin-dependent carboxylases. Eur J Biochem 215:687–696. doi: 10.1111/j.1432-1033.1993.tb18080.x

Valot B, Langella O, Nano E, Zivy M (2011) MassChroQ : A versatile tool for mass spectrometry quantification. Proteomics 11:3572–3577. doi: 10.1002/pmic.201100120

van der Heul HU, Bilyk BL, McDowall KJ, Seipke RF, van Wezel GP (2018) Regulation of antibiotic production in Actinobacteria: new perspectives from the post-genomic era. Nat Prod Rep 35:575–604. doi: 10.1039/c8np00012c

van der Meij A, Worsley SF, Hutchings MI, van Wezel GP (2017) Chemical ecology of antibiotic production by actinomycetes. FEMS Microbiol Rev 41:392–416. doi: 10.1093/femsre/fux005

van Keulen G, Dyson PJ (2014) Production of specialized metabolites by *Streptomyces coelicolor* A3 (2). Adv Appl Microbiol 89:217–266. doi: 10.1016/B978-0-12-800259-9.00006-8

Wang H, Zhao G, Ding X (2017) Morphology engineering of *Streptomyces coelicolor* M145 by sub-inhibitory concentrations of antibiotics. Sci Rep 7:13226. doi: 10.1038/s41598-

017-13493-y

Wang J, Wang W, Wang L, Zhang G, Fan K, Tan H, Yang K (2011) A novel role of 'pseudo' γ-butyrolactone receptors in controlling γ-butyrolactone biosynthesis in *Streptomyces*. Mol Microbiol 82:236–250. doi: 10.1111/j.1365-2958.2011.07811.x

Wang L, Tian X, Wang J, Yang H, Fan K, Xu G, Yang K, Tan H (2009) Autoregulation of antibiotic biosynthesis by binding of the end product to an atypical response regulator. Proc Nat Acad Sci 106:8617-8622. doi: 10.1073/pnas.0900592106

Wang R, Mast Y, Wang J, Zhang W, Zhao G, Wohlleben W, Lu Y, Jiang W (2013) Identification of two-component system AfsQ1/Q2 regulon and its cross-regulation with GlnR in *Streptomyces coelicolor*. Mol Microbiol 87:30–48. doi: 10.1111/mmi.12080

Wang W, Li S, Li Z, Zhang J, Fan K, Tan G, Ai G, Lam SM, Shui G, Yang Z, Lu H, Jin P, Li Y, Chen X, Xia X, Liu X, Dannelly HK, Yang C, Yang Y, Zhang S, Alterovitz G, Xiang W, Zhang L (2020) Harnessing the intracellular triacylglycerols for titer improvement of polyketides in *Streptomyces*. Nat Biotechnol 38:76-83. doi: 10.1038/s41587-019-0335-4

Wietzorrek A, Bibb MJ (1997) A novel family of proteins that regulates antibiotic production in streptomycetes appears to contain an OmpR-like DNA-binding fold. Mol Microbiol 25:1181–1184. doi: 10.1046/j.1365-2958.1997.5421903.x

Wilkinson CJ, Hughes-Thomas ZA, Martin CJ, Böhm I, Mironenko T, Deacon M, Wheatcroft M, Wirtz G, Staunton J, and Leadlay PF (2002). Increasing the efficiency of heterologous promoters in actinomycetes. J Mol Microbiol Biotechnol 4:417-426.

Xu G, Wang J, Wang L, Tian X, Yang H, Fan K, Yang K, Tan H (2010) "Pseudo" γ-butyrolactone receptors respond to antibiotic signals to coordinate antibiotic biosynthesis. J Biol Chem 285:27440–27448. doi: 10.1074/jbc.M110.143081

Yagüe P, Willemse J, Koning RI, Rioseras B, López-García C, Gonzalez-Quiñonez N, Lopez-Igesias C, Shliaha P V, Rogowska-Wrzesinska A, Koster AJ, Jensen ON, van Wezel GP, Manteca Á (2016) Subcompartmentalization by cross-membranes during early growth of *Streptomyces* hyphae. Nat Commun 7:12467. doi: 10.1038/ncomms12467

Yagüe P, Rodríguez-García A, López-García MT, Martín JF, Rioseras B, Sánchez J, Manteca Á (2013) Transcriptomic analysis of *Streptomyces coelicolor* differentiation in solid sporulating cultures: first compartmentalized and second multinucleated mycelia have different and distinctive transcriptomes. PLoS One 8:e60665. doi: 10.1371/journal.pone.0060665

Yeats C, Bentley S, Bateman A (2003) New knowledge from old: *in silico* discovery of novel protein domains in *Streptomyces coelicolor*. BMC Microbiol l3:3. doi: 10.1186/1471-2180-3-3

Zeytuni N, Zarivach R (2012) Review structural and functional discussion of the tetra-trico-peptide repeat, a protein interaction module. Structure 20:397–405. doi: 10.1016/j.str.2012.01.006

Zhang Z, Du C, de Barsy F, Liem M, Liakopoulos A, van Wezel GP, Choi YH, Claessen D, Rozen DE (2020) Antibiotic production in *Streptomyces* is organized by a division of labor through terminal genomic differentiation. Sci Adv 6:eaay5781. doi: 10.1126/sciadv.aay5781

7. APPENDIX

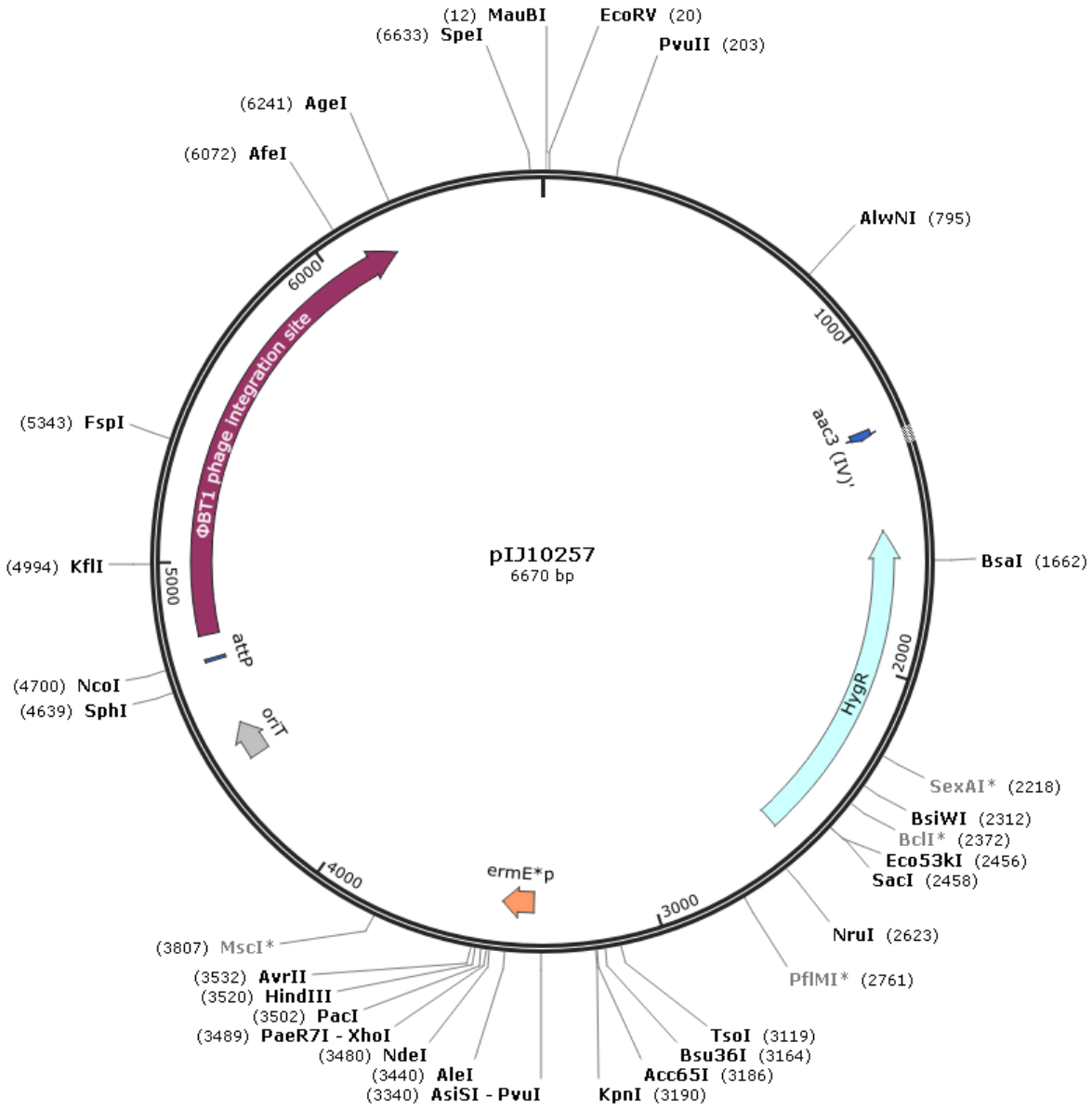

Appendix Figure 1. Map of the expression vector pIJ10257. Unique restriction sites are indicated in bold (http://actinobase.org/index.php/PIJ10257).

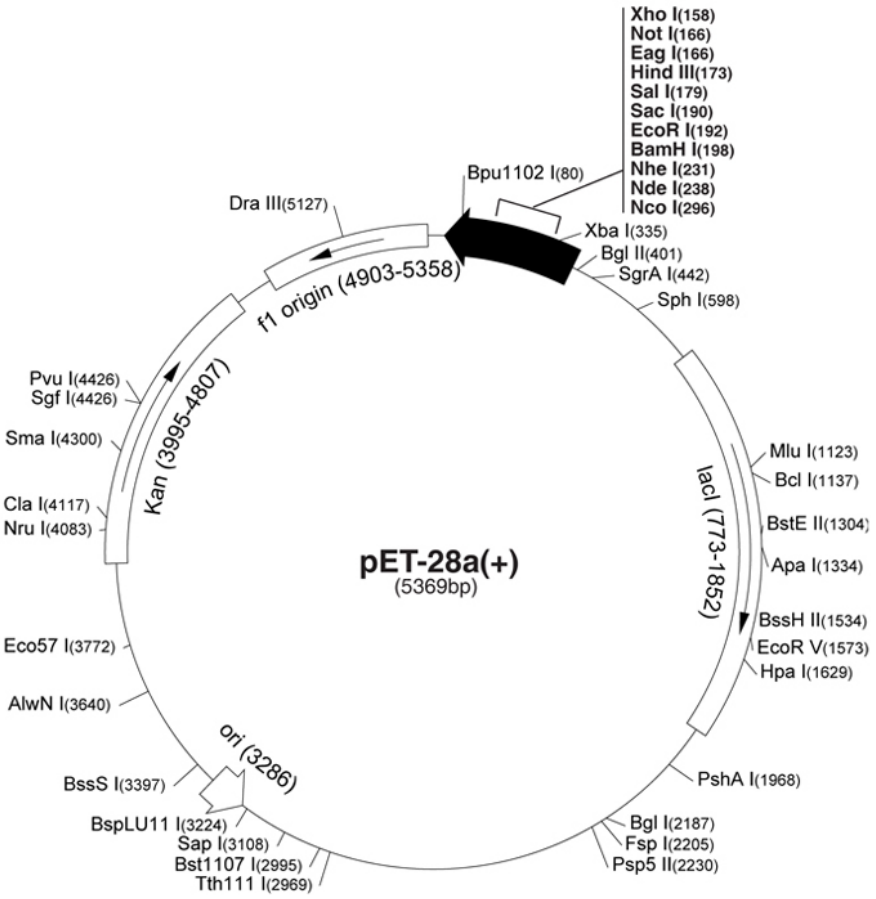

Appendix Figure 2. Map of the expression vector pET28a.
(https://bip.weizmann.ac.il/plasmidb/queryplasmid?vector_or_plasmid_name=pET28a)

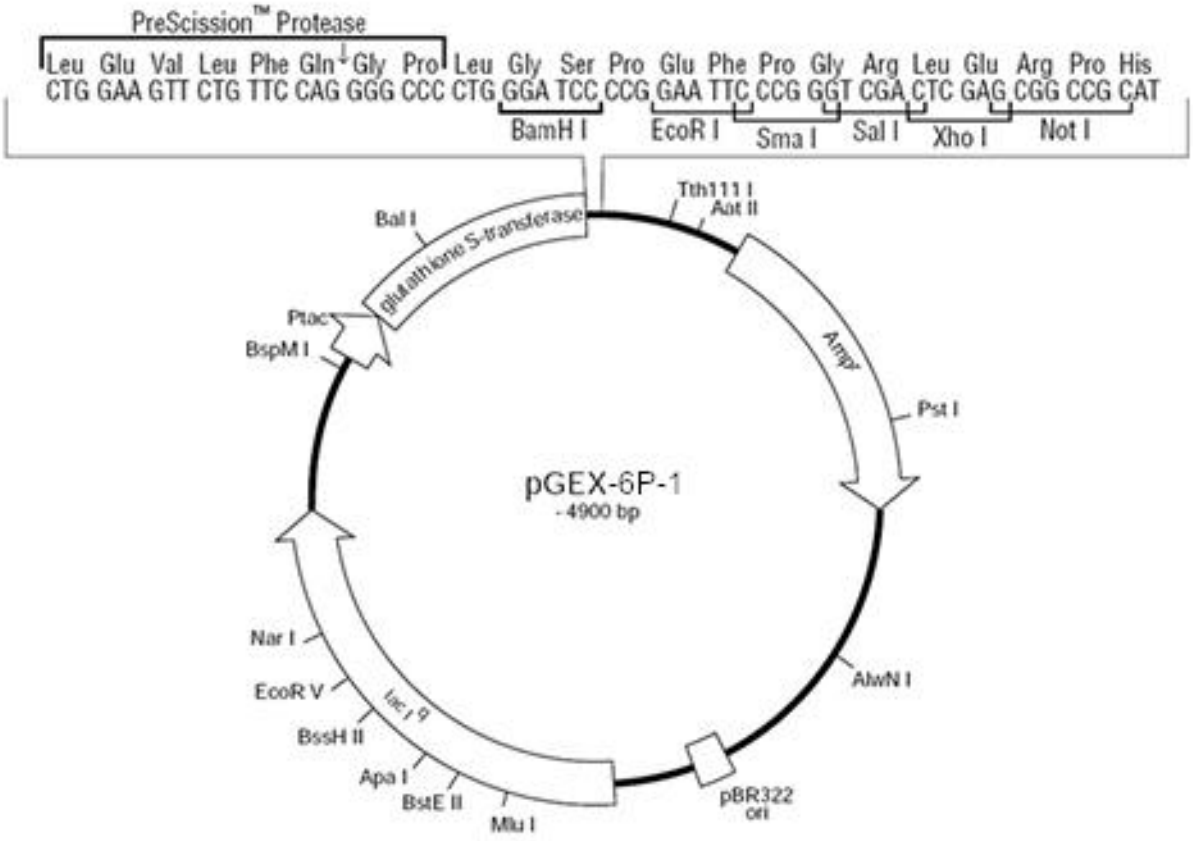

Appendix Figure 3. Map of the expression vector pGEX-6P-1 (https://www.lifescience-market.com/plasmid-c-94/pgex-6p-1-p-63185.html).

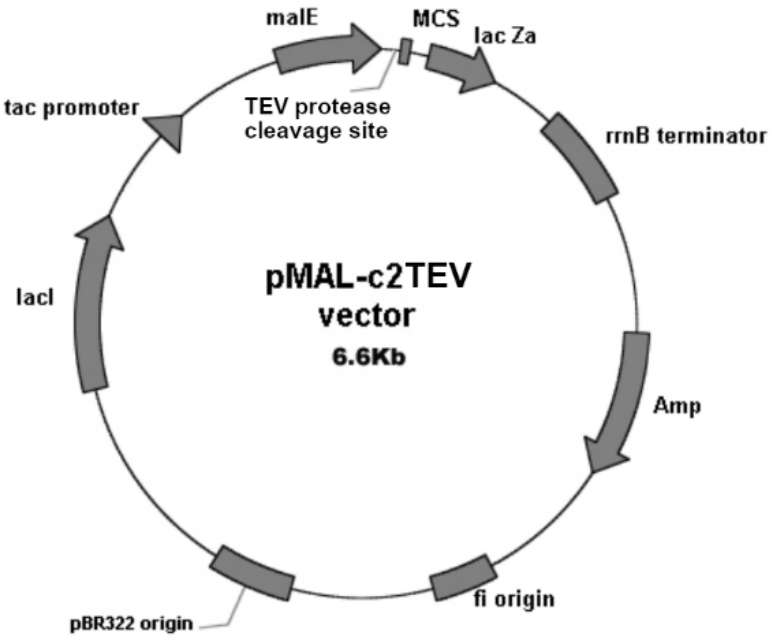

Appendix Figure 4. Map of the expression vector pMAL-c2TEV. (http://www.dingguo.com/Asset/emspics/UP_2012051106493313.pdf)

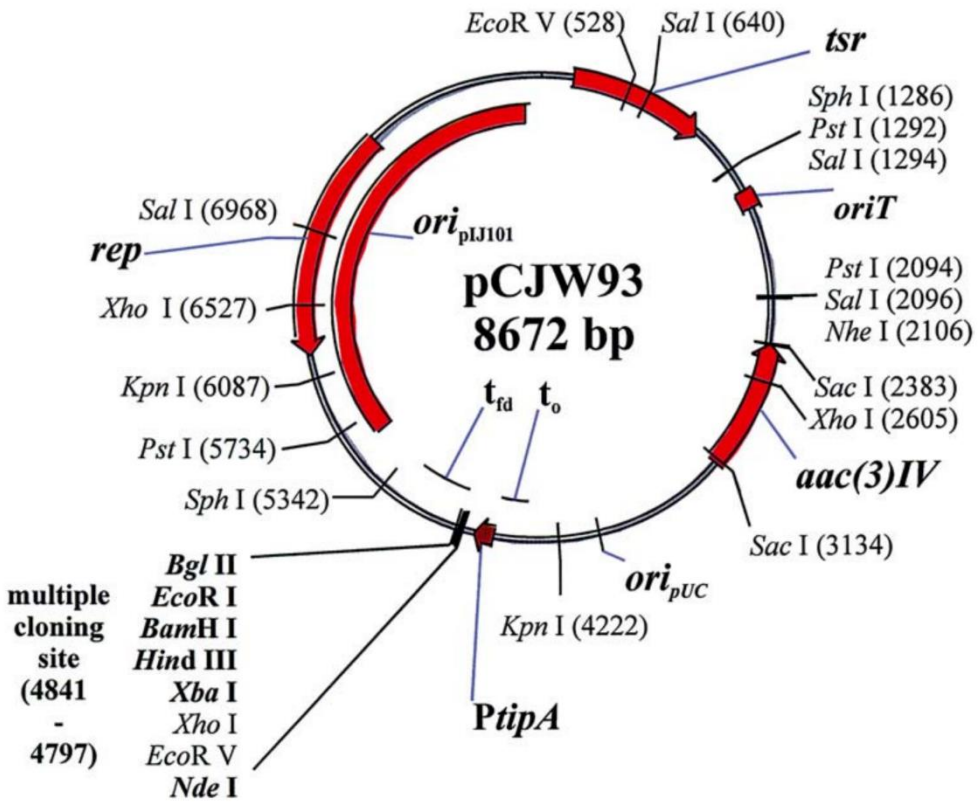

Appendix Figure 5. Map of the expression vector pCJW93 (Wilkinson et al. 2002).

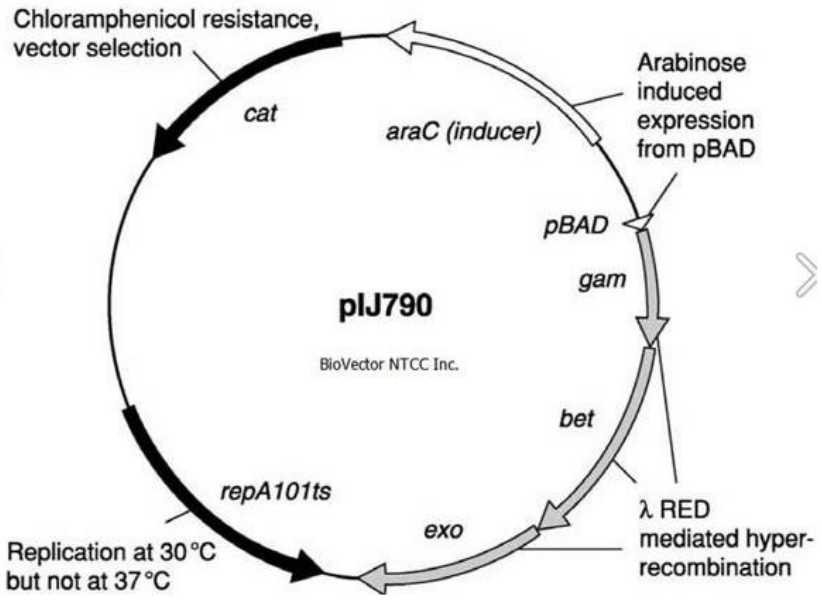

Appendix Figure 6. Map of the recombineering vector pIJ790 (http://www.bioon.com.cn/reagent/show_product.asp?id=4132920)

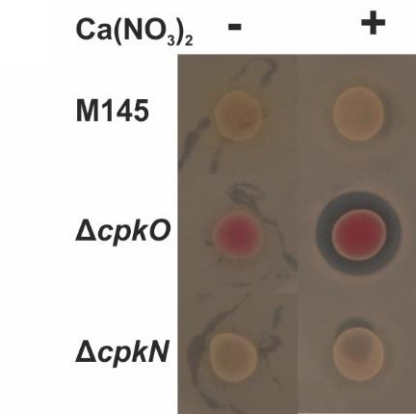

Appendix Figure 7. Calcium-dependent antibiotic (CDA) bioassay in *S. coelicolor* A3(2) M145, Δ*cpkO* and Δ*cpkN* (courtesy of Magdalena Kotowska, Institute of Immunology and Experimental Therapy). 20 µl of *S. coelicolor* A3(2) strains spore suspensions (OD_{600} = 0.3) were spotted on solid medium 79NG (20 ml of medium) and grown at 30°C for 27 h. The plates were then overlayed with 12 ml of soft nutrient agar (1% of agar) (Kieser et al. 2000) containing 32 mM $Ca(NO_3)_2$ mixed with 120 µl of overnight liquid culture of *Bacillus mycoides* PCM2009 indicator strain and incubated for 18 h. In the control plate $Ca(NO_3)_2$ was omitted.

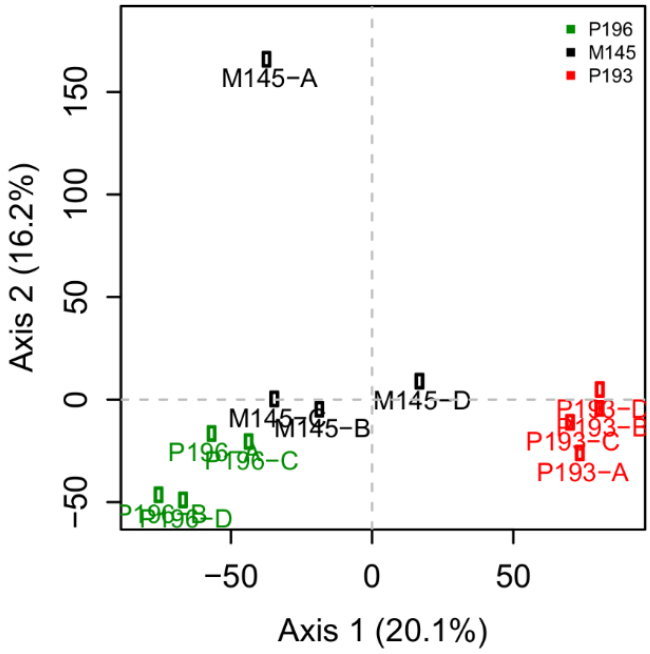

Appendix Figure 8. Primary component analysis as an indicator of proteomics sample preparation quality/reproducibility. Sample M145 A was excluded from further studies.

Appendix Table 1. List of all proteins quantified in *S. coelicolor* A3(2) M145, Δ*cpkO* and Δ*cpkN* strains by XIC, SC or PC quantification methods after proteomics data post-processing. Table information: Entry (UniProt) - primary (citable) protein accession number from UniProt, Ordered locus (UniProt) - SCO# number from UniProt designating gene order on the chromosome

Entry (UniProt)	Ordered locus (UniProt)	Protein names
Q9RI62	SCO0116	
Q9RI60	SCO0118	
Q9RIZ8	SCO0167	
Q9RIZ7	SCO0168	
Q9RIY6	SCO0179	
Q9RI47	SCO0199	
Q9RI46	SCO0200	
Q9RI43	SCO0203	
Q9RI42	SCO0204	
Q9RI40	SCO0208	
Q9RI35	SCO0213	
Q9RI32	SCO0216	
Q9RI31	SCO0217	
Q9S1R9	SCO0222	
Q9S1R2	SCO0229	
Q9S1P6	SCO0245	
Q9S1P5	SCO0246	
Q9S1P4	SCO0247	
Q9S2E4	SCO0256	
Q8CK64	SCO0259	
Q9RKA2	SCO0260	
Q9RK93	SCO0269	
Q9S2D7	SCO0276	
Q9S2D6	SCO0277	
Q9RL03	SCO0315	
Q9RJK9	SCO0379	
Q9RJK8	SCO0380	
Q9RJK6	SCO0382	
Q9RJK5	SCO0383	
Q9RJK4	SCO0384	
Q9RJK3	SCO0385	
Q9RJK2	SCO0386	
Q9RJK1	SCO0387	
Q9RJK0	SCO0388	
Q9RJJ7	SCO0391	
Q9RJJ6	SCO0392	
Q9RJJ5	SCO0393	
Q9RJJ4	SCO0394	
Q9RJJ3	SCO0395	
Q9RJJ2	SCO0396	
Q9RJJ0	SCO0398	
Q9RJI9	SCO0399	
Q9RJI8	SCO0400	
Q9RJI7	SCO0401	
Q9RJT1	SCO0405	
Q9RJS3	SCO0413	
Q9RL45	SCO0441	PxpA
Q9RJH2	SCO0462	
Q9RJG5	SCO0469	
Q9RJF5	SCO0479	
Q9RK14	SCO0492	
Q9RK13	SCO0493	
Q9RK12	SCO0494	
Q9RK11	SCO0495	
Q9RK08	SCO0498	
Q9RK07	SCO0499	
Q9RK06	SCO0500	
Q9RJM5	SCO0506	NadE
Q9RJL9	SCO0513	
Q9RJL5	SCO0520	
Q9RK83	SCO0526	
P48859	SCO0527	ScoF
Q9RK64	SCO0546	
Q9RJH9	SCO0560	KatG
Q93JH4	SCO0568	
Q93RZ5	SCO0575	PepE
Q9RJQ8	SCO0582	
Q9RJQ7	SCO0583	
Q9RJQ0	SCO0590	
Q9RJP8	SCO0592	
Q9R408	SCO0596	DpsA
Q9RJN7	SCO0607	
Q9RJN6	SCO0608	SlbR
Q9RD61	SCO0621	
Q8CK50	SCO0641	
Q9RJB9	SCO0645	
Q9RJ96	SCO0669	
Q9RK35	SCO0681	
Q9RK34	SCO0682	
Q9RK33	SCO0683	
Q9L2I7	SCO0722	
Q9EWU0	SCO0731	
Q9EWT1	SCO0740	
Q9RJD0	SCO0763	
Q9RJC6	SCO0767	
Q8CK46	SCO0769	
Q9EWS4	SCO0774	
Q7AKR5	SCO0775	
Q9EWS0	SCO0782	
Q9EWR4	SCO0788	
Q9RD80	SCO0797	
Q9RD74	SCO0803	
Q9RD73	SCO0804	
Q9RD72	SCO0805	
Q9XAA4	SCO0821	
Q9XA79	SCO0846	
Q9RCV9	SCO0852	
Q9RCV1	SCO0860	
Q9RCU8	SCO0863	
Q9RD38	SCO0871	
Q9RD26	SCO0884	
Q9RD25	SCO0885	TrxC
Q9RD22	SCO0888	
Q9RD05	SCO0906	
Q9RD03	SCO0908	
Q9RD01	SCO0910	EgtA
Q9RD00	SCO0911	EgtB
Q9RCZ9	SCO0912	EgtC
Q8CK43	SCO0913	EgtD
Q9RCY8	SCO0922	
Q9RCY2	SCO0928	
Q9RIV8	SCO0948	

Entry (UniProt)	Ordered locus (UniProt)	Protein names
Q9RIU9	SCO0957	
P72394	SCO0961	GlgC
Q9RIT6	SCO0971	
P58286	SCO0978	PanD
Q93J59	SCO0985	MetE
Q93J57	SCO0987	
Q9EX47	SCO0991	
Q9EX46	SCO0992	
Q9EX45	SCO0993	
Q9EX43	SCO0995	
Q9EX42	SCO0996	
Q9EX40	SCO0998	
Q7AKR0	SCO0999	SodF2
Q9EX32	SCO1008	
Q9EX27	SCO1013	
Q9EX20	SCO1020	
Q9K3N6	SCO1024	
Q9K3M1	SCO1039	
Q9K3K6	SCO1054	
Q9K426	SCO1073	
Q9K421	SCO1078	
Q9K419	SCO1080	
Q9K3R3	SCO1085	
Q9K3R1	SCO1087	
Q9K3R0	SCO1088	
Q9K3Q7	SCO1091	
Q9EX17	SCO1109	
Q9EX13	SCO1113	
Q9EX12	SCO1114	Ung1
Q9EX10	SCO1116	
Q9EX04	SCO1122	

Entry (UniProt)	Ordered locus (UniProt)	Protein names
Q9EWZ4	SCO1132	
Q9EWZ3	SCO1133	
Q9EWY2	SCO1144	
Q9KZI9	SCO1156	
Q9KZI3	SCO1162	
Q9KZI2	SCO1163	
Q9L0B8	SCO1169	XylA
Q9RK00	SCO1170	XylB
Q9RJZ6	SCO1174	ThcA
Q9RJY9	SCO1181	
Q9RJY8	SCO1182	
Q9RJY7	SCO1183	
Q9RJX3	SCO1197	
Q9RJX2	SCO1198	
Q9RJX1	SCO1199	
Q8CK36	SCO1201	
Q9FCA1	SCO1212	
Q9FC99	SCO1214	PfkA3
Q9FC98	SCO1215	
Q9FC91	SCO1222	
Q9FC90	SCO1223	
Q9FCD9	SCO1228	
Q9FCD8	SCO1229	
Q9FCD7	SCO1230	Tap
Q9FCC4	SCO1243	
Q9FCC3	SCO1244	BioB
Q9FCC2	SCO1245	BioA
Q9FCC1	SCO1246	BioD
Q8CK34	SCO1254	
Q9K3I0	SCO1260	
Q9K3H9	SCO1261	

Entry (UniProt)	Ordered locus (UniProt)	Protein names
Q9K3F2	SCO1289	
Q93IX6	SCO1294	
Q93IX4	SCO1296	
Q93IX0	SCO1300	
Q93IW6	SCO1304	
Q8CK32	SCO1319	
P40175	SCO1321	Tuf3
Q9K3Z8	SCO1335	
Q9K3Z6	SCO1337	
Q9K3Z3	SCO1340	
Q9K3Z0	SCO1343	Ung2
Q9K3Y8	SCO1345	
Q9K3Y7	SCO1346	
P0A3Z3	SCO1352	PepP2
Q9AKA1	SCO1361	
Q9AK96	SCO1366	
Q9AK91	SCO1371	
Q9AK88	SCO1374	
Q9KZQ0	SCO1382	
Q9KZP4	SCO1388	
Q9KZP3	SCO1389	
Q9KZN9	SCO1393	
Q9KZN7	SCO1395	
Q9KZN3	SCO1399	
Q9KZN1	SCO1401	
Q9KZN0	SCO1402	
Q9KZM8	SCO1404	
Q9KZM7	SCO1405	
Q9KZM6	SCO1406	
Q8CK29	SCO1407	
Q9RKW7	SCO1408	

Entry (UniProt)	Ordered locus (UniProt)	Protein names
Q9RKW9	SCO1410	
Q9RKY0	SCO1421	RbpA
Q9RKY1	SCO1422	
Q9RKY2	SCO1423	
Q9RKY3	SCO1424	
Q9RKY4	SCO1425	
Q9RKY7	SCO1428	
Q9RKZ2	SCO1434	
Q9EWK0	SCO1439	HisE
Q9EWJ9	SCO1440	RibH
Q9EWJ8	SCO1441	RibA
Q9EWJ6	SCO1443	Rib
Q9L106	SCO1453	
Q9L105	SCO1454	
Q9L104	SCO1455	
Q9L0Z8	SCO1461	
Q9L0Z5	SCO1464	Rpe
Q9L0Y9	SCO1470	
Q9L0Y7	SCO1472	
Q9L0Y6	SCO1473	Fmt
Q9L0Y3	SCO1476	MetK
Q8CK27	SCO1477	
Q9KXS1	SCO1478	RpoZ
Q9KXS0	SCO1479	Gmk
Q9KXR9	SCO1480	SihF
Q9KXR8	SCO1481	PyrF
Q9KXR7	SCO1482	PyrD
Q9KXR5	SCO1484	CarA
Q9KXR4	SCO1485	
Q9KXR3	SCO1486	PyrC
Q9KXR2	SCO1487	PyrB

Entry (UniProt)	Ordered locus (UniProt)	Protein names
Q9KXR1	SCO1488	PyrR
Q7AKQ8	SCO1489	BldD
Q9KXR0	SCO1490	NusB
Q9KXQ9	SCO1491	Efp
Q9KXQ6	SCO1494	AroB
Q9KXQ5	SCO1495	AroK
Q9KXQ1	SCO1499	MltG
Q9KXQ0	SCO1500	
Q9KXP8	SCO1502	
Q9KXP7	SCO1503	
Q9KXP4	SCO1506	
Q9KXP3	SCO1507	
Q9KXP2	SCO1508	HisS
Q9KXP1	SCO1509	
Q9KXP0	SCO1510	
P52560	SCO1513	RelA
P52561	SCO1514	Apt
Q9L292	SCO1517	
Q9L291	SCO1518	RuvB
Q9L290	SCO1519	RuvA
Q9L288	SCO1521	
Q9L287	SCO1522	PdxT
Q9L286	SCO1523	PdxS
Q9L285	SCO1524	
Q9L284	SCO1525	
Q9L283	SCO1526	
Q9L282	SCO1527	
Q9L280	SCO1529	
Q9L279	SCO1530	
Q9L269	SCO1540	
Q9L266	SCO1543	
Q8CK25	SCO1545	

Entry (UniProt)	Ordered locus (UniProt)	Protein names
Q9L1D4	SCO1548	
Q9L1D1	SCO1551	
Q9L1D0	SCO1552	
Q9L1C9	SCO1553	CysG
Q9L1C8	SCO1554	CobT
Q9L1C6	SCO1556	
Q9L1C5	SCO1557	
Q9L1C3	SCO1559	MetN
Q9L1C2	SCO1560	
Q9L1B9	SCO1563	
Q9L1B5	SCO1566	
Q9L1B3	SCO1568	
Q9L1B2	SCO1569	
Q9L1B1	SCO1570	ArgH
Q9L1B0	SCO1571	
O88055	SCO1595	PheS
O88058	SCO1598	RplT
O88059	SCO1599	RpmI
O88061	SCO1601	
O88062	SCO1602	
P14706	SCO1604	
O88066	SCO1609	
Q9RJ81	SCO1620	
Q9RJ80	SCO1621	
Q9RJ79	SCO1622	
Q9RJ78	SCO1623	
Q9RJ75	SCO1626	CvnE9
Q9RJ72	SCO1629	CvnB9
Q9RJ71	SCO1630	CvnA9
Q9RJ70	SCO1631	
Q9RJ68	SCO1633	TatA
Q9RJ65	SCO1636	

Entry (UniProt)	Ordered locus (UniProt)	Protein names
Q9RJ63	SCO1638	
Q9RJ62	SCO1639	
Q9RJ61	SCO1640	PafA
Q7AKQ6	SCO1643	PrcA
Q7AKQ5	SCO1644	PrcB
Q7AKQ4	SCO1646	Pup
O87595	SCO1647	
Q9RJ58	SCO1648	Arc
O87593	SCO1649	
Q9RJ57	SCO1651	
Q9RJ54	SCO1654	
Q9EWH3	SCO1657	
P15360	SCO1658	GylR
Q9ADA7	SCO1660	GlpK2
Q9ADA6	SCO1661	
Q9ADA5	SCO1662	
Q9ADA4	SCO1663	MshC
Q9ADA1	SCO1666	
Q9AD98	SCO1669	
Q9AD96	SCO1671	
Q9AD91	SCO1676	
Q9S261	SCO1691	
Q9S253	SCO1699	
Q9S252	SCO1700	
Q9S251	SCO1701	
Q9S247	SCO1705	
Q9S246	SCO1706	
Q9S2B5	SCO1715	HmgA
Q9S2A4	SCO1726	
Q9EWX6	SCO1750	
Q9EWX1	SCO1755	
Q9EWW7	SCO1759	

Entry (UniProt)	Ordered locus (UniProt)	Protein names
Q9EWW6	SCO1760	Cmk
Q8CK19	SCO1761	
Q9S234	SCO1766	
Q9S233	SCO1767	
Q9S232	SCO1768	
Q9S229	SCO1771	
Q9S228	SCO1772	
Q9S227	SCO1773	Ald
Q9S224	SCO1776	PyrG
Q9S223	SCO1777	
Q9S219	SCO1781	NadK2
Q9S218	SCO1782	
Q9S215	SCO1785	
Q9S213	SCO1787	
Q9S212	SCO1788	
Q9S211	SCO1789	
Q9S210	SCO1790	
Q9S208	SCO1792	
Q9X9Z8	SCO1794	
Q9X9Z6	SCO1796	
Q9X9Z4	SCO1798	
Q9X9Z3	SCO1799	
Q9AJX1	SCO1806	
Q9S281	SCO1808	
Q9S280	SCO1809	
Q9S274	SCO1815	
Q8CK16	SCO1816	
Q9RJ51	SCO1817	
Q9RJ48	SCO1820	
Q9RJ37	SCO1831	
Q9RJ30	SCO1838	
Q9RJ29	SCO1839	

Entry (UniProt)	Ordered locus (UniProt)	Protein names
Q9RJ28	SCO1840	
Q9RJ26	SCO1842	
Q9RJ21	SCO1847	CobD
Q9RJ20	SCO1848	CobQ
Q9RJ19	SCO1849	
Q9RJ18	SCO1850	
Q9RJ15	SCO1853	
Q93RX1	SCO1855	
Q93RX0	SCO1856	
Q93RW9	SCO1857	
Q93RW8	SCO1858	
Q93RW6	SCO1860	
Q93RW5	SCO1861	
Q93RW2	SCO1864	EctA
Q93RW1	SCO1865	EctB
Q93RW0	SCO1866	EctC
Q93RV9	SCO1867	EctD
Q93RV8	SCO1868	
Q93RV7	SCO1869	
Q93RV6	SCO1870	
Q93RV5	SCO1871	
Q93RV4	SCO1872	
Q93RV3	SCO1873	
Q9X9V5	SCO1917	
Q8CK13	SCO1919	
Q9XAD6	SCO1920	
Q9XAD5	SCO1921	Csd
Q9XAD4	SCO1922	
Q9XAD2	SCO1924	
Q9XAC8	SCO1928	
Q9XAB8	SCO1938	
Q9XAB7	SCO1939	Pgl
Q9Z523	SCO1942	Pgi2
Q9Z519	SCO1946	Pgk
Q9Z518	SCO1947	Gap
Q9Z514	SCO1951	
Q9Z513	SCO1952	
Q9Z512	SCO1953	UvrC
Q9Z508	SCO1957	
Q9Z507	SCO1958	UvrA
Q9Z506	SCO1959	
Q9Z505	SCO1960	
Q9Z502	SCO1964	
Q8CK11	SCO1966	UvrB
Q9S2L4	SCO1989	
Q9S2L2	SCO1991	
Q9S2L0	SCO1993	
Q9S2K7	SCO1996	CoaE
Q9S2K6	SCO1997	
Q9S2K0	SCO2003	PolA
Q9S2J9	SCO2004	
Q9S2J8	SCO2005	
Q9S2J5	SCO2008	
Q9S2J3	SCO2010	
Q9S2J1	SCO2012	
Q9S2J0	SCO2013	
Q9S2I9	SCO2014	
Q9S2I2	SCO2021	
Q9S2U8	SCO2034	Lgt1
O68816	SCO2036	TrpA
O05625	SCO2037	TrpB
Q9S2U2	SCO2043	TrpE
Q9S2U0	SCO2045	
Q9S2T7	SCO2048	HisF
P16249	SCO2051	HisH
P16247	SCO2052	HisB
P16246	SCO2053	HisC
Q9S2T2	SCO2057	
Q9S2S7	SCO2062	
Q9Z618	SCO2064	HnaE
Q9S2S3	SCO2067	
Q9R2D3	SCO2069	
Q9S2X8	SCO2073	
Q9S2X7	SCO2074	LspA
Q9S2X5	SCO2076	IleS
Q9S2X4	SCO2077	
Q9S2X2	SCO2079	SepF2
Q9S2X1	SCO2080	
P45497	SCO2081	
P45500	SCO2082	FtsZ
Q9ZBA5	SCO2084	MurG
Q9S2W9	SCO2086	MurD
Q9S2W4	SCO2092	RsmH
Q9S2W3	SCO2093	
Q9S2W0	SCO2096	
Q9S2V9	SCO2097	
Q9S2V8	SCO2098	
Q9S2V5	SCO2101	
Q9S2V3	SCO2103	
Q9S2V2	SCO2104	ThiE
Q8CK07	SCO2105	
Q9S2N3	SCO2110	
Q9S2N2	SCO2111	Nfo
Q9S2N0	SCO2113	Bfr
P80574	SCO2115	AroH
Q9S2M7	SCO2116	
Q9S2M4	SCO2120	
Q9S2M3	SCO2121	
Q9S2M0	SCO2124	
P0A4E1	SCO2126	GlkA
P40182	SCO2127	
Q9X7Y8	SCO2129	
Q9X7Z0	SCO2131	
Q9X7Z1	SCO2132	
O68608	SCO2147	TrpD1
Q9X806	SCO2148	QcrB
Q9X810	SCO2152	
Q9X815	SCO2157	
Q9X816	SCO2158	
Q9X819	SCO2161	
Q9F364	SCO2162	NadA
Q8CK05	SCO2164	
Q9S2R9	SCO2167	
Q9S2R8	SCO2168	
Q9S2R7	SCO2169	
Q9S2R4	SCO2172	
Q9S2R3	SCO2173	
Q9S2R1	SCO2175	CobT
Q9S2Q5	SCO2181	
Q9S2P5	SCO2191	
Q9S2P2	SCO2194	LipA
Q9S2P0	SCO2196	
Q9S2N9	SCO2197	
Q9S2N8	SCO2199	
Q8CK03	SCO2206	
Q7AKP2	SCO2210	
Q9KZ18	SCO2219	
Q9KZ12	SCO2225	

Entry (UniProt)	Ordered locus (UniProt)	Protein names
Q9KZ09	SCO2228	
Q7AKP1	SCO2231	
P72396	SCO2232	MalR
Q8CK02	SCO2234	GlnE
Q9Z4V7	SCO2235	
Q9ADI9	SCO2237	
Q9ADI8	SCO2238	NadE
Q9RDS4	SCO2243	
Q9RDR7	SCO2250	
Q9RKS2	SCO2256	PanB
Q9RKR9	SCO2259	
Q9RKR3	SCO2265	
Q9RKR2	SCO2266	Map
Q9RKQ8	SCO2270	
Q9RKQ0	SCO2278	
Q9RKP9	SCO2279	
Q9RKP6	SCO2282	
Q9RKP3	SCO2285	
Q9RKP1	SCO2287	
Q9L016	SCO2297	
Q9L015	SCO2298	
Q9L014	SCO2299	
Q9L012	SCO2301	
Q9KXK8	SCO2312	
Q9KXK4	SCO2316	
Q9KXK3	SCO2317	
Q9KXJ6	SCO2324	
Q9KXJ0	SCO2330	
Q9KXI2	SCO2338	
Q9KXI1	SCO2339	
Q9KY41	SCO2349	
Q9KY34	SCO2356	

Entry (UniProt)	Ordered locus (UniProt)	Protein names
Q9KY28	SCO2362	
Q9KY27	SCO2363	
Q9KY26	SCO2364	
Q9KY24	SCO2366	
Q9KY23	SCO2367	
Q9KY20	SCO2370	
Q9KY19	SCO2371	AceE
Q8CJZ8	SCO2373	
Q9RDQ7	SCO2377	
Q9RDQ4	SCO2380	
Q9RDQ0	SCO2384	
Q9RDP8	SCO2386	FasR
Q7AKN9	SCO2387	
P72392	SCO2388	FabH
Q7AKN8	SCO2389	AcpP
Q9RDP7	SCO2390	
Q9RDP4	SCO2393	
Q9RDP2	SCO2395	
Q9RDP0	SCO2397	
Q9RDN3	SCO2404	
Q9RDN2	SCO2405	
Q9RDN1	SCO2406	
Q9RDN0	SCO2407	
Q9L0A9	SCO2437	
Q9L0A8	SCO2438	
Q9L0A7	SCO2439	
Q9L0A6	SCO2440	
Q9L0A4	SCO2442	
Q9L0A2	SCO2444	
Q9L085	SCO2461	
Q9L2F2	SCO2464	
Q9S1N5	SCO2469	

Entry (UniProt)	Ordered locus (UniProt)	Protein names
Q9L2C9	SCO2490	
Q9RDC6	SCO2497	
Q9L2H5	SCO2508	
Q9L2H4	SCO2509	UppS1
Q9L2G6	SCO2517	EcrA2
Q9L2G5	SCO2518	EcrA1
Q9L2G4	SCO2519	EcrB
Q9L2G3	SCO2520	
Q9L2G1	SCO2522	
Q9L2G0	SCO2523	
Q9L2F9	SCO2524	
Q9L2F8	SCO2525	
O31046	SCO2528	LeuA
Q9L2L5	SCO2532	
Q8CJZ2	SCO2534	
Q9RDF3	SCO2538	
Q9RDF2	SCO2539	Era
Q9RDE5	SCO2546	
Q9RDE3	SCO2548	
Q9RDD8	SCO2553	
Q9RDD7	SCO2554	DnaJ2
Q9RDD6	SCO2555	HrcA
Q9RDD4	SCO2557	
Q9RDD2	SCO2559	
Q9RDD0	SCO2561	
Q9RDM2	SCO2564	
Q9RDL6	SCO2570	
Q9RDL0	SCO2576	
Q9RDK9	SCO2577	RsfS
Q9RDK7	SCO2579	NadD
Q9RDK4	SCO2582	
Q9RDK1	SCO2585	ProA

Entry (UniProt)	Ordered locus (UniProt)	Protein names
Q9RDJ9	SCO2587	ProB
Q9RDJ7	SCO2589	
Q8CJZ1	SCO2590	
Q9L1I4	SCO2592	
Q9L1I3	SCO2593	
P95722	SCO2595	ObgE
Q9L1I1	SCO2596	RpmA
Q9L1I0	SCO2597	RplU
Q9L1H8	SCO2599	
Q9L1H7	SCO2600	
Q9L1H5	SCO2602	
Q9L1H1	SCO2606	
Q9L1G9	SCO2608	Pbp2
Q9L1G8	SCO2609	MreD
Q9L1G7	SCO2610	MreC
Q9L1G6	SCO2611	MreB
Q8CJZ0	SCO2616	
Q9F316	SCO2617	ClpX
Q9ZH58	SCO2618	ClpP2
Q9F315	SCO2619	ClpP1
Q9F309	SCO2625	
Q9L206	SCO2627	
O51917	SCO2633	SodF1
Q9L201	SCO2634	
Q9L1Z8	SCO2637	
Q9L1Z4	SCO2641	
Q9L256	SCO2665	
Q9L255	SCO2666	
Q9L254	SCO2667	
Q9L253	SCO2668	
Q9L250	SCO2671	
Q9L245	SCO2676	

Entry (UniProt)	Ordered locus (UniProt)	Protein names
Q9L1J1	SCO2726	MsdA
Q8CJY6	SCO2730	
Q9RDJ2	SCO2733	
Q9RDI0	SCO2747	
Q9RDH9	SCO2748	RbsK
Q9RDH4	SCO2753	
Q9RDH3	SCO2754	
Q9RDG7	SCO2761	
Q9RDG5	SCO2763	
Q9RDG1	SCO2767	
Q9RDF9	SCO2769	
Q8CJY5	SCO2770	
Q9L082	SCO2771	
Q9L078	SCO2775	
Q9L077	SCO2776	AccD1
Q9L076	SCO2777	AccC
Q9L075	SCO2778	
Q7AKN2	SCO2779	AcdH
Q9L074	SCO2780	
Q9L069	SCO2785	
Q9L067	SCO2787	
Q9L062	SCO2792	BldH
P57666	SCO2793	Orn
Q9F3I7	SCO2794	
Q9F3I6	SCO2795	
Q9F3H5	SCO2806	
Q93J81	SCO2816	
Q93J75	SCO2822	
Q93J72	SCO2825	
Q9RDC3	SCO2828	
Q9RDC2	SCO2829	
Q9RDC0	SCO2831	
Q9RDB5	SCO2836	
Q9RDB4	SCO2837	
Q9RDB3	SCO2838	
Q9RDA8	SCO2843	
Q9RDA4	SCO2847	
Q9RDA2	SCO2849	
Q9RD96	SCO2855	
Q9RD88	SCO2863	
Q9KZS2	SCO2879	
Q9KZS1	SCO2880	
Q9KZR9	SCO2882	
Q9KZR8	SCO2883	
Q9KZR7	SCO2884	
Q9KZR6	SCO2885	
Q9KZR4	SCO2887	
Q9KZR0	SCO2893	
Q9KZQ4	SCO2899	
Q9KZQ2	SCO2901	
Q9S2H9	SCO2902	
Q9S2H8	SCO2903	
Q9S2H7	SCO2904	Rph
Q9S2H4	SCO2907	NagE2
Q9S2H3	SCO2908	
Q9S2H1	SCO2910	CysM
Q9S2H0	SCO2911	
Q9S2G8	SCO2913	
Q9S2G7	SCO2914	
Q9S2G6	SCO2915	
Q9S2G4	SCO2917	
Q9S2G3	SCO2918	
Q9S2G1	SCO2920	
Q9S2F6	SCO2925	
Q9S2F4	SCO2927	Hpd
Q9S2E8	SCO2936	
Q9L1R8	SCO2940	
Q9L1R7	SCO2941	
Q8CJY1	SCO2942	
Q9L1V1	SCO2943	
Q9L1U8	SCO2946	
Q9L1U7	SCO2947	
Q9L1U5	SCO2949	MurA
P0A3H5	SCO2950	Hup1
Q9L1U4	SCO2951	
Q9L1U3	SCO2952	
Q9L1T5	SCO2960	
Q9L1S7	SCO2968	
Q9L1S6	SCO2969	
P54740	SCO2973	PkaB
Q9L060	SCO2975	
Q9L057	SCO2978	
Q9L055	SCO2980	
Q9L049	SCO2986	
Q9L047	SCO2988	
Q9EWH8	SCO2996	
Q9KYX9	SCO3001	
Q9KYX3	SCO3008	
Q9KYX2	SCO3009	Hpf
Q9KYX0	SCO3011	LpqB
Q9KYW9	SCO3012	
Q9KYW8	SCO3013	
Q9KYW7	SCO3014	MtnA
Q9KYW6	SCO3015	
Q9KYW3	SCO3018	
Q9KZM1	SCO3023	AhcY
Q9KZM0	SCO3024	
Q9KZL9	SCO3025	
Q9KZL6	SCO3028	
Q9KZL1	SCO3033	
Q9KZK9	SCO3036	CofD
Q9KZK8	SCO3037	FbiB
Q9KZK4	SCO3041	
Q93J54	SCO3048	
Q93J53	SCO3049	
Q93J51	SCO3052	
Q93J48	SCO3055	
Q8CJX8	SCO3060	PurK
Q9RIS7	SCO3066	PrsI
Q9RIS6	SCO3067	ArsI
Q9KZ78	SCO3070	HutI
Q9KZ77	SCO3071	
Q9KZ76	SCO3072	
Q9KZ75	SCO3073	HutU
Q9KZ74	SCO3074	
Q9KZ73	SCO3075	
Q9KZ71	SCO3077	
Q9KZ69	SCO3079	
Q9KZ60	SCO3089	
Q9KZ58	SCO3091	Cfa
Q8CJX7	SCO3092	
Q9F2Q6	SCO3093	
Q9F2Q5	SCO3094	
Q9F2P9	SCO3100	
Q9F2P8	SCO3101	
Q9F2P6	SCO3104	
Q9F2P1	SCO3109	Mfd
Q9F2N9	SCO3111	

Entry (UniProt)	Ordered locus (UniProt)	Protein names
Q9F2N5	SCO3115	
Q9F2N2	SCO3118	
Q8CJX6	SCO3122	GlmU
Q9K3T9	SCO3124	RplY
Q9K3T8	SCO3125	Pth
Q9RNU9	SCO3127	Ppc
Q9K3S8	SCO3136	GalK
Q9K3S6	SCO3138	
Q9K3R9	SCO3145	
Q9K3R8	SCO3146	
Q9K3R5	SCO3149	RsmA
Q9RKD6	SCO3151	
Q9RKD4	SCO3153	RsmI
Q9RKD3	SCO3154	
Q9RKD1	SCO3156	
Q9RKD0	SCO3157	
Q9RKC5	SCO3162	
Q9RKC2	SCO3165	
Q9RKC1	SCO3166	
Q9RKC0	SCO3167	
Q9RKB3	SCO3174	
Q9RKB2	SCO3175	
Q9RKA9	SCO3179	
Q9RKA7	SCO3181	
Q9KYV7	SCO3188	
Q9KYV1	SCO3194	
Q9KYU0	SCO3206	
Q9Z4X1	SCO3210	
Q9Z4X0	SCO3211	TrpC2
Q9Z4W9	SCO3212	TrpD2
Q9Z4W8	SCO3213	TrpG
Q9Z4W7	SCO3214	TrpE2
Q9Z4W6	SCO3215	GlmT
Q9Z4W5	SCO3216	
Q9Z389	SCO3217	CdaR
Q9Z388	SCO3218	
Q9Z4W3	SCO3221	
Q9S6T6	SCO3224	
Q7AKM3	SCO3226	AbsA2
Q8CJX3	SCO3227	HpgT
Q9Z4X8	SCO3228	Hmo
Q9Z4X7	SCO3229	HmaS
Q9Z4X6	SCO3230	CdaPS1
Q9Z4X5	SCO3231	CdaPS2
Q8CJX2	SCO3232	CdaPS3
Q9Z4Z8	SCO3233	
Q9Z4Z7	SCO3234	HasP
Q9Z4Z6	SCO3235	
Q9Z4Z5	SCO3236	AsnO
Q9Z4Z4	SCO3237	
Q9Z4Z3	SCO3238	
Q9Z4Z2	SCO3239	
Q9Z4Z1	SCO3240	
Q9Z4Z0	SCO3241	
Q9Z4Y9	SCO3242	
Q9Z4Y8	SCO3243	
Q9Z4Y7	SCO3244	
Q9Z4Y6	SCO3245	HcmO
Q9Z4Y5	SCO3246	FabH2
Q9Z4Y4	SCO3247	HxcO
Q9Z4Y3	SCO3248	FabF3
Q9Z4Y2	SCO3249	Acp
Q9X8D2	SCO3259	
Q9X8D4	SCO3261	
Q9X8E2	SCO3269	
Q9X8E6	SCO3273	
Q9X8E8	SCO3275	
Q9X8F5	SCO3282	
Q9X877	SCO3285	
Q9X878	SCO3286	
Q9X890	SCO3298	
Q9X893	SCO3301	
Q9X894	SCO3302	
Q9X895	SCO3303	LysS
Q9WX27	SCO3306	
Q9WX26	SCO3307	
Q9WX25	SCO3308	
P54919	SCO3311	HemB
Q9WX18	SCO3316	
Q9WX16	SCO3318	HemC1
Q9WX14	SCO3320	Rex
Q9WX12	SCO3322	
Q9WX11	SCO3323	BldN
Q9WX10	SCO3324	RsbN
Q9WX09	SCO3325	
Q9WX08	SCO3326	
Q9WX06	SCO3328	BdtA
Q9WX01	SCO3333	
Q8CJX0	SCO3334	TrpS1
Q9X8G1	SCO3337	ProC
Q9X8G4	SCO3340	
Q9X8G6	SCO3342	
Q9X8L6	SCO3352	DisA
Q9S6T7	SCO3355	
Q9X8M3	SCO3366	
Q9X8M4	SCO3367	
Q9X8M6	SCO3369	
Q9X8N1	SCO3375	Lsr2
Q9X8N6	SCO3380	CoaX
Q9X8N7	SCO3381	
Q9X8N8	SCO3382	NadB
Q9X844	SCO3383	PanC
Q9X845	SCO3384	
Q9X8H8	SCO3398	
Q9X8I1	SCO3401	
Q9X8I3	SCO3403	FolE
Q9X8I5	SCO3405	
Q9X8I6	SCO3406	TilS
Q9X8I7	SCO3407	
Q9X8J2	SCO3412	
Q9X8K0	SCO3421	
Q9RKG4	SCO3473	
Q9RKG3	SCO3474	
Q9RKG2	SCO3475	
Q9RKG1	SCO3476	
Q9RKF9	SCO3478	
Q9RKF8	SCO3479	
Q9RKF7	SCO3480	
Q9RKF3	SCO3484	
Q9RKF2	SCO3485	
Q9RKF1	SCO3486	
Q9RKF0	SCO3487	
Q8CJW4	SCO3500	
Q9X8B3	SCO3538	
Q9X908	SCO3542	Tmk
Q9X909	SCO3543	TopA
Q9X914	SCO3548	
Q9WVX8	SCO3549	RsbV

Entry (UniProt)	Ordered locus (UniProt)	Protein names
Q9X929	SCO3564	NhaA3
Q9X930	SCO3565	
Q9X931	SCO3566	
Q9XA45	SCO3568	
Q9XA44	SCO3569	Nth
Q9XA40	SCO3573	
Q9XA38	SCO3575	
Q9XA36	SCO3577	
Q9XA35	SCO3578	
Q8CJW2	SCO3580	
Q9X935	SCO3582	
Q9XAJ5	SCO3607	
Q9XAJ4	SCO3608	
Q9XAJ1	SCO3611	
Q9XAI8	SCO3614	Asd
Q9XAI5	SCO3617	
Q9XAI4	SCO3618	RecR
Q9XAI3	SCO3619	
Q9XAI1	SCO3621	
Q9X8P6	SCO3629	PurA
Q9X8R1	SCO3644	KynB
Q9X8R2	SCO3645	KynU
Q9X8R3	SCO3646	KynA
Q9X8R8	SCO3651	
Q9X8R9	SCO3652	
Q9X8S5	SCO3658	
Q8CJV9	SCO3661	ClpB
Q9KYQ8	SCO3662	
Q9KYQ6	SCO3664	
Q9KYQ3	SCO3667	
P40170	SCO3669	DnaJ1
Q9X8V5	SCO3673	
Q9X8V8	SCO3676	
Q9X8V9	SCO3677	
Q9X8W0	SCO3678	Dcd
Q9L0X7	SCO3727	
Q9L0X3	SCO3731	
Q9L0X2	SCO3732	
Q7AKL2	SCO3748	
Q9F2M0	SCO3761	
Q9F2L5	SCO3766	
Q9F2L4	SCO3767	
Q9F2L3	SCO3768	
Q9F2K2	SCO3779	
Q9F2J9	SCO3782	
Q9F2I9	SCO3792	MetG
Q9F325	SCO3793	
Q9F324	SCO3794	
Q8CJV6	SCO3800	
Q9XA76	SCO3801	ApeB
Q9XA70	SCO3807	
Q9XA66	SCO3811	
Q9XA62	SCO3815	
Q9XA57	SCO3820	
Q9S2C0	SCO3821	PksC
Q9XA56	SCO3822	
Q9XA55	SCO3823	
Q9XA52	SCO3826	
Q9XA50	SCO3828	
Q8CJV5	SCO3831	
Q9XA31	SCO3833	
Q9XA30	SCO3834	
Q9XA29	SCO3835	
Q9XA25	SCO3839	
Q9XA24	SCO3840	
Q9XA23	SCO3841	
Q9XA21	SCO3843	FhaA
Q9XA19	SCO3845	
Q9XA18	SCO3846	
Q9XA13	SCO3851	
Q9XA09	SCO3855	
Q9XA08	SCO3856	
Q9XA07	SCO3857	
Q9XA06	SCO3858	UppS2
Q9XA02	SCO3862	
Q9KXX6	SCO3872	
P36176	SCO3876	RecF
Q7AKL1	SCO3877	
P27902	SCO3879	DnaA
O54569	SCO3883	YidC
Q7BUY9	SCO3884	Jag
O54571	SCO3885	RsmG
Q9S6U0	SCO3886	
Q9S6U1	SCO3887	
P52230	SCO3889	TrxA
P52215	SCO3890	TrxB
Q9X8S9	SCO3893	
Q9X8T0	SCO3894	
Q9X8T2	SCO3896	
Q9X8T5	SCO3899	
Q9X8T6	SCO3900	
Q9X8T9	SCO3903	
Q9X8U2	SCO3906	RpsF
Q9X8U3	SCO3907	Ssb2
P66470	SCO3908	RpsR1
Q9X8U8	SCO3912	
Q9X8U9	SCO3913	
Q9X9T9	SCO3929	
Q9X9T6	SCO3932	
Q9ZBZ0	SCO3940	
Q7AKK9	SCO3941	
Q9ZBY8	SCO3944	Pat
Q9ZBY7	SCO3945	
Q9ZBY5	SCO3947	
Q9ZBY2	SCO3950	
Q9ZBY1	SCO3951	
Q9ZBX5	SCO3957	
Q9ZBX4	SCO3958	
Q9ZBX2	SCO3960	
Q9ZBX1	SCO3961	SerS
Q9ZBW9	SCO3963	
Q8CJV1	SCO3964	
Q93J40	SCO3966	
Q93J39	SCO3967	
Q93J33	SCO3974	
Q93J30	SCO3977	
Q93J28	SCO3979	
Q9ADQ7	SCO3998	
Q9ADP9	SCO4006	
Q9ADP6	SCO4009	
Q9ADN7	SCO4020	
Q9ADN0	SCO4028	
Q9ADM5	SCO4033	
Q9ADM4	SCO4034	SigN
P37977	SCO4036	
Q9AK78	SCO4039	
Q9AK76	SCO4041	Upp
Q9AK69	SCO4048	

Entry (UniProt)	Ordered locus (UniProt)	Protein names
Q9AK68	SCO4049	
Q9AK67	SCO4050	
Q9AK59	SCO4058	
Q9RKL5	SCO4067	DnaX
Q9RKL3	SCO4069	
Q9RKL2	SCO4070	
Q7AKK4	SCO4075	
Q9RKK7	SCO4077	PurS
Q7AKK3	SCO4086	PurF
Q7AKK2	SCO4087	PurM
Q9RKJ8	SCO4088	
Q9RKJ4	SCO4092	
Q9RKJ0	SCO4096	
Q8CJU8	SCO4109	
Q9F305	SCO4111	TrmB
Q9F303	SCO4113	
Q7AKK1	SCO4114	
Q9KYE8	SCO4122	
Q9KYE4	SCO4126	
Q9KYE3	SCO4127	
Q9KYE2	SCO4128	
Q9KYE1	SCO4129	
Q9KYE0	SCO4130	
Q9KYD7	SCO4133	
Q9KZW5	SCO4136	
Q9KZV6	SCO4145	Ppk
Q9KZV0	SCO4151	MshD
Q9KZU5	SCO4156	
Q05954	SCO4158	
Q9KZT9	SCO4163	
Q8CJU5	SCO4164	CysA
Q9K4H3	SCO4165	

Entry (UniProt)	Ordered locus (UniProt)	Protein names
Q9K4F9	SCO4179	
Q9K4F7	SCO4181	
Q9K4F4	SCO4186	
Q9FCH3	SCO4196	
Q9FCH1	SCO4198	
Q9FCH0	SCO4199	
Q9FCG5	SCO4204	MshA
Q9FCG2	SCO4207	
Q9FCF7	SCO4213	
Q9FCE6	SCO4224	
Q8CJU3	SCO4228	PhoU
Q9L0R1	SCO4230	PhoP
Q9L0R0	SCO4231	
Q9L0Q9	SCO4232	
Q9L0Q8	SCO4233	IspD
Q9L0Q6	SCO4235	CysS
Q9L0Q5	SCO4236	
Q9L0Q3	SCO4238	
Q9L0P9	SCO4242	
Q9L0P8	SCO4243	
Q9L0P6	SCO4245	
Q9L0P4	SCO4247	
Q9L0P3	SCO4248	
Q9L0P0	SCO4251	
Q9L0N8	SCO4253	
Q9L0N7	SCO4254	
Q9L0N6	SCO4255	
Q9L0N5	SCO4256	
Q9L0N3	SCO4258	
Q9L0N2	SCO4259	
Q8CJU2	SCO4260	
Q9K4F1	SCO4261	

Entry (UniProt)	Ordered locus (UniProt)	Protein names
Q9KXW1	SCO4280	
Q9KXW0	SCO4281	
Q9KXV9	SCO4282	
Q9KXV8	SCO4283	
Q9KXV5	SCO4286	
Q9KXV3	SCO4288	
Q9KXV1	SCO4290	
Q9KXU7	SCO4294	
Q9KXU6	SCO4295	ScoF4
Q9KXU5	SCO4296	GroL2
Q9KXU4	SCO4297	
Q9KXU3	SCO4298	
Q9KXT4	SCO4307	MurQ
Q9KXT0	SCO4311	
Q9KXS9	SCO4312	
Q9KXS8	SCO4313	
Q9KXS7	SCO4314	
Q9KXS5	SCO4316	
Q9KXN6	SCO4321	
Q9KXN4	SCO4323	
Q9KXN2	SCO4325	
Q9KXN1	SCO4326	MqnD
Q9KXM7	SCO4330	
Q9KXM6	SCO4331	
Q9KXM5	SCO4332	EcrC
Q8CJU0	SCO4346	
Q9F2Z0	SCO4357	
Q9K3X3	SCO4371	
Q9K3V7	SCO4387	PdxH
Q9K3V6	SCO4388	
Q9K3V4	SCO4390	
Q7AKJ7	SCO4394	DmdR1

Entry (UniProt)	Ordered locus (UniProt)	Protein names
Q9K3V0	SCO4395	
Q9K3U8	SCO4397	
Q9K3U3	SCO4402	
Q9F379	SCO4409	
Q9F377	SCO4411	
Q9F371	SCO4417	
P54741	SCO4423	AfsK
P25941	SCO4426	AfsR
Q9KZZ7	SCO4429	FbiC
Q9KZZ0	SCO4436	
Q9KZY7	SCO4439	
Q9KZY6	SCO4440	
Q9KZY5	SCO4441	
Q9KZY2	SCO4444	
Q9KZX6	SCO4450	
Q9KZX3	SCO4453	
Q9F2S2	SCO4467	
Q9F2R8	SCO4471	
Q9F2R7	SCO4472	
Q9F2R5	SCO4474	
Q9F2R4	SCO4475	
Q9KYP5	SCO4488	
Q9KYP0	SCO4493	
Q9L0U8	SCO4496	
Q9L0U6	SCO4498	
Q9L0T9	SCO4505	
Q9L0T8	SCO4506	MqnA
Q9L0T6	SCO4508	HfkA
Q9L0T5	SCO4509	
Q9L0S9	SCO4515	
Q9L0S0	SCO4524	
Q9L0R9	SCO4525	

Entry (UniProt)	Ordered locus (UniProt)	Protein names
Q9L0R8	SCO4526	
Q9L0R7	SCO4527	
Q9F3F9	SCO4541	
Q9F3F8	SCO4543	
Q9XD94	SCO4545	
Q9F3F7	SCO4546	
Q8CJT3	SCO4548	
Q9XAQ0	SCO4558	
Q9XAQ1	SCO4559	
Q9XAQ2	SCO4560	Def3
Q9XAQ5	SCO4563	NuoB1
Q9XAQ6	SCO4564	NuoC
Q9XAQ7	SCO4565	NuoD2
Q9XAQ8	SCO4566	
Q9XAQ9	SCO4567	NuoF
Q9XAR0	SCO4568	NuoG
Q9XAR1	SCO4569	NuoH
Q9XAR2	SCO4570	NuoI1
Q9XAR3	SCO4571	
Q9XAR5	SCO4573	NuoL
Q9XAR6	SCO4574	
Q9XAR7	SCO4575	NuoN
Q9XAR9	SCO4577	
Q9XAS2	SCO4580	
Q9F2X8	SCO4583	
Q9F2X7	SCO4584	
Q9F2X6	SCO4585	
Q9F2X4	SCO4587	
Q9F2X1	SCO4590	
Q9F2W8	SCO4593	
Q9F2W7	SCO4594	
Q9F2W6	SCO4595	
Q9F2W5	SCO4596	AbrC3
Q8R5N2	SCO4601	
Q9F2V5	SCO4606	
Q9F2V2	SCO4609	HtpX2
Q9F2V1	SCO4610	
Q04296	SCO4628	
Q9L0M9	SCO4631	
Q9L0M7	SCO4633	
P66233	SCO4635	RpmG2
Q9L0M3	SCO4637	
Q9L0L9	SCO4641	
Q9L0L7	SCO4643	MurB
P0A4G8	SCO4646	SecE
P0A463	SCO4648	RplK
P41109	SCO4651	
P41103	SCO4652	RplJ
P41102	SCO4653	RplL
Q9L0K6	SCO4657	
Q9L0K5	SCO4658	
P0A4A3	SCO4659	RpsL
P40174	SCO4662	Tuf1
Q9L0J7	SCO4668	
Q9L0J6	SCO4669	
Q9L0J3	SCO4672	
Q9L0J2	SCO4673	
Q9L0J1	SCO4674	
Q9L0J0	SCO4675	
Q9L0G5	SCO4677	
Q9L0G4	SCO4678	
Q9L0G2	SCO4680	
Q9L0G1	SCO4681	
Q9L0G0	SCO4682	
Q9L0F9	SCO4683	GdhA
Q9L0F5	SCO4687	
Q9L0F3	SCO4689	
Q9L0F0	SCO4692	
P66337	SCO4701	RpsJ
Q9L0E0	SCO4702	RplC
Q9L0D9	SCO4703	RplD
Q9L0D4	SCO4708	RpsC
Q9L0D3	SCO4709	RplP
Q9L0D2	SCO4710	RpmC
Q9L0D1	SCO4711	RpsQ
Q9L0D0	SCO4712	RplN
Q9L0C9	SCO4713	RplX
P66417	SCO4715	RpsZ
P49399	SCO4716	RpsH
P46788	SCO4718	RplR
P46787	SCO4721	RplO
P46785	SCO4722	SecY
P43414	SCO4723	Adk
Q7AKJ0	SCO4724	Map
P60515	SCO4725	InfA
O86773	SCO4727	RpsM
P72403	SCO4728	RpsK
O86777	SCO4732	
Q53874	SCO4734	RplM
O86780	SCO4739	
O86782	SCO4741	
O86783	SCO4742	NnrE
O86786	SCO4745	Alr
O86791	SCO4750	
O86793	SCO4752	TsaD
O86795	SCO4754	
P0A345	SCO4761	GroS
P40171	SCO4762	GroL1
O86803	SCO4764	
Q9L0I7	SCO4770	GuaB
Q9L0I3	SCO4774	
Q9L0I1	SCO4776	
Q9L0I0	SCO4777	
Q9L0H8	SCO4779	
Q9L0H2	SCO4785	GuaA
Q9KY72	SCO4792	
Q9KY67	SCO4797	
Q9KY52	SCO4812	
Q9KY51	SCO4813	PurN
Q9K3J6	SCO4824	FolD
Q9K3J5	SCO4825	
Q9K3J3	SCO4827	Mdh
Q9K3J1	SCO4829	
Q9K3J0	SCO4830	
Q9K3I9	SCO4831	
Q9KZB1	SCO4835	
Q9KZA9	SCO4837	GlyA
Q9KZ99	SCO4847	
Q9KZ96	SCO4850	
Q9KZ89	SCO4857	
Q9EWE6	SCO4861	
Q9EWD8	SCO4869	
Q9EWD6	SCO4871	
Q9AK42	SCO4884	
Q9AK41	SCO4885	
Q9AK40	SCO4886	
Q9AK39	SCO4887	
Q9AK36	SCO4890	

Entry (UniProt)	Ordered locus (UniProt)	Protein names
Q9AK31	SCO4895	
Q9AK25	SCO4901	Add1
Q9AK21	SCO4905	
Q04943	SCO4906	AfsQ2
Q04942	SCO4907	AfsQ1
Q9EWV0	SCO4912	
Q9AD83	SCO4914	
Q9EWV1	SCO4915	
Q9AD82	SCO4916	
Q9EWF0	SCO4919	
Q9AD80	SCO4920	
Q9EWV4	SCO4921	
Q9EWV6	SCO4923	
Q7AKI7	SCO4926	PccB
P40135	SCO4928	Cya
Q9EWW2	SCO4934	
Q9EWF1	SCO4945	
Q9ADK5	SCO4955	
Q9EWF7	SCO4956	MsrA
Q9EWF8	SCO4957	
Q9EWG2	SCO4961	
Q9AD75	SCO4963	
Q9ADK0	SCO4967	Mca
Q9EWG4	SCO4968	
Q9EWG5	SCO4969	
Q9EWG8	SCO4972	
Q9EWH0	SCO4975	
Q93JL5	SCO4979	PckG
Q93JK8	SCO4986	
Q93JK7	SCO4987	
Q93JK6	SCO4988	
Q93JK5	SCO4989	

Entry (UniProt)	Ordered locus (UniProt)	Protein names
Q93JK4	SCO4990	
Q93JK3	SCO4991	
Q93JK0	SCO4994	
Q93JJ8	SCO4996	
Q9KY97	SCO5005	
Q9KY96	SCO5006	
Q9KY93	SCO5009	
Q9KY88	SCO5014	
Q9KY80	SCO5022	
Q9KY78	SCO5024	
Q9KY76	SCO5026	
Q9FBP8	SCO5028	
Q7AKI6	SCO5031	AhpD
Q9FBP5	SCO5032	AhpC
Q9FBP3	SCO5034	
Q9FBN9	SCO5039	
Q9FBN8	SCO5040	
Q9FBN6	SCO5042	FumC
Q9FBN4	SCO5044	
Q9FBN2	SCO5047	
Q9FBN1	SCO5048	
Q9FBM4	SCO5055	XseB
Q9FBM1	SCO5058	IspH
Q9ADE8	SCO5059	
Q93IZ3	SCO5077	ActVA-2
Q7AKH8	SCO5079	ActVA-4
Q93IY5	SCO5100	
Q93IY4	SCO5101	
Q93IY1	SCO5104	
Q93IU3	SCO5112	
Q93IU1	SCO5114	
Q93IU0	SCO5115	

Entry (UniProt)	Ordered locus (UniProt)	Protein names
Q9F348	SCO5122	
Q9F344	SCO5126	MshB
Q9F342	SCO5128	
Q9F334	SCO5136	
Q9FBL9	SCO5139	
Q9FBL8	SCO5140	
Q9FBL3	SCO5145	
Q9FBK7	SCO5151	
Q9FBK0	SCO5158	
Q9FBJ7	SCO5161	
Q9FBJ4	SCO5164	
Q9FBJ2	SCO5166	
Q9FBJ1	SCO5167	
Q9FBI9	SCO5169	
Q9FBI8	SCO5170	
Q9FBI7	SCO5172	
Q9FCL0	SCO5178	MoeB
Q9FCK2	SCO5186	
Q9FCK1	SCO5187	
Q9FCJ6	SCO5192	
Q9FCJ3	SCO5195	
Q9FCJ2	SCO5196	
Q9FCJ1	SCO5197	
Q9FCI9	SCO5199	
Q9FCI8	SCO5200	
Q9FCI5	SCO5203	
Q9K4B1	SCO5208	HisN
Q9K4A8	SCO5211	RsgA
Q9K4A5	SCO5214	
Q7AKG9	SCO5216	SigR
Q9K4A0	SCO5221	Def4
Q9K3C2	SCO5225	NrdB

Entry (UniProt)	Ordered locus (UniProt)	Protein names
Q9K496	SCO5226	
Q9K494	SCO5229	
Q9K492	SCO5231	DasR
Q9K491	SCO5232	
Q9K487	SCO5236	NagB
Q9F3M0	SCO5241	
Q9RIT0	SCO5243	SigH
Q9R3X8	SCO5244	PrsH
Q9F3L5	SCO5249	EshB
Q9F3L3	SCO5251	
Q9F3L2	SCO5252	
P80735	SCO5254	SodN
Q9F3K9	SCO5256	
Q9F3K8	SCO5257	
Q9F3K7	SCO5258	
Q9F3K6	SCO5259	
Q9F3K5	SCO5260	
Q9F3K4	SCO5261	
Q9F3K3	SCO5262	
Q9F3K1	SCO5264	
Q9F3K0	SCO5265	
Q9F3J0	SCO5275	
Q9FBR2	SCO5283	
Q9EVK2	SCO5285	Lon
Q9FBQ8	SCO5288	
Q9XAE0	SCO5291	
Q9XAE1	SCO5292	
Q9XAG1	SCO5312	
Q9XAH0	SCO5330	
Q9XAH1	SCO5331	
Q8CJR7	SCO5332	
Q9ADD1	SCO5336	

Entry (UniProt)	Ordered locus (UniProt)	Protein names
Q9ADD0	SCO5337	
Q9ADB5	SCO5353	LysA
Q9ADB2	SCO5356	ThrB
Q8CJR6	SCO5357	Rho
Q9K4E3	SCO5361	PrmC
P0A302	SCO5366	AtpI
Q9K4D8	SCO5367	AtpB
P0A304	SCO5368	AtpE
Q9K4D0	SCO5381	
Q9K4C6	SCO5385	
Q9K4C3	SCO5388	NucS
Q9K4C2	SCO5389	
Q9K4B9	SCO5392	
Q9K4B8	SCO5393	
Q9K4B6	SCO5395	
Q9K4B5	SCO5396	FilP
Q9L2C3	SCO5397	
Q9L2C2	SCO5398	
Q9L2C1	SCO5399	
Q9L2C0	SCO5400	
Q9L2B5	SCO5405	
Q9L2B4	SCO5406	
Q9L2B2	SCO5408	
Q9L2B1	SCO5409	
Q9L2A2	SCO5420	
Q9L298	SCO5424	AckA
Q8CJR5	SCO5425	Pta
Q9L1K5	SCO5439	
Q59833	SCO5440	GlgB1
Q8CJR4	SCO5444	
Q9L1E7	SCO5458	
Q9L1E1	SCO5464	
Q9L1E0	SCO5465	
O86564	SCO5469	SdaA
O86566	SCO5471	GcvH
O86567	SCO5472	GcvT
O86569	SCO5474	
O86570	SCO5475	
O86571	SCO5476	
O86573	SCO5478	
O86575	SCO5480	
O86583	SCO5488	MnmA
Q9Z589	SCO5490	
Q9Z588	SCO5491	
Q9Z587	SCO5492	
Q9Z585	SCO5494	LigA1
Q9Z582	SCO5497	
Q9Z581	SCO5498	GatC
Q9Z576	SCO5503	
Q9Z575	SCO5504	
Q9Z571	SCO5508	
Q9Z569	SCO5510	
Q9Z567	SCO5512	
Q9Z564	SCO5515	
Q9Z560	SCO5519	PutA
O86504	SCO5522	LeuB
O86505	SCO5523	IlvE
O86515	SCO5533	
O86517	SCO5535	AccB
O86518	SCO5536	AccE
O86519	SCO5537	
O86520	SCO5538	
O86521	SCO5539	
O86522	SCO5540	
Q9R7V6	SCO5541	
O86523	SCO5542	
O86524	SCO5543	
O86525	SCO5544	CvnA1
O86526	SCO5545	
O86533	SCO5552	NdgR
O86534	SCO5553	LeuC
O86535	SCO5554	LeuD
P0A3H7	SCO5556	Hup2
O86538	SCO5557	
Q9ZBS0	SCO5559	GpsA
Q9ZBR9	SCO5560	Ddl
Q9ZBR8	SCO5561	
Q9ZBR7	SCO5562	ThiL
Q9ZBR6	SCO5563	ThiD
Q9ZBR5	SCO5564	RpmB1
Q9ZBR1	SCO5568	CoaD
Q9ZBR0	SCO5569	
Q9ZBQ9	SCO5570	
Q9ZBQ6	SCO5573	MutM
Q9ZBP7	SCO5582	NsdA
O69874	SCO5586	Ffh
O69878	SCO5590	
P0A4Q4	SCO5592	
O69886	SCO5598	
O69893	SCO5605	
O69896	SCO5608	
O69913	SCO5626	PyrH
O86770	SCO5627	Frr
O86768	SCO5629	
O86763	SCO5636	
O86754	SCO5645	RlmN
O86753	SCO5646	
O86750	SCO5649	
O86748	SCO5651	
O86747	SCO5652	
O86744	SCO5655	
O86742	SCO5657	
O86738	SCO5661	
O86737	SCO5662	
O86736	SCO5663	
Q8CJI6	SCO5677	
Q9KYS1	SCO5694	Dxr
Q9KYS0	SCO5695	
Q9KYR9	SCO5696	IspG2
Q9KYR2	SCO5703	RimP
Q9KYR1	SCO5704	NusA
Q9Z528	SCO5709	TruB
Q9Z530	SCO5711	
O86637	SCO5717	
O86639	SCO5719	
Q7AKF6	SCO5723	BldB
O86643	SCO5724	
O86644	SCO5725	
O86647	SCO5728	
O86648	SCO5729	
O86650	SCO5731	
O86653	SCO5734	
O86654	SCO5735	
O86655	SCO5736	RpsO
Q8CJQ6	SCO5737	Pnp
O86835	SCO5738	
O86836	SCO5739	DapB
O86838	SCO5741	

Entry (UniProt)	Ordered locus (UniProt)	Protein names
O86840	SCO5743	ThyX
O86841	SCO5744	DapA2
O86808	SCO5748	OsaA
O86809	SCO5749	OsaB
O86811	SCO5751	RodZ
O86812	SCO5752	RimO
O86819	SCO5759	
O50487	SCO5769	RecA
O50492	SCO5774	
O50493	SCO5775	
O50495	SCO5777	
O69959	SCO5783	
O69963	SCO5787	MiaB
O69964	SCO5788	
O69967	SCO5791	MiaA
O69969	SCO5793	DapF
O69972	SCO5796	HflX
O69974	SCO5798	
O69978	SCO5802	
O69979	SCO5803	LexA
O69980	SCO5804	NrdR
O69981	SCO5805	NrdJ
O69985	SCO5809	
O69990	SCO5813	
O69992	SCO5815	
O69994	SCO5817	
O70007	SCO5831	
O50510	SCO5836	
O50516	SCO5842	
O50517	SCO5843	
O50518	SCO5844	
O50528	SCO5854	
O50529	SCO5855	
O50531	SCO5857	
O50533	SCO5859	HemH
Q8CJQ3	SCO5860	
P0A4I1	SCO5862	CutR
P0A4I7	SCO5863	CutS
O54130	SCO5864	
O54133	SCO5867	
O54134	SCO5868	Dut
O54140	SCO5874	
O54141	SCO5875	
Q53949	SCO5876	TrkA
O54142	SCO5878	
O54143	SCO5879	RedW
Q7AKF4	SCO5881	
O54147	SCO5884	
O54149	SCO5886	
O54153	SCO5890	
O54155	SCO5892	
O54156	SCO5893	
O54158	SCO5895	
Q8CJQ2	SCO5896	
O54095	SCO5897	
O54099	SCO5901	
O54116	SCO5920	
O54181	SCO5952	
Q93JF6	SCO5971	
Q93JF2	SCO5975	ArcA
Q93JE5	SCO5982	
Q8CJP9	SCO5998	
Q7AKF3	SCO5999	SacA
Q93RY8	SCO6003	
O50499	SCO6005	
O50502	SCO6008	Rok7B7
O50503	SCO6009	
O50504	SCO6010	
O50505	SCO6011	
Q8CJP7	SCO6013	Dxs2
O69849	SCO6019	
O69856	SCO6026	
O69857	SCO6027	
O69858	SCO6028	
O69860	SCO6030	
O69869	SCO6039	
Q8CJP6	SCO6041	
O69834	SCO6046	
O69840	SCO6052	
Q9X824	SCO6057	
Q9X827	SCO6060	MurC
Q9X828	SCO6061	
Q9X829	SCO6062	
Q9X832	SCO6065	
Q9X833	SCO6066	
Q9X835	SCO6068	
Q9X836	SCO6069	
Q9X837	SCO6070	
Q9X842	SCO6076	
Q9ADI5	SCO6078	TreZ
Q9ADI0	SCO6083	
Q9ADH9	SCO6084	
Q9ADH8	SCO6085	
Q9ADH2	SCO6091	
Q9ADG9	SCO6094	SsuC
Q9ADG7	SCO6096	SsuA
Q9ADG6	SCO6097	CysN
Q9ADG5	SCO6098	CysD
Q9ADG4	SCO6099	CysC
Q9ADG3	SCO6100	CysH
Q9ADG1	SCO6102	SirA/CysI
Q9ADF7	SCO6106	
Q9ADF4	SCO6109	
Q9Z556	SCO6116	
Q9Z551	SCO6121	
Q9Z539	SCO6133	
Q9Z538	SCO6134	
Q9ZBU1	SCO6147	XyoA
Q9ZBU0	SCO6148	
Q9ZBS6	SCO6162	
Q9ZBS5	SCO6163	
Q9ZBS4	SCO6164	
Q8CJP0	SCO6165	
Q9ZBP3	SCO6166	
Q9Z5A7	SCO6195	MACS1
Q9Z5A6	SCO6196	FadD1
Q9Z5A4	SCO6198	
Q9Z597	SCO6205	GlxR
Q8CJN8	SCO6211	
Q9RKV8	SCO6218	
O86587	SCO6222	
O86589	SCO6224	
Q9RKU9	SCO6243	AceB1
Q9RKU5	SCO6247	AllB
Q9RKU4	SCO6248	AlC
Q9RKT5	SCO6257	
Q9RKT2	SCO6260	
Q7AKF1	SCO6265	ScbR

Entry (UniProt)	Ordered locus (UniProt)	Protein names
Q7AKF0	SCO6266	ScbA
Q9RKS7	SCO6267	ScbB
Q9RKS5	SCO6269	CpkPβ
Q9RKS4	SCO6270	CpkPα
Q9EX55	SCO6272	ScF
Q9EX54	SCO6273	CpkC
Q9EX53	SCO6274	CpkB
Q8CJN6	SCO6275	CpkA
Q93S13	SCO6276	CpkD
Q93S12	SCO6277	CpkE
Q93S11	SCO6278	CpkF
Q93S10	SCO6279	CpkG
Q93S09	SCO6280	CpkO
Q93S08	SCO6281	CpkH
Q93S07	SCO6282	CpkI
Q93S06	SCO6283	CpkJ
Q93S05	SCO6284	CpkK
Q93S03	SCO6286	ScbR2
Q9LAS9	SCO6287	ScoT
Q93RY4	SCO6288	CpkN
Q93RY0	SCO6292	
Q93RX9	SCO6293	
O86608	SCO6339	
O86609	SCO6340	
O86610	SCO6341	
O69937	SCO6409	Map
O69939	SCO6411	
Q8CJN1	SCO6412	
O69817	SCO6423	LplA
Q9ZBH4	SCO6439	
Q9ZBG8	SCO6445	
Q9ZBG4	SCO6449	

Entry (UniProt)	Ordered locus (UniProt)	Protein names
Q9ZBG1	SCO6452	
Q9ZBF9	SCO6454	
Q9ZBF7	SCO6456	
Q8CJM8	SCO6465	
Q9ZBK8	SCO6466	
Q9ZBK6	SCO6468	Psd
Q9ZBK5	SCO6469	
Q9ZBK0	SCO6474	
Q9ZBJ2	SCO6482	
Q9ZBJ0	SCO6484	
Q9ZBI7	SCO6487	
Q9ZBI6	SCO6488	
Q9ZBI5	SCO6489	DppA
Q8CJM7	SCO6492	
Q9ZC20	SCO6493	
O86699	SCO6517	
O86713	SCO6531	
O86718	SCO6536	
O86731	SCO6549	
Q9ZBW7	SCO6551	
Q9ZBV4	SCO6564	FabH4
Q9ZBV3	SCO6565	
O69954	SCO6579	
O87848	SCO6593	
O86540	SCO6606	
O86552	SCO6618	
O86555	SCO6621	
O86557	SCO6623	
O86560	SCO6626	
O86678	SCO6631	
O86679	SCO6632	
O86682	SCO6635	

Entry (UniProt)	Ordered locus (UniProt)	Protein names
O86683	SCO6636	
Q7AKE6	SCO6637	
O86684	SCO6638	
O86685	SCO6639	
O86689	SCO6643	
O86695	SCO6649	
O88014	SCO6658	
O88016	SCO6660	
O88017	SCO6661	Zwf
O88018	SCO6662	Tal1
O88019	SCO6663	
Q9XAH7	SCO6687	
Q9XAN4	SCO6696	
Q9XAM9	SCO6701	PcaF
Q9XAL3	SCO6717	
Q9X7N7	SCO6731	
Q9X7N8	SCO6732	
Q9X7P2	SCO6736	
Q9X7P8	SCO6742	
Q9X7P9	SCO6743	
Q9X7Q1	SCO6745	
Q9X7Q6	SCO6750	Idi
Q8CJL9	SCO6752	
Q9WW65	SCO6753	
Q9X7U9	SCO6754	
Q9X7V0	SCO6755	
Q9X7V1	SCO6756	
Q9X7V2	SCO6757	
Q9X7V3	SCO6758	
Q9X7V5	SCO6760	
Q9X7V7	SCO6762	
Q9X7V8	SCO6763	

Entry (UniProt)	Ordered locus (UniProt)	Protein names
Q9X7V9	SCO6764	
Q9X7W1	SCO6766	
Q9X7W3	SCO6768	Dxs1
Q9X7W4	SCO6769	
Q9X7W7	SCO6772	
Q9X7X1	SCO6776	
Q9L233	SCO6799	Tdh
Q9L232	SCO6800	Kbl
Q9L221	SCO6811	
Q9L216	SCO6816	
Q9L214	SCO6818	GpmI
Q9L213	SCO6819	AroA2
Q9L211	SCO6821	
Q8CJL8	SCO6824	
Q9L1W0	SCO6825	
Q9L1V9	SCO6826	
Q9L1V8	SCO6827	
Q9L1V7	SCO6828	
Q9L1Q3	SCO6862	
Q9KYC4	SCO6906	
Q9KYJ3	SCO6948	
Q9KZC9	SCO6960	
Q9KZC3	SCO6966	
Q9KZC2	SCO6967	PcaF
Q9KZC1	SCO6968	
Q9KZB8	SCO6971	
Q8CJL4	SCO6975	
Q9KZH4	SCO6978	
Q9KZH3	SCO6979	
Q9KZH2	SCO6980	
Q9KZH1	SCO6981	
Q9KZH0	SCO6982	

Entry (UniProt)	Ordered locus (UniProt)	Protein names
Q9KZG9	SCO6983	
Q9KZG4	SCO6988	
Q9L033	SCO7022	
Q9L027	SCO7028	
Q9L024	SCO7031	
Q8CJL2	SCO7034	
P24532	SCO7036	ArgG
Q9FC43	SCO7040	
Q9FC27	SCO7057	
Q9FC18	SCO7066	FadH
Q9FC12	SCO7072	
Q9FC11	SCO7073	
Q9FC84	SCO7102	
Q9FC63	SCO7123	
Q8CJL0	SCO7137	
Q9FBV0	SCO7141	
Q9FBS4	SCO7168	
Q8CJK8	SCO7173	
Q9FBY9	SCO7193	
Q9FBY5	SCO7197	
Q9K467	SCO7218	
Q9K466	SCO7219	
Q9K4H9	SCO7246	
Q9X7U7	SCO7252	
Q9X7T2	SCO7268	Add2
Q9X7T1	SCO7269	
Q9X7S9	SCO7271	
Q9X7R6	SCO7284	RnhA
Q9X7R4	SCO7286	
Q9K4M2	SCO7292	
Q9K4L8	SCO7296	
Q9K4L7	SCO7297	
Q9K4L6	SCO7298	
Q9K4L5	SCO7299	
Q9K4L4	SCO7300	
Q9K4L0	SCO7304	
Q9K4J4	SCO7320	
Q9K4J3	SCO7321	
Q8CJK4	SCO7322	
Q9KY15	SCO7323	
Q9KY14	SCO7324	
Q9KY13	SCO7325	
Q9KY11	SCO7327	
Q9KY00	SCO7343	HemC2
Q9KYM9	SCO7356	
Q9KYM7	SCO7358	
Q9KYM1	SCO7366	
Q9L178	SCO7399	
Q9L177	SCO7400	
Q9L173	SCO7404	
Q9L142	SCO7417	
Q9L141	SCO7418	
Q9L139	SCO7420	
Q9L138	SCO7421	
Q9L137	SCO7422	
Q9L131	SCO7428	
Q9L124	SCO7436	
Q9L117	SCO7443	
Q9ADJ5	SCO7464	
Q9ADJ4	SCO7465	
Q9ADJ2	SCO7467	
Q93JC7	SCO7469	
Q93JC6	SCO7470	
Q93JC5	SCO7471	
Q93JC4	SCO7472	
Q93JC3	SCO7473	
Q93JC2	SCO7474	
Q93JC1	SCO7475	
P58481	SCO7516	HtpG
Q93J01	SCO7519	
Q9KYZ3	SCO7536	
Q9KYZ0	SCO7539	
Q9F3C1	SCO7554	
Q9F395	SCO7580	
Q9F389	SCO7586	
Q9F387	SCO7588	
Q9F3E9	SCO7608	
Q9F3E0	SCO7617	
Q7AKC7	SCO7629	
Q9F3Q7	SCO7630	
Q9F3Q5	SCO7632	
Q9F3P9	SCO7638	Eno2
Q9F3N5	SCO7652	
Q9F3N4	SCO7653	
Q9F3N3	SCO7654	
Q9F3N2	SCO7655	
Q9F3N0	SCO7657	
Q9AJZ8	SCO7730	
Q9AJZ5	SCO7733	
Q9FBX5	SCO7809	

Appendix Table 2. Proteomic comparison of *S. coelicolor* A3(2) M145, Δ*cpkO* and Δ*cpkN* strains - proteins with statistically significant abundance changes (ANOVA-adjusted p value < 0.01). Table information: Entry (UniProt) - primary (citable) protein accession number from UniProt, Ordered locus (UniProt) - SCO# number from UniProt designating gene order on the chromosome. Quantification methods: XIC - in log10, the sum of MS1 peak intensities (expressed as the sum of surface area under the peaks) of all peptides assigned to a protein, SC - the number of MS2 spectra assigned to a protein, PC - the number of MS1 chromatogram peaks assigned to a protein. *Abundance ratio could not be calculated (NA) if the protein was not detected in M145 strain.

			Abundance			Quantification	Abundance ratio*		
Entry (UniProt)	Ordered locus (UniProt)	Protein names	ΔcpkN mean	M145 mean	ΔcpkO mean	method	ΔcpkN/M145	ΔcpkO/M145	ANOVA-adjusted p value
Q9RI62	SCO0116		6.80	6.47	6.71	XIC	2.12	1.72	0.005879358
Q9RIZ8	SCO0167		0.75	0.33	3.50	SC	2.25	10.5	0.007178997
Q9RIZ7	SCO0168		2.00	0.33	7.25	SC	6.00	21.75	4.83526E-06
Q9RIY6	SCO0179		7.30	7.12	7.94	XIC	1.49	6.59	0.00412016
Q9RI47	SCO0199		7.58	7.22	8.04	XIC	2.29	6.63	0.006792997
Q9RI46	SCO0200	UspA	3.25	2.33	10.00	SC	1.39	4.29	8.61078E-05
Q9RI43	SCO0203	OsdK	2.75	6.00	9.75	SC	0.46	1.63	0.001631922
Q9RI42	SCO0204	OsdR	8.03	7.88	8.41	XIC	1.41	3.40	0.007647983
Q9RI40	SCO0208		2.00	2.00	6.25	PC	1.00	3.13	0.006011215
Q9RI35	SCO0213	NarK2	0.00	0.00	2.75	SC	NA	NA	0.000128036
Q9RI32	SCO0216	NarG2	9.00	3.67	22.75	SC	2.45	6.20	9.78944E-12
Q9RI31	SCO0217	NarH2	1.50	0.00	6.00	SC	NA	NA	2.913E-06
Q9RK93	SCO0269		0.25	4.67	4.25	SC	0.05	0.91	0.000198898
Q9S2D7	SCO0276		7.33	7.68	6.98	XIC	0.45	0.20	0.006009422
Q9RL03	SCO0315		9.00	15.33	18.00	SC	0.59	1.17	0.009780509
Q9RJK9	SCO0379	CatA	9.39	10.04	9.41	XIC	0.23	0.24	9.47629E-05
Q9RJK6	SCO0382		7.94	8.03	8.39	XIC	0.82	2.30	0.009255314
Q9RJK5	SCO0383		7.30	7.61	8.14	XIC	0.48	3.34	8.44918E-05
Q9RJK3	SCO0385		0.25	4.00	7.00	SC	0.06	1.75	1.89485E-06

Q9RJK2	SCO0386		7.14	7.49	7.80	XIC	0.44	2.05	0.000890241
Q9RJK1	SCO0387		7.00	20.00	31.50	SC	0.35	1.58	7.73093E-14
Q9RJK0	SCO0388		6.88	7.34	7.75	XIC	0.35	2.57	0.001200023
Q9RJJ7	SCO0391		0.00	0.33	4.25	SC	0.00	12.75	5.45534E-06
Q9RJJ6	SCO0392		7.86	8.25	8.66	XIC	0.41	2.61	0.000482347
Q9RJJ5	SCO0393		7.09	7.32	7.69	XIC	0.58	2.34	0.006952851
Q9RJJ4	SCO0394		7.07	7.39	7.72	XIC	0.48	2.15	0.003529369
Q9RJJ3	SCO0395		8.13	8.58	8.96	XIC	0.36	2.41	5.12891E-05
Q9RJJ2	SCO0396		7.06	7.49	7.94	XIC	0.37	2.80	0.001405833
Q9RJJ0	SCO0398		7.45	7.80	8.06	XIC	0.44	1.82	0.002037399
Q9RJI9	SCO0399		6.52	6.86	7.22	XIC	0.46	2.29	0.00873209
Q9RJI8	SCO0400		7.14	7.50	7.98	XIC	0.44	3.02	0.001781999
Q9RJI7	SCO0401		6.99	7.45	7.79	XIC	0.35	2.23	0.006129385
Q9RJH2	SCO0462		7.74	8.09	8.03	XIC	0.45	0.88	0.001801338
Q9RK14	SCO0492		25.50	8.67	25.25	SC	2.94	2.91	4.13566E-07
Q9RK12	SCO0494		9.04	8.85	8.83	XIC	1.53	0.94	0.000719009
Q9RK11	SCO0495		7.66	7.35	7.33	XIC	2.05	0.97	0.007036601
Q9RK08	SCO0498		17.00	7.00	10.00	SC	2.43	1.43	0.002079034
Q9RJH9	SCO0560	CatC	9.04	9.22	9.19	XIC	0.66	0.94	0.009884252
Q9RJQ7	SCO0583		0.50	2.33	10.25	SC	0.21	4.39	6.50366E-10
Q9RJP8	SCO0592		0.50	2.00	6.50	SC	0.25	3.25	2.20153E-05
Q9RD61	SCO0621		6.77	7.08	6.34	XIC	0.49	0.18	0.00705484
Q9RK35	SCO0681		45.25	43.00	23.50	SC	1.05	0.55	1.3746E-06
Q9RK33	SCO0683		1.00	4.00	6.50	SC	0.25	1.63	0.000858809
Q9RJD0	SCO0763		7.45	7.59	7.80	XIC	0.72	1.63	0.000331081
Q8CK46	SCO0769		7.95	8.12	8.22	XIC	0.67	1.26	0.00137016
Q9EWS4	SCO0774		7.25	7.61	7.84	XIC	0.44	1.73	0.002247519
Q9RD73	SCO0804		7.78	7.99	8.07	XIC	0.62	1.22	0.004855111
Q9XAA4	SCO0821		7.06	7.30	7.73	XIC	0.57	2.66	0.001499171
Q9RD25	SCO0885	TrxC	8.00	8.37	7.80	XIC	0.43	0.27	0.000969869

Q9RD22	SCO0888		8.35	9.28	7.97	XIC	0.12	0.05	3.79036E-05
Q9RCZ9	SCO0912	EgtC	7.31	7.63	7.71	XIC	0.49	1.22	0.003529369
Q8CK43	SCO0913	EgtD	8.17	8.47	8.57	XIC	0.51	1.26	0.000265561
Q9RIV8	SCO0948	Am1	7.17	7.41	7.37	XIC	0.58	0.92	0.006598498
Q9RIU9	SCO0957		7.71	7.23	7.03	XIC	3.00	0.64	0.000121904
P72394	SCO0961	GlgC	0.00	0.00	3.00	SC	NA	NA	5.1764E-05
P58286	SCO0978	PanD	8.02	7.87	7.56	XIC	1.42	0.49	0.003979309
Q93J59	SCO0985	MetE	7.25	13.67	23.00	SC	0.53	1.68	4.13566E-07
Q9EX46	SCO0992		7.30	7.70	8.14	XIC	0.41	2.78	0.000265876
Q9EX45	SCO0993		8.21	8.43	8.73	XIC	0.60	1.98	0.001504742
Q9EX43	SCO0995		7.92	8.19	8.42	XIC	0.54	1.70	0.005463046
Q9K3N6	SCO1024		11.00	4.33	14.00	SC	2.54	3.23	0.000786589
Q9K426	SCO1073		8.59	8.51	8.38	XIC	1.21	0.75	0.008948284
Q9K3R3	SCO1085		8.27	8.03	7.83	XIC	1.72	0.63	0.002640316
Q9EX17	SCO1109		0.50	6.33	0.00	SC	0.08	0.00	3.21372E-08
Q9EX10	SCO1116		8.82	8.67	8.62	XIC	1.43	0.89	0.001126952
Q9EX04	SCO1122		7.29	7.25	7.87	XIC	1.08	4.14	0.001405833
Q9EWZ4	SCO1132		1.50	17.33	4.25	SC	0.09	0.25	7.51139E-13
Q9EWZ3	SCO1133		6.75	7.47	6.73	XIC	0.19	0.18	9.18942E-05
Q9EWY2	SCO1144		7.30	7.31	7.93	XIC	0.99	4.21	0.002040251
Q9KZI2	SCO1163		7.36	7.47	7.65	XIC	0.78	1.51	0.008664653
Q9RK00	SCO1170	XylB	7.70	7.77	7.89	XIC	0.84	1.32	0.006036551
Q9RJZ6	SCO1174	ThcA	8.55	8.97	8.75	XIC	0.38	0.60	0.00965747
Q9FC91	SCO1222		7.00	7.36	8.19	XIC	0.43	6.71	0.00065728
Q9FC90	SCO1223		7.94	8.11	8.83	XIC	0.67	5.20	0.002928101
Q9FCD8	SCO1229		6.53	6.73	6.71	XIC	0.63	0.95	0.006405492
Q9FCD7	SCO1230	Tap	1.50	4.33	0.25	SC	0.35	0.06	0.001895262
Q9FCC3	SCO1244	BioB	9.17	8.42	7.96	XIC	5.69	0.35	8.15932E-06
Q9FCC2	SCO1245	BioA	8.36	7.89	7.17	XIC	2.99	0.19	6.68645E-06
Q9FCC1	SCO1246	BioD	8.22	7.70	6.93	XIC	3.36	0.17	5.82078E-05

Q9K3F2	SCO1289		1.25	5.67	7.25	SC	0.22	1.28	0.000412308
Q93IX6	SCO1294		8.70	8.34	9.13	XIC	2.30	6.22	8.05729E-05
P40175	SCO1321	Tuf3	3.75	3.00	0.00	SC	1.25	0.00	0.000143708
Q9KZP4	SCO1388		8.88	8.99	9.20	XIC	0.77	1.61	0.001302369
Q9KZM8	SCO1404		14.00	8.33	18.25	SC	1.68	2.19	0.009730079
Q9RKY7	SCO1428		17.00	22.00	29.00	SC	0.77	1.32	0.009730079
Q9EWJ8	SCO1441	RibA	7.38	6.90	6.57	XIC	2.97	0.47	0.000529627
Q9EWJ6	SCO1443	Rib	8.10	8.03	7.75	XIC	1.19	0.53	0.003246341
Q9L0Y3	SCO1476	MetK	9.22	9.23	9.51	XIC	0.97	1.91	0.001126952
Q9KXP1	SCO1509		6.95	6.56	6.91	XIC	2.47	2.25	0.004697702
Q9L290	SCO1519	RuvA	7.27	7.41	7.79	XIC	0.73	2.38	0.002009855
Q9L287	SCO1522	PdxT	8.25	7.90	7.66	XIC	2.26	0.57	0.00040408
Q9L1C9	SCO1553	CysG	8.79	8.34	7.87	XIC	2.87	0.34	6.26071E-05
O88059	SCO1599	RpmI	9.39	8.14	8.28	XIC	18.04	1.40	2.56857E-05
Q9RJ80	SCO1621		8.15	7.83	7.79	XIC	2.13	0.93	0.001899255
Q9RJ78	SCO1623		8.48	8.28	8.15	XIC	1.57	0.74	0.006792997
Q9RJ75	SCO1626	CvnE9	6.62	7.50	7.36	XIC	0.13	0.72	0.002343005
Q9RJ72	SCO1629	CvnB9	6.74	7.55	7.07	XIC	0.15	0.33	0.001200023
Q9RJ71	SCO1630	CvnA9	7.30	8.11	7.68	XIC	0.15	0.37	0.001281959
Q9RJ61	SCO1640	PafA	8.62	8.72	8.91	XIC	0.80	1.56	0.001053079
Q7AKQ6	SCO1643	PrcA	8.80	9.09	9.00	XIC	0.51	0.83	0.009255314
Q7AKQ5	SCO1644	PrcB	8.83	9.05	9.06	XIC	0.61	1.03	0.001313456
Q7AKQ4	SCO1646	Pup	8.17	8.40	8.52	XIC	0.59	1.31	0.001938115
Q9RJ58	SCO1648	Mpa	9.01	9.23	9.32	XIC	0.60	1.21	0.000719009
Q9RJ57	SCO1651		8.41	8.29	8.18	XIC	1.31	0.77	0.000353515
Q9RJ54	SCO1654		8.26	8.21	8.42	XIC	1.13	1.63	0.004855111
Q9EWH3	SCO1657	MetH	10.00	17.00	38.00	SC	0.59	2.24	2.32104E-15
Q9AD91	SCO1676		8.72	8.71	8.88	XIC	1.02	1.50	0.003529369
Q9S247	SCO1705		7.89	8.24	8.34	XIC	0.44	1.25	0.004030128
Q9EWX6	SCO1750		7.71	7.96	8.06	XIC	0.57	1.26	0.002117118

Q9EWW7	SCO1759		8.61	8.07	7.94	XIC	3.51	0.76	9.18942E-05
Q9S234	SCO1766		7.29	7.19	8.00	XIC	1.26	6.49	0.00040408
Q9S233	SCO1767		0.25	0.00	4.00	SC	NA	NA	1.62761E-05
Q9S227	SCO1773	Ald	54.00	47.67	68.25	SC	1.13	1.43	0.005990058
Q9S224	SCO1776	PyrG	9.02	8.86	8.66	XIC	1.42	0.62	0.001124393
Q9S215	SCO1785		7.89	7.55	7.52	XIC	2.21	0.94	0.006553773
Q9S208	SCO1792		6.99	6.73	6.63	XIC	1.81	0.80	0.007534308
Q9X9Z6	SCO1796		8.46	8.69	8.71	XIC	0.59	1.05	0.00440298
Q9RJ29	SCO1839		8.30	8.59	8.80	XIC	0.52	1.62	0.000820869
Q93RW6	SCO1860		0.25	9.33	1.50	SC	0.03	0.16	1.97654E-09
Q93RW5	SCO1861		7.19	6.90	7.17	XIC	1.94	1.87	0.001899255
Q93RW2	SCO1864	EctA	8.33	7.94	7.88	XIC	2.43	0.86	0.003246341
Q93RW1	SCO1865	EctB	8.54	7.92	7.75	XIC	4.21	0.68	6.61521E-05
Q93RW0	SCO1866	EctC	8.75	8.36	8.63	XIC	2.42	1.82	0.001801338
Q93RV9	SCO1867	EctD	9.08	8.71	9.01	XIC	2.38	2.03	0.0002514
Q93RV8	SCO1868		7.30	7.74	8.10	XIC	0.36	2.25	0.000328849
Q93RV7	SCO1869		2.00	5.00	0.00	SC	0.40	0.00	2.94515E-05
Q9XAD4	SCO1922		9.23	9.34	9.11	XIC	0.79	0.59	0.00038046
Q9XAD2	SCO1924		9.12	9.23	9.04	XIC	0.77	0.65	0.003246341
Q9Z507	SCO1958	UvrA	19.50	29.67	12.25	SC	0.66	0.41	2.21135E-05
Q9S2K6	SCO1997	Asp1	7.12	7.47	6.69	XIC	0.45	0.17	0.000140195
Q9S2J5	SCO2008		9.41	9.65	9.48	XIC	0.58	0.69	0.000358494
Q9S2J3	SCO2010		7.65	7.97	7.82	XIC	0.49	0.72	0.004331953
Q9S2I2	SCO2021		6.95	7.25	7.28	XIC	0.49	1.07	0.001495169
O68816	SCO2036	TrpA	7.64	7.50	8.15	XIC	1.40	4.48	0.000226724
O05625	SCO2037	TrpB	8.01	7.93	8.43	XIC	1.19	3.15	0.00051165
Q9S2S3	SCO2067		9.36	9.18	9.52	XIC	1.52	2.18	0.003917372
Q9S2W3	SCO2093		8.53	8.21	7.76	XIC	2.09	0.35	0.000526558
Q9S2N3	SCO2110	PkaF	7.45	7.11	6.93	XIC	2.18	0.65	0.003718914
Q9S2N0	SCO2113	Bfr	6.71	7.14	7.64	XIC	0.37	3.16	0.000503766

P40182	SCO2127		6.96	7.20	7.26	XIC	0.58	1.17	0.009756059
Q9X7Z1	SCO2132		7.06	7.03	7.42	XIC	1.08	2.49	0.004527585
Q9X810	SCO2152		7.02	7.14	7.44	XIC	0.75	1.98	0.001200023
Q9S2R4	SCO2172		7.76	7.80	8.04	XIC	0.92	1.73	0.004527585
Q9S2P5	SCO2191		0.00	0.00	4.00	SC	NA	NA	1.32474E-06
Q9KZ12	SCO2225		8.18	7.73	7.46	XIC	2.80	0.53	0.003659562
Q9RDR7	SCO2250		0.75	3.00	4.75	SC	0.25	1.58	0.008720675
Q9RKS2	SCO2256	PanB	7.32	7.16	6.41	XIC	1.45	0.18	0.000371147
Q9RKP3	SCO2285		8.01	8.04	7.86	XIC	0.93	0.66	0.007343564
Q9KY19	SCO2371	AceE	8.75	17.00	25.75	SC	0.51	1.51	3.75699E-07
Q9RDQ0	SCO2384		7.02	7.19	7.45	XIC	0.67	1.82	0.000226724
Q7AKN9	SCO2387	FabD	8.65	8.41	8.51	XIC	1.73	1.23	0.005863542
P72392	SCO2388	FabH	9.14	8.93	8.86	XIC	1.63	0.85	0.003616451
Q9RDP7	SCO2390	FabF	9.37	9.23	9.18	XIC	1.37	0.90	0.000121904
Q9RDP0	SCO2397		7.18	7.47	6.95	XIC	0.52	0.30	0.001824211
Q9RDN3	SCO2404		8.73	9.06	8.86	XIC	0.47	0.64	0.009756059
Q9RDN0	SCO2407		7.15	7.66	7.22	XIC	0.31	0.37	0.002410714
Q9S1N5	SCO2469		7.81	7.99	8.18	XIC	0.66	1.56	0.001200023
Q9L2H5	SCO2508		8.10	7.80	7.98	XIC	2.02	1.51	0.002037399
Q9L2G6	SCO2517	EcrA2	7.47	7.45	8.16	XIC	1.05	5.10	1.01158E-05
Q9L2G5	SCO2518	EcrA1	0.00	0.00	6.25	SC	NA	NA	2.53133E-10
Q9L2G4	SCO2519	EcrB	7.66	7.98	8.90	XIC	0.47	8.39	0.000120853
Q9L2G3	SCO2520		6.51	7.07	7.49	XIC	0.27	2.63	0.001001596
Q9L2F9	SCO2524		7.51	7.62	7.88	XIC	0.78	1.82	0.006408321
P95722	SCO2595	ObgE	8.02	8.10	7.79	XIC	0.83	0.50	0.00412016
Q9L1H7	SCO2600		7.93	7.59	7.71	XIC	2.17	1.29	0.003458136
Q9L1H1	SCO2606		8.15	7.72	7.97	XIC	2.69	1.80	5.93689E-05
Q9L1G8	SCO2609	MreD	9.18	8.89	7.25	XIC	1.93	0.02	0.00261015
Q9L206	SCO2627		8.87	8.70	8.69	XIC	1.47	0.97	0.003723758
O51917	SCO2633	SodF1	8.61	8.55	8.84	XIC	1.15	1.98	0.000686293

Q9L201	SCO2634		8.28	8.88	8.01	XIC	0.25	0.13	0.000625874
Q9L1Z8	SCO2637		7.81	8.01	8.11	XIC	0.63	1.26	0.003529369
Q9L250	SCO2671		8.23	8.05	7.62	XIC	1.51	0.37	0.000890241
Q9L1J1	SCO2726	MsdA	8.51	8.61	8.76	XIC	0.80	1.40	0.00412016
Q8CJY6	SCO2730		7.50	7.38	6.71	XIC	1.31	0.21	0.004527585
Q9RDI0	SCO2747		1.25	3.33	6.50	SC	0.38	1.95	0.00241774
Q9RDG5	SCO2763		6.59	7.20	6.13	XIC	0.24	0.09	0.001200023
Q9RDF9	SCO2769		7.88	7.71	7.68	XIC	1.47	0.92	0.001856924
Q8CJY5	SCO2770		8.94	8.80	8.70	XIC	1.38	0.80	0.008580303
Q9L082	SCO2771		7.71	7.82	7.93	XIC	0.78	1.28	0.005863542
Q7AKN2	SCO2779	AcdH	9.44	9.71	9.59	XIC	0.55	0.76	0.002803888
Q93J81	SCO2816		3.25	18.00	2.25	SC	0.18	0.13	5.10382E-13
Q9RDA2	SCO2849		7.54	8.33	7.25	XIC	0.16	0.08	0.000625874
Q9KZS2	SCO2879		8.07	8.28	8.38	XIC	0.62	1.26	0.001574661
Q9KZR8	SCO2883		8.17	8.26	8.44	XIC	0.83	1.53	0.001941642
Q9KZR7	SCO2884		8.95	9.10	9.24	XIC	0.70	1.38	0.000265876
Q9S2H4	SCO2907	NagE2	7.03	6.84	6.76	XIC	1.54	0.83	0.001938115
Q9S2H1	SCO2910	CysM	8.28	8.47	7.88	XIC	0.64	0.26	9.18942E-05
Q9S2G1	SCO2920		7.98	8.44	7.70	XIC	0.35	0.18	0.009255314
Q9S2F6	SCO2925		0.25	1.00	4.75	SC	0.25	4.75	0.000114795
Q9S2E8	SCO2936		4.00	0.67	0.75	PC	6.00	1.13	0.003144879
Q9L1U8	SCO2946		7.48	7.74	7.24	XIC	0.56	0.32	0.00824535
Q9L057	SCO2978		8.75	14.67	23.50	SC	0.60	1.60	7.97314E-06
Q9L055	SCO2980		0.00	1.00	4.00	SC	0.00	4.00	6.98931E-05
Q9KYX2	SCO3009	Hpf	8.46	8.58	8.84	XIC	0.75	1.80	0.002410714
Q9KYW3	SCO3018		8.12	8.05	8.28	XIC	1.18	1.70	0.009756059
Q9KZM1	SCO3023	AhcY/SahH	9.30	9.33	9.81	XIC	0.92	3.01	0.001226091
Q93J48	SCO3055		6.99	6.74	7.20	XIC	1.77	2.86	0.009756059
Q9KZ77	SCO3071		7.48	7.32	7.51	XIC	1.45	1.53	0.006036551
Q9KZ58	SCO3091	Cfa	7.59	8.31	7.65	XIC	0.19	0.22	0.000134366

Q8CJX7	SCO3092		9.06	8.82	8.77	XIC	1.76	0.89	0.001899255
Q9F2P8	SCO3101		0.25	1.67	5.25	SC	0.15	3.15	7.30549E-05
Q9K3T9	SCO3124	RplY	9.24	9.21	9.01	XIC	1.07	0.63	0.0071763
Q9K3R8	SCO3146		8.08	7.96	7.78	XIC	1.30	0.66	0.008800679
Q9RKD0	SCO3157		6.73	6.68	6.30	XIC	1.10	0.41	0.001574661
Q9RKC5	SCO3162		1.50	4.00	0.25	SC	0.38	0.06	0.004205545
Q9KYV1	SCO3194		7.27	6.51	6.70	XIC	5.83	1.58	3.79036E-05
Q9KYU0	SCO3206		0.00	4.00	0.00	SC	0.00	0.00	2.27578E-06
Q9Z4X1	SCO3210		7.84	8.22	8.54	XIC	0.42	2.09	0.002788709
Q9Z4X0	SCO3211	TrpC2	6.72	7.30	7.61	XIC	0.26	2.04	0.002195458
Q9Z4W9	SCO3212	TrpD2	7.53	8.09	8.25	XIC	0.28	1.44	0.003928472
Q9Z4W8	SCO3213	TrpG	6.84	7.16	7.68	XIC	0.48	3.27	0.004281045
Q9Z4W7	SCO3214	TrpE2	4.00	17.33	24.75	SC	0.23	1.43	6.63249E-14
Q9Z4W6	SCO3215	GlmT	8.22	8.65	8.92	XIC	0.36	1.85	0.001677264
Q9Z389	SCO3217	CdaR	7.25	18.67	7.00	SC	0.39	0.37	3.30867E-05
Q9Z388	SCO3218		8.08	8.43	8.86	XIC	0.44	2.64	0.001499171
Q8CJX3	SCO3227	HpgT	8.05	8.49	8.86	XIC	0.36	2.34	0.002803888
Q9Z4X8	SCO3228	Hmo	7.56	7.99	8.36	XIC	0.37	2.34	0.000569224
Q9Z4X7	SCO3229	HmaS	8.66	8.97	9.12	XIC	0.48	1.41	0.00170599
Q9Z4X6	SCO3230	CdaPS1	9.35	9.46	9.98	XIC	0.78	3.29	0.000482347
Q9Z4X5	SCO3231	CdaPS2	153.25	191.67	249.50	PC	0.80	1.30	1.09168E-19
Q8CJX2	SCO3232	CdaPS3	9.11	9.32	9.74	XIC	0.61	2.66	0.000169633
Q9Z4Z8	SCO3233		10.25	15.00	34.50	SC	0.68	2.30	1.24351E-12
Q9Z4Z7	SCO3234	HasP	8.26	8.36	9.07	XIC	0.79	5.11	0.000358494
Q9Z4Z6	SCO3235		8.28	8.55	8.89	XIC	0.53	2.17	0.002111082
Q9Z4Z5	SCO3236	AsnO	8.98	9.26	9.58	XIC	0.53	2.09	0.008992508
Q9Z4Z4	SCO3237		7.44	7.79	8.30	XIC	0.45	3.20	0.001499171
Q9Z4Z3	SCO3238		7.51	7.76	8.32	XIC	0.57	3.63	0.000719009
Q9Z4Z2	SCO3239		8.37	8.70	8.92	XIC	0.47	1.67	0.001304611
Q9Z4Z1	SCO3240		7.01	7.29	7.84	XIC	0.52	3.51	0.006405492

Q9Z4Z0	SCO3241		7.28	7.69	7.95	XIC	0.40	1.84	0.004929954
Q9Z4Y9	SCO3242		7.08	7.54	8.03	XIC	0.35	3.08	0.001431028
Q9Z4Y8	SCO3243		8.28	8.71	8.93	XIC	0.37	1.66	0.007121931
Q9Z4Y7	SCO3244		1.50	7.00	5.25	SC	0.21	0.75	0.003838603
Q9Z4Y6	SCO3245	HcmO	6.75	16.67	20.50	SC	0.40	1.23	3.24003E-06
Q9Z4Y5	SCO3246	FabH4	7.68	8.12	8.37	XIC	0.37	1.77	0.001380344
Q9Z4Y4	SCO3247	HxcO	8.47	8.96	9.20	XIC	0.32	1.72	0.000884304
Q9Z4Y3	SCO3248	FabF3	8.05	8.42	8.66	XIC	0.42	1.74	0.003879199
Q9Z4Y2	SCO3249	Acp	8.29	8.56	8.92	XIC	0.53	2.26	0.001290474
Q9WX11	SCO3323	BldN	0.25	4.33	3.25	SC	0.06	0.75	0.001103188
Q9WX10	SCO3324	RsbN	0.00	4.00	1.50	SC	0.00	0.38	0.000288659
Q9WX06	SCO3328	BdtA	6.92	7.09	7.60	XIC	0.69	3.29	0.004083677
Q8CJX0	SCO3334	TrpS1	6.92	6.97	6.65	XIC	0.90	0.48	0.009614205
Q9X8M6	SCO3369		0.00	1.00	3.75	SC	0.00	3.75	0.000146232
Q9X8N8	SCO3382	NadB	7.72	7.61	7.53	XIC	1.30	0.84	0.001431028
Q9X8R2	SCO3645	KynU	6.93	7.27	6.99	XIC	0.46	0.52	0.009880161
Q9X8R3	SCO3646	KynA	6.85	7.30	6.58	XIC	0.36	0.19	0.003979309
Q8CJV9	SCO3661	ClpB	52.50	91.00	51.00	SC	0.58	0.56	3.43848E-10
Q9L0X2	SCO3732		4.75	0.33	0.00	SC	14.25	0.00	9.29199E-07
Q9F2L5	SCO3766		7.50	7.19	7.31	XIC	2.03	1.30	0.009756059
Q9XA31	SCO3833		6.87	7.25	7.31	XIC	0.43	1.15	0.006813933
Q9XA25	SCO3839		7.63	7.15	7.64	XIC	3.03	3.10	0.00433407
Q9XA13	SCO3851		7.65	7.21	7.47	XIC	2.79	1.81	0.00380947
Q9XA02	SCO3862		7.92	8.17	8.47	XIC	0.56	1.99	0.000342109
Q7AKL1	SCO3877		8.83	8.74	8.54	XIC	1.22	0.62	0.007355589
P27902	SCO3879	DnaA	7.76	7.71	7.58	XIC	1.12	0.74	0.00605367
P52215	SCO3890	TrxB	8.83	9.17	8.80	XIC	0.46	0.43	0.006553773
Q9X9T9	SCO3929		7.39	7.36	7.77	XIC	1.07	2.55	0.001200023
Q9ZBY7	SCO3945	CydA	0.50	0.67	8.00	SC	0.75	12.00	7.5245E-09
Q9ZBY5	SCO3947	CydCD	0.50	0.00	3.75	SC	NA	NA	0.000139034

Q93J30	SCO3977		7.82	7.70	8.04	XIC	1.30	2.17	0.002799784
Q9ADP9	SCO4006		2.75	6.67	9.75	SC	0.41	1.46	0.001613099
Q9ADM4	SCO4034	SigN	0.00	2.67	3.75	SC	0.00	1.41	0.000182517
Q7AKK3	SCO4086	PurF	8.64	8.35	8.40	XIC	1.96	1.12	0.008183699
Q9RKJ0	SCO4096		7.05	6.69	6.28	XIC	2.31	0.40	0.001739336
Q8CJU8	SCO4109		7.69	8.03	7.61	XIC	0.46	0.38	0.005879358
Q9F303	SCO4113		7.45	7.63	7.64	XIC	0.66	1.03	0.001903164
Q8CJU5	SCO4164	CysA	9.37	9.65	9.01	XIC	0.52	0.23	3.79036E-05
Q9K4H3	SCO4165		8.63	8.77	8.33	XIC	0.72	0.36	0.000720274
Q9FCG5	SCO4204	MshA	3.50	6.00	1.00	PC	0.58	0.17	0.00266049
Q9FCF7	SCO4213		2.50	5.33	9.75	SC	0.47	1.83	0.000670952
Q9L0Q9	SCO4232		8.75	8.51	8.25	XIC	1.74	0.55	0.000482347
Q9L0P9	SCO4242		8.86	8.76	8.63	XIC	1.27	0.75	0.006563859
Q9L0N5	SCO4256		7.10	7.12	6.77	XIC	0.96	0.44	0.007768894
Q9K4F1	SCO4261		8.05	7.57	7.33	XIC	3.01	0.58	0.0002514
Q9KXV5	SCO4286		7.55	7.29	7.13	XIC	1.81	0.69	0.002107349
Q9KXU4	SCO4297		8.51	8.88	7.46	XIC	0.43	0.04	0.000115678
Q9KXN6	SCO4321		4.50	9.67	12.75	SC	0.47	1.32	0.001602554
Q9KXN4	SCO4323		7.38	7.14	7.48	XIC	1.74	2.20	0.008948284
Q9KXM5	SCO4332	EcrC	2.75	4.33	12.00	SC	0.63	2.77	7.96821E-06
Q9KZY2	SCO4444		8.24	7.89	8.18	XIC	2.23	1.94	0.007463004
Q9L0T8	SCO4506	MqnA	8.31	8.05	8.07	XIC	1.81	1.03	0.002107349
Q9L0T6	SCO4508		11.50	2.67	10.50	SC	4.31	3.94	0.000145401
Q9L0S9	SCO4515		7.38	7.49	7.62	XIC	0.78	1.33	0.008505963
Q9XAQ5	SCO4563	NuoB1	7.00	7.38	7.73	XIC	0.42	2.28	0.001941642
Q9XAQ6	SCO4564	NuoC	7.04	7.59	7.98	XIC	0.28	2.43	0.003752862
Q9XAQ7	SCO4565	NuoD2	7.04	7.54	7.83	XIC	0.31	1.92	0.002731605
Q9XAQ8	SCO4566	NuoE	7.46	7.73	8.03	XIC	0.54	2.01	0.006405492
Q9XAQ9	SCO4567	NuoF	3.00	5.33	9.75	SC	0.56	1.83	0.002788126
Q9XAR0	SCO4568	NuoG	8.09	8.64	8.80	XIC	0.28	1.45	0.007610869

Q9XAR1	SCO4569	NuoH	1.50	3.33	9.25	SC	0.45	2.78	1.56572E-05
Q9XAR2	SCO4570	NuoI1	7.45	7.77	8.21	XIC	0.48	2.79	0.000482347
Q9XAR3	SCO4571	NuoJ	6.71	7.34	7.58	XIC	0.24	1.74	0.001941616
Q9XAR5	SCO4573	NuoL	6.68	7.46	7.79	XIC	0.16	2.12	0.001946371
Q9XAR6	SCO4574	NuoM	6.78	7.17	7.49	XIC	0.40	2.10	0.002601099
Q9F2X7	SCO4584		6.30	6.30	6.64	XIC	1.00	2.19	0.00412016
Q9F2X4	SCO4587		0.00	13.33	0.00	SC	0.00	0.00	1.39594E-21
Q9F2X1	SCO4590		7.45	7.57	7.25	XIC	0.75	0.48	0.009456512
Q9F2W8	SCO4593		0.00	12.67	0.00	SC	0.00	0.00	1.81623E-20
Q9F2W6	SCO4595		56.50	49.67	36.00	SC	1.14	0.72	0.00059075
Q9L0L9	SCO4641		2.50	0.00	0.00	SC	NA	NA	0.000313562
P41109	SCO4651		7.99	7.57	7.64	XIC	2.64	1.17	0.002195458
Q9L0J6	SCO4669		6.61	7.47	6.44	XIC	0.14	0.09	0.006553773
Q9L0J3	SCO4672		0.00	4.00	0.00	SC	0.00	0.00	2.27578E-06
Q9L0J2	SCO4673		6.50	4.33	0.00	SC	1.50	0.00	1.71138E-07
Q9L0J1	SCO4674		9.25	5.00	0.00	SC	1.85	0.00	1.80085E-10
Q9L0J0	SCO4675		8.76	8.46	8.16	XIC	2.02	0.50	0.00038046
Q9L0G5	SCO4677	RsfA	0.00	0.00	6.25	SC	NA	NA	2.53133E-10
Q9L0G4	SCO4678		8.47	8.28	7.19	XIC	1.55	0.08	6.205E-06
Q9L0G2	SCO4680		8.50	3.33	0.00	SC	2.55	0.00	9.79788E-10
Q9L0G1	SCO4681		9.06	8.72	7.17	XIC	2.18	0.03	7.57932E-07
Q9L0G0	SCO4682		15.50	5.67	0.00	SC	2.74	0.00	4.9745E-18
Q9L0F9	SCO4683	GdhA	7.72	8.37	7.77	XIC	0.22	0.25	9.18942E-05
Q9L0F5	SCO4687		8.05	8.69	8.14	XIC	0.23	0.28	8.15932E-06
Q9L0F0	SCO4692		7.30	7.95	7.50	XIC	0.23	0.36	0.00440298
Q9L0E0	SCO4702	RplC	9.68	9.60	9.49	XIC	1.21	0.78	0.003973515
Q9L0D4	SCO4708	RpsC	9.86	9.77	9.66	XIC	1.22	0.77	0.003843123
Q9L0D3	SCO4709	RplP	9.51	9.41	9.31	XIC	1.26	0.78	0.004855111
P46788	SCO4718	RplR	9.59	9.52	9.41	XIC	1.18	0.78	0.003928472
P72403	SCO4728	RpsK	9.42	9.35	9.22	XIC	1.18	0.75	0.002142361

O86780	SCO4739		8.26	8.04	8.03	XIC	1.65	0.98	0.006108167
O86791	SCO4750		7.39	7.27	7.47	XIC	1.32	1.58	0.005949157
Q9K3J6	SCO4824	FolD	8.91	8.78	9.01	XIC	1.35	1.69	0.008183699
Q9EWE6	SCO4861		0.00	0.67	4.25	SC	0.00	6.38	1.6252E-05
Q9AK25	SCO4901	Add1	7.94	8.14	8.05	XIC	0.63	0.80	0.004376851
Q9AD80	SCO4920		6.92	7.60	7.20	XIC	0.21	0.40	0.00084646
Q9EWV4	SCO4921	AccA2	9.79	9.62	9.22	XIC	1.46	0.39	9.18942E-05
Q9EWW2	SCO4934		9.16	8.74	8.94	XIC	2.60	1.58	3.71066E-05
Q9EWF7	SCO4956	MsrA	8.14	8.65	8.14	XIC	0.31	0.31	0.005863542
Q9ADK0	SCO4967	Mca	8.55	8.78	8.40	XIC	0.59	0.42	0.00092816
Q9EWG5	SCO4969		1.00	2.67	14.25	SC	0.38	5.34	2.39543E-13
Q9EWG8	SCO4972		0.50	2.33	8.25	SC	0.21	3.54	2.59457E-07
Q93JL5	SCO4979	PckG	9.59	9.32	9.59	XIC	1.89	1.89	0.00084646
Q93JK6	SCO4988		7.58	7.73	7.42	XIC	0.70	0.49	0.00416073
Q93JJ8	SCO4996		1.00	0.00	4.25	SC	NA	NA	0.000141226
Q9KY97	SCO5005		6.25	6.89	6.80	XIC	0.23	0.82	0.00305307
Q9KY96	SCO5006		6.74	7.23	7.24	XIC	0.33	1.02	0.00499063
Q9KY93	SCO5009		0.25	1.00	4.75	SC	0.25	4.75	0.000114795
Q9FBP8	SCO5028		5.75	9.00	14.00	SC	0.64	1.56	0.004581681
Q7AKI6	SCO5031	AhpD	9.03	8.93	8.77	XIC	1.27	0.70	0.000574556
Q9FBP5	SCO5032	AhpC	60.50	24.67	13.25	SC	2.45	0.54	1.56496E-29
Q9FBN6	SCO5042	FumC	8.35	8.77	8.29	XIC	0.38	0.33	0.00084646
Q7AKH8	SCO5079		0.00	1.67	5.50	SC	0.00	3.30	1.86967E-06
Q93IY4	SCO5101		7.89	8.30	8.52	XIC	0.39	1.67	0.008680843
Q93IY1	SCO5104		7.42	7.35	7.60	XIC	1.15	1.76	0.000858351
Q93IU0	SCO5115	BldKD	8.93	8.94	8.76	XIC	0.97	0.65	0.000331081
Q9FBJ2	SCO5166		8.61	8.51	8.29	XIC	1.24	0.59	0.000370036
Q9FCL0	SCO5178	MoeB	9.24	9.49	9.13	XIC	0.57	0.44	0.001130578
Q9K494	SCO5229		6.67	6.94	6.66	XIC	0.54	0.52	0.007629052
Q9F3L5	SCO5249	EshB	7.14	8.13	7.54	XIC	0.10	0.26	0.000271487

Q9F3K8	SCO5257		8.00	8.05	8.29	XIC	0.90	1.74	0.00040408
Q9F3K7	SCO5258		7.61	7.77	7.54	XIC	0.68	0.58	0.008680843
Q9F3K4	SCO5261		38.25	27.33	19.00	SC	1.40	0.70	1.825E-05
Q9F3J0	SCO5275		9.75	18.67	25.00	SC	0.52	1.34	9.70451E-06
Q9EVK2	SCO5285	Lon	8.36	8.69	7.92	XIC	0.48	0.17	0.003523844
Q9XAG1	SCO5312		0.50	0.67	3.75	SC	0.75	5.63	0.004399026
Q9XAH1	SCO5331		7.19	7.13	7.38	XIC	1.14	1.77	0.009614205
Q9K4B6	SCO5395		6.99	6.86	7.25	XIC	1.36	2.47	0.003246341
Q9K4B5	SCO5396	FilP	9.11	9.21	9.01	XIC	0.80	0.63	0.00261015
Q9L2B2	SCO5408		0.00	1.33	3.00	SC	0.00	2.25	0.001613099
Q59833	SCO5440	GlgB1	0.50	3.67	7.00	SC	0.14	1.91	1.56572E-05
Q8CJR4	SCO5444	GlgP	3.25	6.67	15.25	SC	0.49	2.29	2.88079E-07
Q9L1E7	SCO5458		7.84	6.97	7.64	XIC	7.29	4.63	0.0001525
Q9L1E0	SCO5465		8.29	9.20	8.05	XIC	0.12	0.07	0.000271487
Q9Z589	SCO5490		0.00	5.67	0.00	SC	0.00	0.00	4.979E-09
Q9Z560	SCO5519	PutA	9.19	9.03	8.81	XIC	1.42	0.59	0.005340349
O86504	SCO5522	LeuB	7.51	7.41	7.32	XIC	1.25	0.80	0.001431028
O86517	SCO5535	AccB	9.28	8.97	8.95	XIC	2.05	0.97	0.000482347
O86518	SCO5536	AccE	7.33	6.53	6.62	XIC	6.31	1.21	0.001801338
O86525	SCO5544	CvnA1	8.70	8.50	8.49	XIC	1.56	0.97	0.003246341
O86526	SCO5545		7.72	7.59	7.44	XIC	1.35	0.71	0.008800679
O86535	SCO5554	LeuD	4.75	0.67	1.00	SC	7.13	1.50	0.001707329
Q9ZBR9	SCO5560	Ddl	7.75	7.66	7.52	XIC	1.22	0.72	0.00705564
Q9ZBR8	SCO5561		7.03	7.21	7.50	XIC	0.66	1.92	0.002040251
Q9ZBR5	SCO5564	RpmB1	8.84	8.74	8.52	XIC	1.26	0.60	0.008526814
Q9ZBP7	SCO5582	NsdA	1.00	7.00	1.50	SC	0.14	0.21	0.000122422
O69878	SCO5590		7.91	7.76	7.69	XIC	1.39	0.84	0.007137727
O69886	SCO5598		7.20	7.40	7.11	XIC	0.64	0.51	0.001800667
O86768	SCO5629		6.50	6.87	6.99	XIC	0.43	1.32	0.001445593
O86737	SCO5662		8.19	8.16	8.44	XIC	1.06	1.88	0.009649843

O86653	SCO5734		7.58	7.22	7.27	XIC	2.28	1.11	0.00705484
Q8CJQ6	SCO5737	Pnp	9.90	9.81	9.71	XIC	1.24	0.80	0.001765533
O86812	SCO5752	RimO	8.41	8.16	8.20	XIC	1.76	1.09	0.002896206
O50487	SCO5769	RecA	8.27	8.37	8.04	XIC	0.79	0.47	9.18942E-05
O69974	SCO5798		8.53	8.49	8.30	XIC	1.09	0.65	0.001941642
O69979	SCO5803	LexA	8.15	8.43	8.21	XIC	0.52	0.61	0.006052745
O69980	SCO5804	NrdR	6.99	7.18	6.94	XIC	0.64	0.57	0.00961502
O54142	SCO5878	RedX	0.25	0.00	10.25	SC	NA	NA	1.63464E-15
O54143	SCO5879	RedW	7.14	6.86	7.65	XIC	1.87	6.11	0.00031161
O54147	SCO5884		0.75	0.00	4.75	PC	NA	NA	7.75429E-06
O54153	SCO5890	RedN	6.46	6.24	7.42	XIC	1.63	15.16	5.82078E-05
O54155	SCO5892	RedL	1.75	0.33	19.25	SC	5.25	57.75	1.54183E-23
O54156	SCO5893	RedK	6.67	6.72	7.32	XIC	0.88	3.92	0.002202663
O54158	SCO5895	RedI	1.50	1.67	15.25	SC	0.90	9.15	9.60455E-15
Q8CJQ2	SCO5896	RedH	6.87	6.98	7.74	XIC	0.77	5.77	0.001200023
O54095	SCO5897	RedG	1.25	1.67	13.25	SC	0.75	7.95	1.46136E-12
O54116	SCO5920		3.25	0.33	0.00	SC	9.75	0.00	0.000162157
Q7AKF3	SCO5999	SacA	110.00	129.00	147.00	SC	0.85	1.14	0.00018436
Q9X842	SCO6076		7.32	7.59	7.60	XIC	0.54	1.02	0.002337166
Q9ADI5	SCO6078	TreZ	7.40	7.76	7.85	XIC	0.44	1.23	0.001395418
Q9ADH2	SCO6091		3.25	4.33	10.00	SC	0.75	2.31	0.001764371
Q9ADG7	SCO6096	SsuA	7.54	8.05	7.37	XIC	0.31	0.21	0.002928101
Q9ADG6	SCO6097	CysN	8.19	8.71	7.77	XIC	0.31	0.12	0.000543394
Q9ADG5	SCO6098	CysD	7.96	8.43	7.41	XIC	0.34	0.10	5.82078E-05
Q9ADG4	SCO6099	CysC	3.00	8.67	3.00	SC	0.35	0.35	0.006581824
Q9ADG3	SCO6100	CysH	2.25	4.00	0.00	SC	0.56	0.00	0.000250713
Q9ADG1	SCO6102	SirA/CysI	8.16	8.42	7.59	XIC	0.56	0.15	0.001817736
Q9Z5A7	SCO6195	MACS1	9.00	15.33	21.75	SC	0.59	1.42	0.00015483
Q9Z5A6	SCO6196	FadD1	0.00	1.00	7.50	SC	0.00	7.50	6.8352E-10
Q9Z5A4	SCO6198		8.32	8.74	8.52	XIC	0.39	0.61	0.004927302

Q9Z597	SCO6205	GlxR	7.40	7.22	6.83	XIC	1.52	0.41	0.004030128
Q8CJN8	SCO6211		7.04	7.13	7.41	XIC	0.82	1.92	0.006813933
Q9RKU5	SCO6247	AllB	7.81	7.73	8.31	XIC	1.18	3.79	0.001434136
Q9RKU4	SCO6248	Alc	10.00	13.00	24.00	SC	0.77	1.85	2.26397E-05
Q7AKF1	SCO6265	ScbR	8.72	8.76	9.09	XIC	0.91	2.13	0.001130578
Q7AKF0	SCO6266	ScbA	6.43	6.57	7.93	XIC	0.73	23.21	0.000214979
Q9RKS7	SCO6267	ScbB	7.12	7.06	8.20	XIC	1.13	13.80	0.00040408
Q9RKS5	SCO6269	CpkPβ	17.00	12.67	7.00	SC	1.34	0.55	0.00123494
Q9RKS4	SCO6270	CpkPα	56.00	48.33	34.75	SC	1.16	0.72	0.000277115
Q9EX55	SCO6272	ScF	18.25	14.00	0.00	SC	1.30	0.00	5.50775E-22
Q9EX54	SCO6273	CpkC	9.29	8.72	8.13	XIC	3.68	0.26	0.002009855
Q9EX53	SCO6274	CpkB	8.93	8.56	8.53	XIC	2.39	0.93	0.001545388
Q8CJN6	SCO6275	CpkA	9.37	8.96	8.45	XIC	2.56	0.31	0.000305494
Q93S13	SCO6276	CpkD	9.38	8.94	6.40	XIC	2.72	0.00	2.58998E-06
Q93S12	SCO6277	CpkE	8.97	8.76	7.62	XIC	1.61	0.07	8.4056E-06
Q93S11	SCO6278	CpkF	9.37	9.02	7.27	XIC	2.26	0.02	0.000121904
Q93S10	SCO6279	CpkG	9.74	9.65	8.68	XIC	1.24	0.11	0.007137727
Q93S09	SCO6280	CpkO	13.75	9.67	0.00	SC	1.42	0.00	4.1624E-16
Q93S08	SCO6281	CpkH	4.25	3.00	0.00	SC	1.42	0.00	5.24476E-05
Q93S07	SCO6282	CpkI	10.71	10.72	8.76	XIC	0.97	0.01	2.58998E-06
Q93S06	SCO6283	CpkJ	9.84	9.71	8.54	XIC	1.36	0.07	0.000569224
Q93S05	SCO6284	CpkK	25.75	18.67	0.00	SC	1.38	0.00	8.19047E-31
Q93S03	SCO6286	ScbR2	7.25	7.33	0.00	SC	0.99	0.00	1.99826E-09
Q9LAS9	SCO6287	ScoT	0.00	4.33	0.00	SC	0.00	0.00	6.72874E-07
Q93RY4	SCO6288	CpkN	0.00	3.67	0.50	PC	0.00	0.14	0.000103497
Q93RY0	SCO6292		8.17	8.45	7.71	XIC	0.53	0.18	0.000214979
O69939	SCO6411		0.00	1.33	4.50	SC	0.00	3.38	2.34642E-05
O69817	SCO6423	LplA	7.39	7.97	7.33	XIC	0.26	0.23	0.00051165
Q9ZBK6	SCO6468	Psd	8.53	8.43	8.28	XIC	1.23	0.70	0.007029316
Q9ZBJ0	SCO6484		6.61	7.00	7.22	XIC	0.41	1.67	0.002107349

Q8CJM7	SCO6492		1.00	3.33	8.75	SC	0.30	2.63	4.90943E-06
Q9ZBV4	SCO6564	FabH2	8.03	7.29	7.14	XIC	5.48	0.70	0.000305254
O86678	SCO6631		8.15	7.63	7.38	XIC	3.32	0.56	0.003078577
O86683	SCO6636	PglZ	7.53	7.35	7.24	XIC	1.52	0.78	0.006683308
Q9XAN4	SCO6696		0.00	0.33	2.50	SC	0.00	7.50	0.002060584
Q9XAL3	SCO6717		8.64	8.23	8.04	XIC	2.61	0.64	0.001903164
Q9X7P2	SCO6736		7.66	8.22	8.03	XIC	0.28	0.65	0.002346626
Q9X7Q1	SCO6745		7.31	7.55	7.58	XIC	0.57	1.08	0.009979211
Q9X7V9	SCO6764		0.50	5.33	10.50	SC	0.09	1.97	3.80945E-09
Q9X7W1	SCO6766		7.44	7.89	7.80	XIC	0.35	0.80	0.001431028
Q9X7W3	SCO6768	Dxs1	6.74	7.27	7.40	XIC	0.30	1.37	0.001856924
Q9L221	SCO6811		0.00	5.33	0.00	SC	0.00	0.00	1.71151E-08
Q9L216	SCO6816		0.00	14.00	0.00	SC	0.00	0.00	1.11247E-22
Q9L214	SCO6818	GpmI	0.00	7.67	0.00	SC	0.00	0.00	3.09263E-12
Q9L213	SCO6819	AroA	6.65	8.03	6.93	XIC	0.04	0.08	3.71066E-05
Q9L211	SCO6821		0.00	3.33	0.00	SC	0.00	0.00	2.31975E-05
Q8CJL8	SCO6824		0.00	6.00	0.25	SC	0.00	0.04	2.25714E-08
Q9L1W0	SCO6825		0.00	2.67	0.00	SC	0.00	0.00	0.000242219
Q9L1V9	SCO6826		0.00	4.67	0.00	SC	0.00	0.00	2.0243E-07
Q9L1V8	SCO6827		0.25	15.33	0.00	SC	0.02	0.00	3.1683E-23
Q9L1V7	SCO6828		8.02	9.20	8.28	XIC	0.07	0.12	0.000503766
Q9KYC4	SCO6906		0.25	3.00	4.25	SC	0.08	1.42	0.001016197
Q9KZC3	SCO6966		7.20	7.29	7.60	XIC	0.81	2.03	0.006498158
Q9KZC2	SCO6967		7.47	7.82	7.92	XIC	0.45	1.27	0.005158752
Q9KZC1	SCO6968		7.86	8.19	8.26	XIC	0.47	1.18	0.004697702
Q8CJL4	SCO6975		2.00	8.33	9.25	SC	0.24	1.11	0.0001092
Q9KZH2	SCO6980		6.12	6.56	6.47	XIC	0.37	0.82	0.005838255
Q9KZG4	SCO6988		2.50	7.67	8.75	SC	0.33	1.14	0.002064041
Q8CJL2	SCO7034		0.50	0.67	4.25	SC	0.75	6.38	0.001040982
Q9FC18	SCO7066	FadH	8.68	8.34	7.47	XIC	2.17	0.13	9.49499E-05

Q9FBV0	SCO7141		0.50	8.33	0.00	SC	0.06	0.00	3.46919E-11
Q9FBS4	SCO7168	Agl3R	8.18	7.52	7.23	XIC	4.59	0.51	0.001477183
Q9K4H9	SCO7246		7.10	7.16	7.59	XIC	0.88	2.74	0.002256111
Q9X7T1	SCO7269		7.57	7.89	7.87	XIC	0.48	0.94	0.006405492
Q9K4M2	SCO7292		7.21	7.30	7.45	XIC	0.80	1.39	0.005863542
Q9KY13	SCO7325	RsbV/BldG	7.15	7.17	7.58	XIC	0.94	2.59	0.001689645
Q9L178	SCO7399	CdtB	8.75	8.58	8.56	XIC	1.48	0.95	0.004452742
Q9L141	SCO7418		7.82	7.67	7.85	XIC	1.42	1.52	0.001748024
Q9L139	SCO7420	CvnC10	6.67	6.38	6.62	XIC	1.98	1.74	0.006813933
Q9L131	SCO7428	FhbA	7.14	6.76	6.59	XIC	2.39	0.67	0.008539454
Q9L124	SCO7436		0.50	8.33	12.00	SC	0.06	1.44	5.346E-11
Q9L117	SCO7443	Pgm	8.59	8.65	8.77	XIC	0.87	1.31	0.005158752
Q9ADJ2	SCO7467		7.97	7.89	7.60	XIC	1.18	0.51	0.006963042
Q93JC7	SCO7469		4.00	8.00	11.25	SC	0.50	1.41	0.004581681
Q9KYZ3	SCO7536	MmpL	8.00	7.58	8.49	XIC	2.58	8.14	0.000308461
Q9F389	SCO7586		0.00	6.33	0.00	SC	0.00	0.00	4.42195E-10
Q9F3P9	SCO7638	Eno2	0.00	0.00	3.50	SC	NA	NA	7.97314E-06
Q9F3N4	SCO7653		6.67	6.82	7.25	XIC	0.71	2.70	0.001801338
Q9F3N2	SCO7655		7.88	8.12	8.04	XIC	0.58	0.82	0.005949157
Q9F3N0	SCO7657		8.79	8.97	8.53	XIC	0.67	0.36	0.000448087